ČESKÉ VYSOKÉ UČENÍ TECHNICKÉ V PRAZE

Fakulta stavební

Katedra mechaniky

Subsoil Influenced by Groundwater Flow

Podloží ovlivněné prouděním podzemní vody

DISERTAČNÍ PRÁCE

Ing. Miroslav Brouček

Doktorský studijní program: Stavební inženýrství

Studijní obor: Fyzikální a materiálové inženýrství

Školitel: prof. Ing. Pavel Kuklík, CSc.

Praha, 2013

ČESKÉ VYSOKÉ UČENÍ TECHNICKÉ V PRAZE
Fakulta stavební
Thákurova 7, 166 29 Praha 6

PROHLÁŠENÍ

Jméno doktoranda: Miroslav Brouček

Název disertační práce: Podloží ovlivněné prouděním podzemní vody

Prohlašuji, že jsem uvedenou doktorskou disertační práci vypracoval/a samostatně pod vedením školitele prof. Ing. Pavla Kuklíka, CSc.
Použitou literaturu a další materiály uvádím v seznamu použité literatury.

Disertační práce vznikla v souvislosti s řešením projektů: MSM 680770001, GA103/07/0246, GA103/08/1119, GA103/04/11134, GA103/08/1617 a CTU0700811.

v Praze dne 28.2.2013

podpis

ACKNOWLEDGEMENT

At first I would like to express my gratitude to prof. Ing. Pavel Kuklik, CSc. for his never ending support, patience and advices during my entire study.

I also would like to thank colleagues from Centre of Experimental Geotechnics for helping me with the experiments and providing many useful tools and advices during my laboratory experiments and colleagues from the Department of Geotechnics for the possibility to use their software for numerical modelling and measuring devices for lateral pressures measurement.

My thanks also belong to Ing. Martin Lidmila, Ph.D. for his support during the large scale experiments and to doc. Ing Ladislav Satrapa, CSc. for his kindness, which allow me to use the laboratory of Water Management Experimental Centre for my experiments. I wish to thank all other colleagues for their valuable comments, advices and excellent working environment.

Most importantly, I would like to express my deepest thanks to my wife Michaela and my parents for their support and help which allow me to concentrate fully on the subject of the interest.

I would also like to acknowledge the research project MSM 680770001 and grants GA103/07/0246, GA103/08/1119, GA103/04/11134 and 103/08/1617. Part of the work was produced under kind support of the CTU internal grant CTU0700811.

TABLE OF CONTENTS

LIST OF FIGURES

LIST OF TABLES

Czech Technical University in Prague

Abstract

Subsoil Influenced by Groundwater Flow

Miroslav Broucek

Generally three phase porous anisotropic inhomogeneous medium showing significant spatial variability and also the oldest construction and the most common foundation material – the soil. Even though the soil mechanics has rapidly evolved within last 80 years of its modern history, due to numerous phenomena which influence soils behaviour and are based on its natural characteristics the room for improvement exists. This basic space will most likely preserve to the fore coming century as a result of fundamental limits of the applied approaches which cannot completely comprehend with so complex open system and large spatial variability. However, most engineering problems, regarding saturated and even unsaturated soils behaviour, can be resolved with sufficient accuracy using powerful numerical models and methods. Although even models which approximate the reality perfectly have to be supplied with material parameters obtained from either laboratory or in-situ experiment when both classes affect only limited surroundings.

With respect to the wide range of influencing phenomena connected with the presence of liquid phase in the soil, this thesis focuses on two important areas of research. First, there is an internal erosion problem of saturated soils when subjected to groundwater flow. Although, the topic of change of the mechanical parameters of the soil due to the groundwater flow was in the past studied from the point of view of transition zones between core with very low hydraulic conductivity and stabilizing parts in the earth dams resulting in recommendations for grain distribution of the soils used in the transition zones, the methods used in dam engineering are barely suitable for common engineering problems.

Second, the behaviour of soils in unsaturated state under is part of the research. Here the thesis focuses on suction cancellation followed by additional settlement of foundation structures in fine grained and coarse grained soils. However, the last mentioned class is commonly referred as unaffected by suction cancellation.

The area of interest was restricted to "hydro-mechanical" point of view and does not involve any chemical interactions between the phases inside the soil or between the surrounding and solved domain. From the numerical modelling point of view the work is based on continuum approach using finite element method although references the particle float codes where appropriate.

Predominant part of the thesis concentrates on the experimental analysis and its evaluation followed by recommendations. Stand for full scale experiments with varying groundwater table was designed and constructed allowing for observation of all the phenomena and possibility of estimating the effects in situ due to selected measuring technique, i.e. static plate load test.

The results obtained from the full scale experiments proved to be very useful in understanding and evaluating of the processes through which the groundwater influence the behaviour of the subsoil. Some of the results obtained challenge the general assumptions, such as fine particle loss due to groundwater flow or negligibility of the effect of suction for coarse soils. The results were also used to calibrate and confirm the ability of professional codes to approximate the soils behaviour during plate load tests and suction cancellation. The success of the last mentioned simulations was very limited despite the enormous computational time used.

Part of the thesis is devoted to search for a simple solution with large variety of use available and understandable in common engineering practice. Here, the elastic layer theory with adopted varying influence zone theory providing for fast analytical solution is employed.

The thesis also contains recommendations for flood risk assessment, and several comments on practical issues regarding the infiltration policy for large impermeable areas and the influence of hydraulic structures and channel improvements on adjacent areas.

České vysoké učení technické v Praze

Abstrakt

Podloží ovlivněné prouděním podzemní vody

Miroslav Brouček

Popis a porozumění procesům ovlivňujících chování či odezvu zemin v návaznosti na přítomnost nebo pohyb podzemní vody jednoznačně přispěje ke spolehlivějšímu návrhu základových i geotechnických konstrukcí. Jejich ignorování naopak přináší zvýšená rizika chybného návrhu nebo posouzení a z nich vyplývající, převážně materiálové byť velmi vysoké, škody. Přestože dnešní praxe připouští výrazné rozdíly v chování nasycených a nenasycených zemin, je ochotná je bráti do úvahy pouze v případě zemin jemnozrnných či raději přímo jílovitých. V experimentální části práce je pak prokázán nezanedbatelný vliv jednotlivých jevů i pro zeminy hrubozrnné, písčité i štěrkovité.

Jakkoli se může zdát teoretická báze popisující hydraulické i mechanické jevy v pórovitém prostředí dostatečně široká, prostor pro doplnění nebo zjednodušení jinak velice komplexních úloh je dostatečný jak v oblasti lokalizovaného proudění v nasycené zóně spojeného s vyplavováním částic a vnitřní erozí, tak i v oblasti modelování chování zemin nenasycených. V disertační práci je představeno několik konstitutivních modelů popisujících chování zemin při ustáleném i neustáleném stavu kapilárního sání včetně nedávné kritiky stran jejich nekonsistence se základními fyzikálními prvky systému, která zaznívá zejména z důvodu použití techniky „překladu os“ k překonání potíží s kavitačními jevy, které nastávají při experimentech využívaných standardních měřicích technik. Práce dále představuje stručný obecný i matematický popis vnitřní eroze a vyplavování částic.

K zúžení velmi široké zájmové oblasti podloží ovlivněného působením podzemní vody lze přistoupit z různých úhlů pohledu v závislosti na konkrétních podmínkách zkoumaných jevů. Předložená práce si vytyčila cíle v oblasti vnitřní stability zemin při krátkodobém působení extrémních hydraulických gradientů a v oblasti dodatečného sedání potažmo deformací způsobených změnou nenasyceného stavu, která může být vyvolána extrémními přírodními událostmi i lidskou činností.

Vysoce sofistikované numerické modely dokáží dobře vystihnout chování zemin v nenasyceném stavu. Jejich komplexnost a náročnost na výpočetní čas a na kvalifikaci uživatele však téměř vylučují jejich širší použití v současné běžné praxi ponechávajíce jim pouze oblasti akademického bádání a zpětných analýz. Modely řešící úlohy v prostředí nasyceném, případně nenasyceném ovšem bez možnosti změny sání coby stavové proměnné, mají výrazně rozsáhlejší oblast působení, byť i zde je možné pozorovat příklon k jednoduchým a ověřeným modelům Mohr-Coulomba či Drucker-Pragera i přes širokou nabídku modelů kritického stavu.

Práce si vytkla mimo další cíle i zpracování doporučení aplikovatelných na problémy běžné inženýrské praxe. Z tohoto důvodu je hlavní část práce zaměřená na experimentální analýzu jevů na laboratorních modelech a zkoumání možností využití analogie pro přenos pozorovaných jevů na řešení praktických úloh. Popsaný přístup je patrný zejména na laboratorních experimentech na velkých vzorcích, které využívají shodné postupy s in-situ měřením.

Výsledky měření byly využity pro kalibraci a ověřování schopností numerických modelů popsat věrně provedené experimenty, a jsou i dále k dispozici dalším autorům. Zjednodušené a zobecněné závěry vyvozené z měřených dat byly použity pro úpravu výpočtu hloubky deformační zóny pod základy pomocí snížení předkonsolidace, návrh rozšíření ztrátových funkcí při rizikové analýze povodňových škod, upozornění na potenciální škody při zasakování srážkových vod z velkých ploch bez respektu k ustálenému stavu okolí a další inženýrské úlohy.

Chapter 1

INTRODUCTION

Reductionism is true in a sense.
But it's seldom true in a useful sense.

Martin John Rees

The soil was used as a constructing and foundation material for thousands of years and so it can be expected that its behaviour under all conditions is perfectly described, but it is not. This is due to the spatial variability of soil content as well as the variability of processes that influence the soil response (Terzaghi et al., 1996), (Fredlund and Rahardjo, 1993), (Shroff et al., 2003). The fact that soil is in general a three or more phases (Fredlund and Morgenstern, 1977), (Vardoulakis, 2006) medium does not make things easier.

On the other hand nearly all the processes have been observed and, the ones having very significant effect, described. Still there is enough space to improve the knowledge, especially in soils which behaviour is influenced by the groundwater, where the worldwide consensus regarding the stress state variables has not been established.

Typically the problem of particle loss due to the flow of a liquid phase can be studied under different conditions with respect to the assumptions of the particular solution of the problem (sand production in oil industry (Papamichos, 2006), water well production and its walls stability, (Cividini et al., 2009) or stability of hydraulic structures such as weirs and dams (ICOLD, 2013).

1.1. Motivation

The goals of this thesis are motivated strictly by practical issues and financial losses resulting from neglecting the impact of changes in subsoil behaviour due to groundwater flow in both saturated and unsaturated soil or missing standard recommendations for involving these changes into design situations even though the standing standards (EN

1997-1) require engineers to do so. The applied methodical approach, described further, bears in mind the statement from Martin Rees (2010).

During past two decades the Czech Republic was affected by series of big flood events which caused serious damage to many buildings and engineering construction. When the floods passed and the damage to the buildings was studied, broad discussion opened about the effect of the changes in the subsoil on the overall damage of the constructions (Valenta et al., 2006), (Broucek and Kuklik, 2006). Although, the topic of change of the mechanical parameters of the soil due to the groundwater flow was in the past studied from the point of view of transition zones between core with very low hydraulic conductivity and stabilizing parts in the earth dams resulting in recommendations for grain distribution of the soils used in the transition zones (ICOLD, 1994), the methods used in dam engineering are barely suitable for common engineering problems.

As the risk analysis, which can be considered as the only impartial mean for evaluation the effect of floods and flood prevention projects, builds on the assessment of the damage to the buildings, we found it important to search for solution that will clearly state the effect of the groundwater to the building during and most importantly after the flood events. To explain the last sentence it is to be stated that most of the structural damage to the constructions was not caused by hydrodynamic loading and took place sometime after the flood peak.

Another practical problem that extends the research area to unsaturated field is damage observed on engineering structures constructed on artificially compacted soils as well as on natural soils experiencing suction cancellation due to changed hydrogeological conditions. The last mentioned can either be caused by accidents of water supply or sewer system pipelines or are taking place due to infiltration systems constructed as a result of the civil service requirement to infiltrate all of the precipitation water from large impermeable areas (roofs, parking areas, etc.) without any respect to relevant circumstances.

On the other hand, problems with artificially compacted soils can be usually attributed to road and pavements built on the backfilled trenches from engineering networks. Although only a part of the reported cases is caused by the groundwater flow (especially vertical) and its influence on the soil (suction cancellation), due to the high number of cases in total, it is still an important issue for study. Similar issues, additional settlements, were reported on natural soils improved with vibroflotation or sand or gravel piles both Franki and vibroflotated type (Weng et al., 2009).

Last problem that is an active part of the motivation of this research represents accidents and complete failures of several spillways and dam constructions. Last reported case took place in the Slovak Republic in April 2008. It was a complete destruction of one weir block of newly constructed weir structure while adjacent small hydroelectric plant suffered also severe damage.

1.2. Area of interest and methodical approach

As the problem can be studied from different points of view, it has been decided to set the area of interest to gain as much practical information and conclusions as possible while avoiding decrease in generality of the results. All the processes are studied from the geotechnical point of view and the selected area of interest is macroscopic level and phenomenological approach to the processes. Following two areas of interest, their subdivisions and corresponding goals were specified:

1. Increase in overall settlement due to suction cancellation
    - Description of the process and review of relevant methods for rigorous evaluation of the impact – Chapter 2
    - Design of an experiment allowing for quantification of the impact of suction cancellation for different soil types – Chapter 4
    - Recommendations for fast evaluation of the impact using analytical approach – Chapter 5
    - Contribution to the flood risk assessment (involves both areas of interest) – Chapter 6
    - Provide experimental results for confirmation of numerical models – Appendixes B - D
2. Internal erosion due to groundwater flow
    - General description of the process – Chapter 3
    - Stability assessment for soils under extremely high hydraulic gradient – Chapter 4 and Appendix E
    - Contribution to the flood risk assessment (involves both areas of interest) – Chapter 6

The area of interest was restricted to "hydro-mechanical" point of view and does not involve any chemical interactions between the phases inside the soil or between the surrounding and solved domain. It was also decided to avoid the conclusions available only for high-risk, high-pay-off technologies, which in case of soils means only the oil production industry, which works under conditions not applicable to our research.

From the numerical modelling point of view the work is based on continuum approach using finite element method although references the particle float codes where appropriate.

1.3. Historical background

The knowledge describing the movement or position of groundwater table in a phreatic aquifer with high hydraulic conductivity adjacent to a river can be successfully traced back to the ancient Egypt. The great temple of Kom Ombo stands witness to this knowledge containing even today working well measuring water table in the river Nile (also called Nilometer) and notes about observed flood peaks carved in stone for time periods more than 3000 years ago.

G.J. Caesar (Caesar, 40 BC) in his commentaries about the war in Alexandria describes the effort of Egyptian soldiers to deprive his forces of fresh water. The Egyptian troops planned to contaminate wells of besieged Romans with brackish waters from nearby estuaries by abstracting water from series of new wells bored around their positions. Such actions could not be taken without deep understanding of flow through porous media including depression curve development around wells as well as freshwater-saltwater interface position and movement more than eighteen centuries before Henry Darcy presented his experiments (Darcy, 1856) and started modern era in subsurface hydrology and nearly twenty centuries before Karl Terzaghi (1936) described the stress state variable controlling the behaviour of saturated soils.

Detailed description of the behaviour of unsaturated soil cannot be however considered within the "historical background" as the worldwide consensus was not so far established (Lu, 2008). The inability to derive one universal description of the unsaturated soils behaviour is not due to the lack of need, quite the opposite is actually true, but rather due to the complexity of the problem. As presented by Jones and Holtz (1973) the damage inflicted by unsaturated soils is in United States doubles the damage caused by earthquakes, floods and tornados. This statement was supported by Krohn and Slosson (1980) estimating the spendings on repair and reconstruction works induced by the damage caused by expansive soils to exceed seven billions US dollars per annum. Similar problems have been reported in many Asian and South American countries as well e.g. (Rodrigues et al., 2006). Different standing approaches are introduced in the following chapter.

Chapter 2

SATURATED AND UNSATURATED SOILS

The aim of this chapter is to review the theories and approaches used in both saturated and unsaturated soil mechanics. At the beginning we briefly describe the general poromechanics formulation of saturated soils and provide a few comments on coupling the governing equations for individual phases (Charlier et al., 2001), (Charlier et al., 2006). The problem with physical foundations of unsaturated soil mechanics is discussed later in this chapter followed by the description of stress state variables used in unsaturated soils modelling. Last part of this chapter is devoted to the constitutive models used for simulations of carried out experiments and their implementation into software packages. It is to be pointed out that only problems involving small strains are considered in this chapter.

2.1. General poromechanics problem formulation for saturated soils

The presence of groundwater can cause any soil specimen, i.e. porous material, to be either in saturated or unsaturated state. Some processes described further are typically present only in unsaturated or saturated soils. The formulation of the problems is also different for saturated and unsaturated state although recommendations could be found to simulate non-cohesive dry soils such as sands and gravel using the same approach as for the saturated soils, i.e. classical soil mechanics (Fredlund and Rahardjo, 1993). Although classical approach assumes two phase medium (solid and fluid) and therefore seems to be perfectly suitable for dry porous media behaviour description, in practice nearly all soils contain certain amount of water. As shown in the numerical modelling part, classical approach is sufficient for simulation of unsaturated soils behaviour as long as the pore water pressure are bounded by constant Dirichlet boundary conditions, while unsaturated approach is necessary even for cohesionless soils when the suction state changes. The results from experiments with suction cancellation on poorly graded gravel presented in chapter 4 cannot be obtained when employing only classical soil mechanics. Therefore it is important to specify the soil state prior to any numerical modelling and also to carefully evaluate the type of the problem and select correct constitutive model.

Nowadays, large number of constitutive models can be found in the literature. The detailed description of all used constitutive models goes beyond the scope of this thesis and so the description is limited to several models used by the author while the detailed description of other models presented over the last two decades can be found based on the following example of the state-of-the-art reviews (Gens, 1996), (Wheeler and Karube, 1996), (Kohgo, 2003), (Gens et al., 2008), (Sheng and Fredlund, 2008), (Sheng et al, 2008a), (Cui and Sun, 2009) and (Gens, 2009).

Steady state seepage problems and geomechanical problems where loads are very slowly applied are generally described by partial differential equations of elliptic type (with the exception of localized failure in elastoplastic softening material) (Pastor and Mira, 2002). These partial differential equations can be used for case of saturated soils but in case of unsaturated soils where transient problems play major part the equation type is parabolic or hyperbolic (Lewis and Schrefler, 2000), (Pastor and Merodo, 2002).

Flow through the porous media can be described with help of the balance of momentum equation (2.1) and balance of mass equation (2.2). We solve the problem on open domain Ω having boundary Γ.

$$-\nabla p_w + \rho_w . \mathbf{g} = \mathbf{k}_w^{-1} . \mathbf{v} \tag{2.1}$$

where p_w is the pore water pressure, ρ_w is the water density, ∇ is the gradient operator $(\partial_x, \partial_y, \partial_z)^T$, $\mathbf{g}$ is the vector of body forces, $\mathbf{k}_w$ is the permeability tensor and $\mathbf{v}$ is the average velocity of water.

$$\nabla^T . \mathbf{v} + \left(C_S + \frac{1}{Q} \right) \frac{\partial p_w}{\partial t} = 0 \tag{2.2}$$

where p_w is the pore water pressure, t is the time, ∇^T is the divergence operator $(\partial_x, \partial_y, \partial_z)$, C_s is the specific storage coefficient, $1/Q$ is the member that accounts for the compressibility of water and soil particles and $\mathbf{v}$ is the average velocity of water. When combining eq. 2.1 and 2.2 and introducing the potential Φ such that

$$\nabla \Phi = \nabla p_w + \rho_w . \mathbf{g} \ , \qquad (2.3)$$

we obtain

$$\nabla^T \left(k_w \left(\nabla \Phi \right) \right) = \left(C_S + \frac{1}{Q} \right) \frac{\partial p_w}{\partial t} \ , \qquad (2.4)$$

with steady state condition

$$\nabla^T \left(k_w \left(\nabla \Phi \right) \right) = 0 \quad in \, \Omega \, . \qquad (2.5)$$

The weak formulation can be obtained in form

$$\int_\Omega \nabla \psi^T k_w \ \nabla \Phi \ d\Omega = \int_\Gamma \psi \ q \ d\Gamma \ , \qquad (2.6)$$

where q is flow on the boundary normal to boundary as it refers to Neumann boundary condition and ψ is a smooth function from Sobolev space and is square integrable with first derivative also square integrable.

In the mixture the balance of momentum equation reads

$$div \left(\boldsymbol{\sigma} \right) + \mathbf{g} = 0 \qquad (2.7)$$

where $\boldsymbol{\sigma}$ is the total stress tensor, $\mathbf{g}$ is the body force vector and *div* represents the discrete divergence operator. Constitutive behaviour equations for each phase must be provided to ensure closure of the balance equations. The vary basic elastic constitutive model can be written with the help of Terzaghi's mean effective stress (2.10) and assuming incompressible grains bud deformable soil skeleton as follows

$$\sigma'_{ij} = \left[2G \delta_{ik} \delta_{jl} + \left(K - \frac{2}{3} G \right) \delta_{ij} \delta_{kl} \right] \varepsilon_{kl} \qquad (2.8)$$

where K is the bulk modulus and G is the shear modulus. Such constitutive model is to be used strictly for fully saturated but perfectly drained (the bulk modulus is drained) soils and also only for problems that does not go over the scope of elastic deformations. More sophisticated plastic or hypoplastic constitutive relations are described further in this chapter.

It is also important to point out that the equations for flow and deformation of the selected domain should not be solved separately as strong interaction between them exists. In mass balance equation for flow there is a coupling effect present in a storage term and in calculation of the total stress tensor is present also.

Two different approaches are today used for coupling the hydro-mechanical processes. At first it is the monolithical approach that implies identical space and time mashes for each coupled phenomenon. Secondly it is the staggered approach which solves the problems separately with different time and space mesh and even with different numerical codes and then couple them by information transfer at regular meeting point.

2.1.1. Monolithical approach for coupled processes

The monolithical approach in hydromechanical coupling presents a problem with time dimension as well as with mixing fields of different order.

Let us assume the typical geotechnical problem of deformation of soil mass and single fluid flow in pores. Such definition presents 4 degrees of freedom per node in 3D analysis (3 displacements and 1 pore pressure).

The first coupling term is from mass balance. It is the storage term saying that the change in storage is due to the volumetric change of the soil matrix

$$\frac{\partial S}{\partial t} = \frac{\partial \varepsilon_V}{\partial t} \; . \tag{2.9}$$

The second coupling term is the Terzaghi’s definition of total stress (Terzaghi, 1943).

$$\boldsymbol{\sigma} = \boldsymbol{\sigma}' + p_w . \mathbf{I} \, , \tag{2.10}$$

where $\mathbf{I}$ is the unity tensor and $\boldsymbol{\sigma}'$ is the effective stress tensor. Additionally the permeability change due to change in pore volume might be considered described by Kozeny-Carman model e.g. (Eq. 2.11) (Kozeny, 1927), (Carman, 1937), (Davies, 1980)

$$K = K_0 \cdot \left[n^3 / (1-n)^2\right] \cdot \left[(1-n)^2 / n_0^3\right] \qquad (2.11)$$

where n is the porosity of the material, n_0 is reference porosity and K_0 is the hydraulic conductivity at the reference porosity.

Using isoparametric second order finite elements and fully implicit scheme for this problem we obtain linear stress tensor rate field (for elastic material), but the pore pressure field is already quadratic. And so the second coupling term mixes linear and quadratic field. Although this problem can be overcome by using quadratic shape function for the geometry and linear shape function for the pore pressure, new problem arise with the number of spatial integration points.

2.1.2. Staggered approach for coupled processes

The staggered approach uses the advantage of solving the coupled problems as appropriate number of uncoupled problems leaving only the issue of information exchange between the uncoupled processes. This approach can combine the well-known models with good convergence and neglect the often conflicting requirements for time steps we face when using monilithical approach (soil mechanics often requires much shorter time steps in contrast with fluid flow or diffusion problems leading into convergence issues). The idea of staggered approach is clear from following figure.

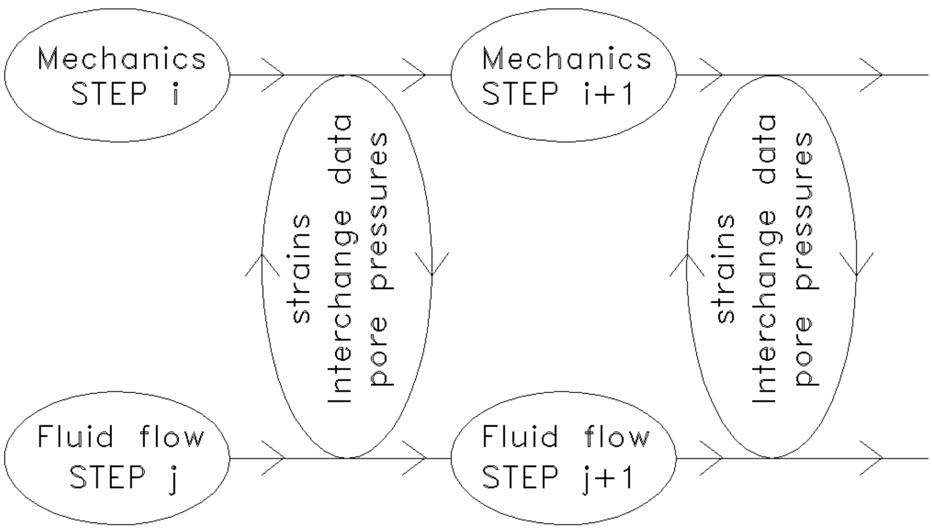

Fig. 1. Staggered approach - descriptive scheme

When the spatially different meshes are used for solution of the processes or even the finite different analysis and finite element analysis are employed, the transfer of the information requires an interpolation scheme. This is due to the fact, that in some meshes the information to be transferred are not available.

The accuracy of the approach is dependent on the frequency of information transfer, which is limited by the time step, and on the type of information exchanged. The stability and accuracy of the approach was proved by several authors eg. (Turska et al., 1993) and (Zienckiewicz et al., 1988).

2.2. Fundamental principles of unsaturated soil mechanics

Major difference between saturated and unsaturated soils is obviously the presence of additional non-wetting phase, usually the air. As in the case of classical soil mechanics, solving practical engineering problems require deep understanding of shear strength, seepage and volume change behaviour of the soil. However fundamental differences exist in the position of theory of consolidation which is shifted towards being used in qualitative way rather than provide clear answers about changes in total stress and corresponding volume changes. The boundary conditions for unsaturated soils are usually also different. Rather than change in total stress typical for saturated soils, change in flux is commonly applied in unsaturated soils problems.

To address the problems of unsaturated soils we must understand that for unsaturated soils the presence of negative pore-water pressures is the most typical characteristic and vice versa soil which have negative pore-water pressures should be described as in unsaturated state. The term "capillarity" was adopted during 1930's describing the observed phenomenon of vertical flux above or more precisely from stable groundwater table, however, the theoretical concept of soil suction itself was developed in the beginning of 20th century (Buckingham, 1907), (Richards, 1928). Further research in this area lead to the statement that strength of unsaturated soils is heavily influenced by the capillarity or stress state in the capillary water respectively (Hogentogler and Barber, 1941).

The definition of suction from thermodynamic context was presented in 1965 by Aitchinson (1965) but already before that the direct shear test were performed by Donald (1956) showing significant increase with increased matric suction. The attempts to develop an effective stress formulation for unsaturated soils similar to saturated concept were in the center of interest during second half of 20th century resulting in several so-called effective stress relations (Bishop, 1959 – see Eq. 2.18).

2.2.1. Physical foundations and measuring techniques

Assuming three phases system in which one phase can be denoted as wetting and one phase that is non-wetting then superficial tension acting between the phases can be generally called suction and defined as follows.

$$s = p_{nw} - p_w \quad \text{or often} \quad s = u_a - u_w \tag{2.12}$$

where p_{nw} is a pore pressure of the non-wetting phase (u_a for air pressure) and p_w is a pore pressure of the wetting phase (u_w for water). The suction is in general a product of chemical disequilibria as well as the capillarity effect. The part of the suction caused by capillarity effect is called matric suction.

For our purpose, i.e. soils influenced by groundwater, the non-wetting phase is an air and the wetting phase is water. The air value is considered to be equal 0 or atmospheric pressure respectively. The matric suction can be defined according to known Laplace's equation.

$$h_w = h_a - \frac{2T_s}{\rho_w . g . r_w} \quad \text{or} \quad s = -\frac{2T_s}{r_w} \tag{2.13}$$

where h_a is the atmospheric pressure, T_s is the superficial or surface tension, which is temperature dependent, ρ_w is the water density, g is the acceleration due to gravity and r_w is an average radius of the capillary menisci.

Due to the difficulties in measuring the menisci's radius, Kelvin (Thomson, 1871) derived the formula describing the relation between the pressure of a vapour above the menisci and the radius of the menisci already in 19th century.

$$\frac{R.T}{M.g} \ln \frac{p_{vs}}{p_{vs}^{\infty}} = -\frac{2T_s}{\rho_w . g . r_w} \tag{2.14}$$

where R is the ideal gas constant, T is the temperature, M is a molar weight of a water, p_{vs} is a pressure of a vapour above the menisci and p_{vs}^{∞} is a saturated vapour pressure.

The suction due to the osmotic effects was defined by van't Hoff as follows.

$$s = -RT\sum_i c_i \tag{2.15}$$

where R is the ideal gas constant, T is the temperature and c is a molar concentration.

Combination of equations (2.11) – (2.13) gives the formula for suction due to capillarity and osmotic pressure.

$$s = RT.\left(\frac{1}{M.g}\ln\frac{p_{vs}}{p_{vs}^{\infty}} - \sum_i c_i\right) \tag{2.16}$$

Measurements of the matric suction and its influence to the behaviour of the soil have been done by several authors in the past from different point of view e.g. (Tadepalli et al., 1992), (Kayadelen et al., 2007). Nearly all of them, however, are based on the axis translation procedure (ATP) which correctness with relation to field conditions was lately questioned (Baker and Frydman, 2009).

The problems with experimental evidence are associated with the values of suction which very often exceed 100 kPa (Krahn and Fredlund, 1972), which is the theoretical value for water cavitation, and so special arrangements and measuring techniques need to be introduced. ATP uses in its interpretation suction according to Eq. 2.10 and to avoid cavitation problems increases the air pore pressure.

It is generally accepted that negative pore-water potential could reach up to 1000 MPa at zero degree of saturation e.g. (Croney and Coleman, 1961), (Vanapalli and Fredlund, 1997). However, tensile strength of pure water obtained from hydrogen bonding on molecular level does not exceed 160 MPa (Speedy, 1982) and so the inconsistency is obvious. The idea of adsorption of water onto the mineral skeleton, which is certainly unaffected by increased air pressure and so explains the measured results (water potentials) from soil-water characteristics curves, was put forward by Baker and Frydman (2009) who also heavily criticize the existing models by stating that "*it is concluded that existing* *constitutive models for unsaturated soils, in their present format, are not consistent with the basic physical elements of the system.*".

2.2.2. Stress state variables

The stress state variables are usually defined as nonmaterial variables required for characterization of the stress conditions in particular point in time and space. From this definition it is clear that state variables must be independent of the characteristics or properties of the material. Constitutive models on the other hand provide relationship between different state variables, such as stress-strain relationship (Fung, 1965). Constitutive models therefore must incorporate physical properties of the material.

In case of unsaturated soils the net stress defined according to Eq. 2.15 is widely used stress state variable.

$$\overline{\sigma}_{ij} = \left(\sigma_{ij} - p_{nw}\delta_{ij}\right) \tag{2.17}$$

where $\overline{\sigma}_{ij}$ is the net stress, p_{nw} is a pore pressure of the non-wetting phase (u_a for air pressure) and δ_{ij} is Kronecker delta. The soil suction defined according to Eq. 2.12 is usually second stress state variable.

The formulation of effective stress which includes suction was presented by Bishop (1959) Eq. 2.18 and by Schrefler (1984) with the use of parameter S_R (degree of saturation) which represents the volume ratio between the phases Eq. 2.19.

$$\sigma_{ij}^{'} = \left(\sigma_{ij} - p_{nw}\delta_{ij}\right) + \chi\left(p_{nw}.\delta_{ij} - p_{w}.\delta_{ij}\right) \tag{2.18}$$

where parameter χ originally depends either on the suction or on the degree of saturation.

$$\sigma_{ij}^{'} = \left(\sigma_{ij} - p_{nw}\delta_{ij}\right) + S_R.s.\delta_{ij}\,, \tag{2.19}$$

which can be rewritten for $p_{nw} = 0$ as follows

$$\sigma_{ij}^{'} = \sigma_{ij} + S_R.s.\delta_{ij} \tag{2.20}$$

From the above described variables and combinations, three different approaches can be recognized when pursuing volume change behaviour.

a) net stress and suction (e.g. Fredlund and Rahardjo, 1993) – independent variables

b) effective stress (e.g. Nuth and Laloui, 2007)– combines both variables into one

c) SFG approach (Sheng et al., 2008b) – compromise approach

All of these approaches are used not only to describe volume change behaviour, but also when solving shear strength based problems as change of shear strength induced by change in the degree of saturation is often primary cause of landslides.

2.3. Numerical modelling – constitutive models

Barcelona Basic Model (Alonso et al., 1990) was the first elastoplastic model that takes into account wetting-collapse behaviour using the net stress. The description of the decomposition of strain variation used in the model follows.

$$\frac{\partial \varepsilon_{ij}}{\partial t} = \frac{\partial \varepsilon_{ij}^{\sigma}}{\partial t} + \frac{\partial \varepsilon_{ij}^{s}}{\partial t} \tag{2.21}$$

where strain variation induced by stress variations are denoted by σ exponent, while strain variation induced by the variation of suction are denoted by s exponent.

Further decomposition assumes the elastic (reversible) part, denoted by e exponent, and plastic (irreversible) part, denoted by p exponent, of the strain variation.

$$\frac{\partial \varepsilon^{\sigma}_{ij}}{\partial t} = \frac{\partial \varepsilon_{ij}^{e,\sigma}}{\partial t} + \frac{\partial \varepsilon_{ij}^{p,\sigma}}{\partial t} \tag{2.22}$$

Combination of equation 2.21 and 2.22 we get a variation of strain caused due to variation of suction.

$$\frac{\partial \varepsilon_{ij}^{s}}{\partial t} = \frac{\partial \varepsilon_{ij}^{e,s}}{\partial t} + \frac{\partial \varepsilon_{ij}^{p,s}}{\partial t} \tag{2.23}$$

The elastic part of the strain variation induced by variation of suction is only volumetric and so following formula can be written

$$\frac{\partial \varepsilon_{ij}^{e,s}}{\partial t} = K^{s} \cdot \frac{\partial s}{\partial t} . \delta_{ij} \qquad (2.24)$$

This relation can be a non-linear one as K^s (solid bulk modulus) generally depends on stress.

Nowadays, numerous constitutive models, designed to improve the pioneering Barcelona Basic Model, are capable to predict wetting induced collapse. However as can be observed in the following figure, room for improvement exists.

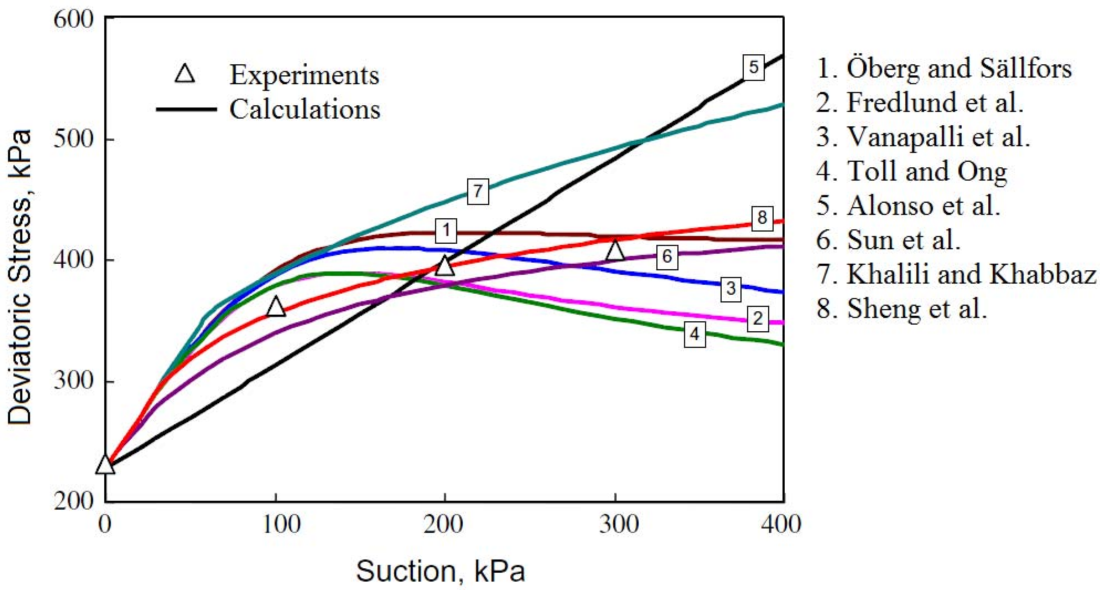

Fig. 2. Comparison of measured (Thu et al., 2007) and calculated (Sheng, 2011 – other authors are included) data for triaxial test on compacted kaolin clay under 200 kPa confining pressure

Further in this part constitutive models implemented in different codes and used for simulations of the proposed experiments are described but the comments regarding the simulations are in Chapter 6. Although the particle float codes from Itasca were also used for modelling of unsaturated soil (Liu and Li, 2008), it was decided to compare only continuum approach models.

2.3.1. Modified Cam-Clay constitutive model

Hereafter presented numerical model of coupled hydro-mechanical of soils was implemented into the SIFEL software package. The model follows Lewis and Schrefler's approach of coupled heat and moisture transfer while employing Darcy's and Fick's laws for moisture transfer, Fourier's law for heat transfer, standard mass and energy balance equations and modified concept of effective stress according to (Bittnar and Sejnoha, 1996), i.e. one stress variable as shown in following equation

$$(1-n)\sigma_{ij}^{s} = (1-n)S_w\sigma_{ij}^{w} + (1-n)S_g\sigma_{ij}^{g} + \sigma_{ij}^{ef} \tag{2.25}$$

where σ_{ij}^{s} is the stress in grains, σ_{ij}^{w} is the stress in liquid phase (water), σ_{ij}^{g} is the stress in gas, σ_{ij}^{ef} is the effective stress, nS_w is a volume fraction of water and nS_g is a volume fraction of gas. In order to describe the deformation of a porous skeleton or actually the rearrangement of grains standard constitutive equation is written in the rate form.

$$\dot{\sigma}_{ij}^{ef} = D_{sk}\left(\dot{\varepsilon} - \dot{\varepsilon}_0\right) \tag{2.26}$$

where D_{sk} is a tangential matrix of porous skeleton while, $\dot{\varepsilon}$ represents the strain rate while $\dot{\varepsilon}_0$ represents strains indirectly associated with stress changes, such as shrinkage and swelling, creep, etc. and also involves the strain of the bulk material due to pore pressure changes. Combining Eq 2.25 and 2.26 while assuming negligible shear stress in fluid we obtain

$$\dot{\sigma}_{ij} = D_{sk}\dot{\varepsilon} - \alpha\delta_{ij}\left(\dot{s}\right) \tag{2.27}$$

where α represents the Biot's constant and suction s is defined in agreement with volume fractions as follows

$$s = S_w p^w + S_g p^g \tag{2.28}$$

The constitutive model reflects a non-linear behaviour observed in isotropic compression tests. The results are usually presented in semi-logarithmic scale as shown in the following figure.

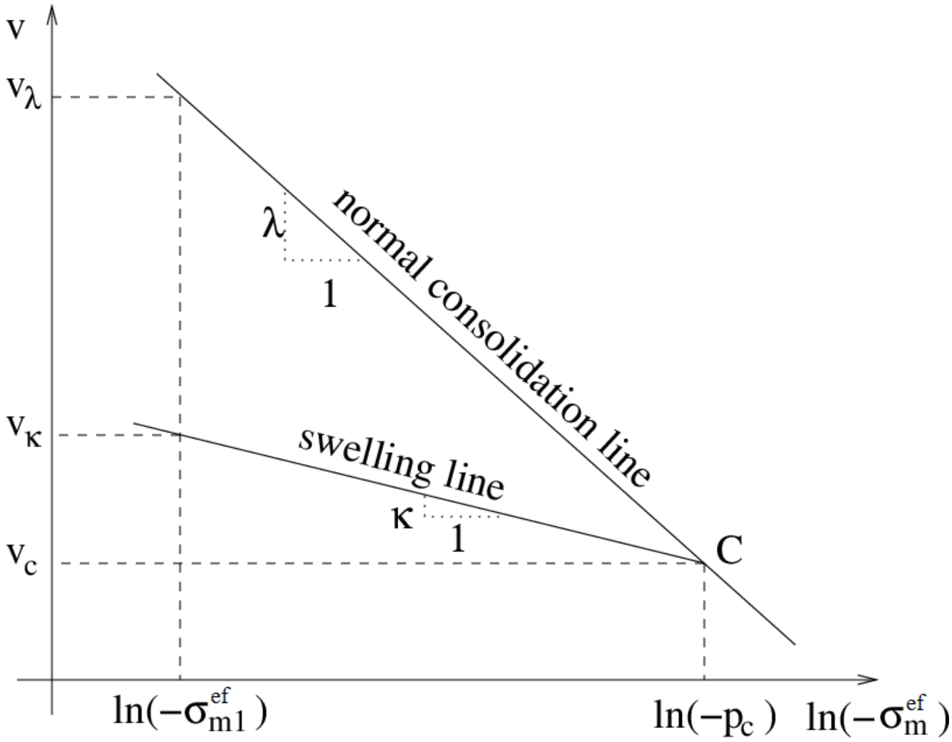

Fig. 3. Normal consolidation and swelling line describing the behaviour of soil during isotropic compression test

The used yield function and yield condition is described in Eq. 2.29 while the visualization of yield surface in mean-deviatoric stress plane is shown in the following figure.

$$f\left(\sigma_{ij}^{ef}\right) = q^2 + M^2 \sigma_m^{ef}\left(\sigma_m^{ef} - p_c\right) = 0 \tag{2.29}$$

where p_c represents the pre-consolidation pressure or hardening parameter respectively which in fact determines the diameter of the yield surface ellipsoid along the σ_m^{ef} (mean effective stress) axis. M is the material parameter related to the friction angle which determines the slope of critical state line and consequently the radius in the deviatoric plane. It is assumed to be $M = 6.\sin\varphi/(3-\sin\varphi)$ for triaxial compression test and $M = 6.\sin\varphi/(3+\sin\varphi)$ for triaxial extension test.

Although implementation of the Cam Clay model was also prepared in the SIFEL package, it was not so far successfully used for simulation of the wetting experiments described in the chapter 4 and therefore the detail description is not provided.

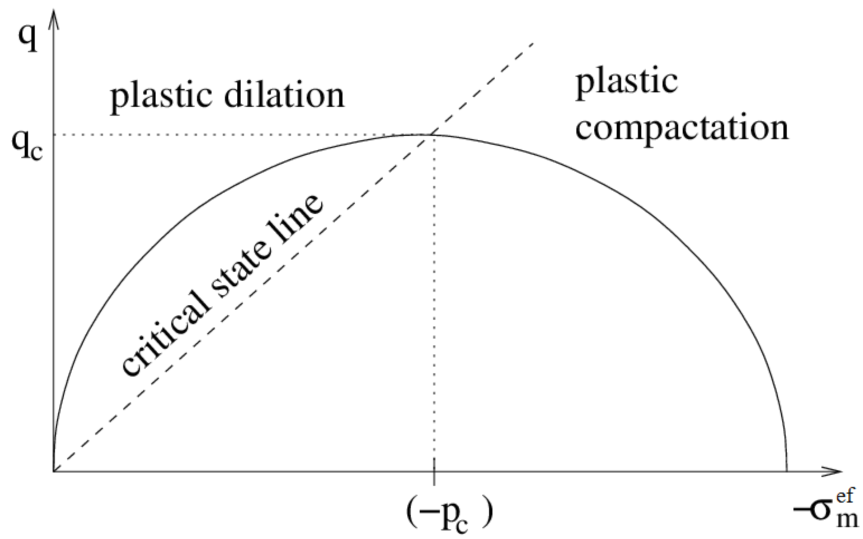

Fig. 4. Yield surface of the Cam-Clay model in the mean-deviatoric stress plane

Apart from unit weight and Poisson's ratio, the model requires 5 additional parameters described in the following table.

Tab. 1. Parameters required by used Modified Cam Clay model

Parameter	Interpretation
λ	slope of the normal consolidation line
κ	slope of the swelling line
e_0	initial void ratio
OCR	overconsolidation ratio
M	slope of the critical state line*

* M can be calculated using φ_c (critical state friction angle)

2.3.2. Hypoplasticity for clays

Hereafter presented model developed by Masin (2005) is based on combination of classical critical state models and generalized hypoplasticity principles and was successfully implemented into GEO 5 FEM version 16 software package (from April 2013 available at http://www.fine.cz/) and used for simulation of unsaturated silt loams with steady no-flow boundary condition. The adjustments required for the model to be used for simulations of typical unsaturated problem are described in the next part of this chapter.

The non-linear behaviour of the clay is in this model governed by generalized hypoplasticity while as limit stress criteria was selected Matsuoka–Nakai failure surface. The normal compression line for isotropic compression is similar to the NCL from Modified Cam Clay model. The intergranular strain concept was not involved within carried out calculations. In most basic form, the model requires five following material parameters.

Tab. 2. Parameters required by used Hypoplastic model for clays

Parameter	Interpretation
N	position of the normal consolidation line for isotropic compression in the *ln (1+e)* vs. *ln p* plane
λ^*	slope of the normal consolidation line for isotropic compression in the *ln (1+e)* vs. *ln p* plane
κ^*	slope of the unloading line for isotropic compression in the *ln (1+e)* vs. *ln p* plane
φ_c	critical state friction angle
r	parameter controlling shear stiffness

The meaning of the parameters and their analogy with modified cam clay parameter is clear from Fig. 5. and calibration procedure is in detail described in Masin (2010).

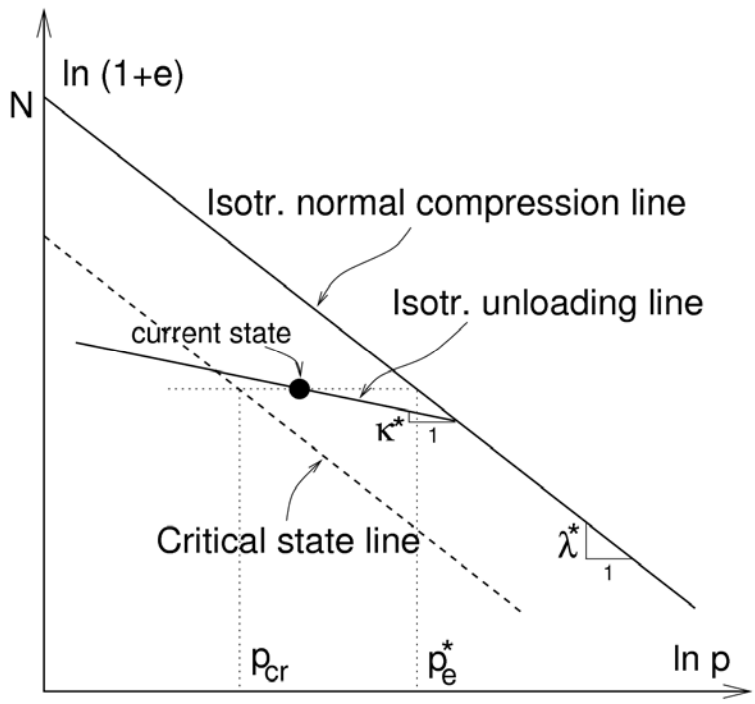

Fig. 5. Definition of parameters N; λ^* and κ^* (Masin, 2005)

In the figure above quantity p_{cr} is defined as the mean stress at the critical state line at the current void ratio and p_e^* is the equivalent pressure at the isotropic normal compression line.

2.3.3. Hypoplasticity for unsaturated soils

Hypoplastic model for unsaturated soils presented by Masin and Khalili (2008) combines principle of effective stress, represented here by "equivalent pore pressure" see Eq. 2.30 and theory of hypoplasticity.

$$u^* = \chi u_w + (1-\chi)u_a \tag{2.30}$$

where χ is defined empirically with help of material parameter s_e (air entry value – separates unsaturated and saturated state of the soil) as follows

$$\chi = \begin{cases} 1 & for\ s \le s_e \\ \left(\dfrac{s_e}{s}\right)^{0,55} & for\ s > s_e \end{cases} \tag{2.31}$$

The model attributes two effects on the soil behaviour to the suction. At first it is the above described influence on the effective stress and second it is the increased inhibition capacity of grain slippage represented by change in size of state boundary surface and bounding system. This can be done even though the mathematical formulation of hypoplastic models does not include either explicit state boundary surface or bounding surface. More details regarding this matter can be found in Masin (2005).

Apart from five parameters necessary for the hypoplastic model, four additional parameters are required to describe the unsaturated behaviour or more precisely two parameters (n and l) to describe the dependence of N and λ^* on suction – see Eq. 2.32 and 2.33, one parameter (m) which controls the structure collapse along the wetting path and one (s_e) to prescribe the air entry or air expulsion value which serves to quantify the unsaturated state.

$$N(s) = N + n\ln\left(\frac{s}{s_e}\right) \tag{2.32}$$

$$\lambda^*(s) = \lambda^* + l \ln\left(\frac{s}{s_e}\right) \tag{2.33}$$

Although eight of total nine parameters are identifiable from laboratory experiments, parameter m must be calibrated by means of parametric study of wetting experiments on overconsolidated soils only after all other parameters are known. Moreover for calibration of s_e is important which type of problem, drying or wetting, is solved as the air entry value (wetting process) and air expulsion value (drying process) differ significantly.

Tab. 3. Parameters required by used hypoplastic model for unsaturated soils

Parameter	Interpretation
m	controls the structure collapse along the wetting path
n	represents dependence of N on suction
l	represents dependence of λ^* on suction
s_e	air entry or expulsion value
N	position of the normal consolidation line for isotropic compression in the *ln (1+e)* vs. *ln p* plane
λ^*	slope of the normal consolidation line for isotropic compression in the *ln (1+e)* vs. *ln p* plane
κ^*	slope of the unloading line for isotropic compression in the *ln (1+e)* vs. *ln p* plane
φ_c	critical state friction angle
r	parameter controlling shear stiffness

(Last five parameters are identical with parameters used by hypoplastic model for clay.)

Chapter 3

INTERNAL EROSION

The erosion of particles due to seepage of fluid phase is responsible for changes of the soil behaviour and subsequently raises many issues in different areas of geotechnical engineering. The internal erosion usually takes place only in fully saturated soils, but the state prior to application of the water under high hydraulic gradient can make significant difference. This is a typical problem for unsaturated levees during initial phase of flood events.

Design recommendations for hydraulic structures are dealing with the term critical gradient. The definition of the critical gradient describes it as a hydraulic gradient that causes internal erosion and loss of particle. Empirical values of critical gradients for different soils are presented in the literature (Bligh, 1910), (Lane, 1935), (Kenney and Lau, 1985) and (Sherard et al., 1984) and the design of the foundation structure should ensure that the actual hydraulic gradients do not exceed the critical values during the effective service life of the construction. The influence of the internal erosion to the stability and deformations of the river structure can be perfectly shown on the recently collapsed spillway structure in Slovak Republic.

Problems with internal erosion are enlarged by difficulties in detecting the initializing phase. Monitoring equipment presents additional significant increase in both investments and operation costs even when used in sparsely. When the erosion is already progressing through the subsoil or dam the time window for successful intervention is very limited.

The scope of this work is strictly limited to hydro-mechanical behaviour and particularly to backward erosion and suffusion. Significant portion of the internal erosion process, however, take place on dispersive soils

The aim of this chapter is to briefly review general approaches regarding modelling of the internal erosion assuming continuum models and validity of averaging principles. Particle float codes from Itasca, e.g. of applications (Lohani et al., 2008), (de Pater and

Dong, 2007) or (Achmus and Abdel-Rahman, 2003), were found far too demanding with respect to the computational power and also their use does not correspond with the selected methodological approach to the studied problems.

3.1. Loss or detachment of particles

The problem of pumping well installed in the urban area is described from the point of view of eroded particles and subsequent settlement of nearby buildings by Cividini (Cividini et al., 2009). At first the erosion law based on experimental results is presented in terms of nondimensional densities. $\rho_f\,(t)$ stands for the ratio of weight of fine fraction within the sample to initial dry weight of the sample. $\rho_{er}\,(t)$ stands for the ratio of weight of eroded material to initial dry weight of the sample. Both densities are function of time and are related by following equation:

$$\rho_f(t) = \rho_{f0} - \rho_{er}(t) \tag{3.1}$$

where ρ_{f0} represent the initial value of nondimensional density ρ_f. At this point it is necessary to stress the main assumption of this model. It is assumed that only the fine fraction of the soil sample is eroded. Although this might be true for small gradients acting very long time, it cannot be universal assumption for all internal erosion processes as shown in the relevant part of chapter 4. The entire erosion law is then stated as

$$\frac{\partial \rho_f(\rho_{f0}, i, t)}{\partial t} = d\,\sqrt{i}\,\left[\rho_f(\rho_{f0}, i, t) - \rho_{f\infty}(\rho_{f0}, i)\right] \tag{3.2}$$

where i is a hydraulic gradient, d is a model parameter and $\rho_{f\infty}$ is the density reached in long term defined from measured results as

$$\rho_{f\infty}(\rho_{f0}, i) = \rho_{f0}\,\left[(1 - c_\infty)\exp\left(-a\,i^b\right) + c_\infty\right] \tag{3.3}$$

where a, b and c_∞ are parameters from back analysis of the experiments.

The decrease of total volume of soil, which governs the settlement, is divided into the decrease of the volume of solids due to the erosion and the variation of the volume of voids. The variation of the nondimensional density of fine particles is directly related with the variation of the volume of solids through the unit weight of grains γ_g and the initial unit weight of dry soil γ_0.

$$(\varepsilon_{vol})_{solid} = \Delta\rho_f \frac{\gamma_0}{\gamma_g} \tag{3.4}$$

Neglecting the case in which no overall volume change occurs, the volume deformation caused by the erosion process can be described as

$$\Delta\rho_f \frac{\gamma_0}{\gamma_g} \le \varepsilon_{vol} \le \Delta\rho_f \tag{3.5}$$

Another engineering problem that deals with internal erosion is a sand production in oil industry. Following model was proposed by Vardoulakis (Vardoulakis and Sulem, 1995). The model assumes that the erosion can only take place in fully saturated soils. Under such conditions the porosity equals moisture content as all pores are assumed to be full of fluid phase. Further, the model assumes three phases, i.e. solid, fluid and fluidized particles. The concentration of fluidized particles is defined as

$$c = \frac{dV_{fs}}{dV_{ff} + dV_{fs}} \tag{3.6}$$

where V_{ff} is the volume of fluid and V_{fs} is the volume of fluidized solids. The mass balance for the fluid phase in case of incompressible fluid is expressed as

$$\frac{\partial}{\partial t}((1-c)n) + \frac{\partial}{\partial x_i}(n(1-c)v_i) = 0 \tag{3.7}$$

where v_i is a fluid velocity and $v_i.n = q_i$. For incompressible particles of the solid phase the mass balance can be expressed as

$$-\frac{\partial}{\partial t}\left(\left(1-c\right)n\right)+\frac{\partial}{\partial x_i}\left(ncv_{is}\right)=0 \tag{3.8}$$

where v_{is} is the velocity of fluidized particles. The porosity diffusion model (Papamichos and Vardoulakis, 2005) assumes that the concentration of the fluidized particles is small and the particles are small enough to have the velocity equals to velocity of the fluid. These assumptions yields the equations stating that all porosity changes in the volume of soil are due to the net transport of grains outside this volume.

$$\frac{\partial n}{\partial t}=\frac{\partial q_{is}}{\partial x_i} \tag{3.9}$$

Where the net transport of grains is defined as $q_{is} = cnv_{is}$, while assuming small concentration of fluidized particles. Regarding the internal erosion it is necessary to mention Einstein-Sakthivadivel erosion model (Einstein, 1937), (Sakthivadivel and Irmay, 1966), which is the base that many other models use. In this model the rate of eroded mass is driven by the discharge of the transported solids.

$$\frac{\partial m}{\partial t}=\Lambda\,\rho_s\,\left(1-\theta\right)c\theta\,v_{is} \tag{3.10}$$

where Λ is the empirical erosion constant.

3.2. Preferential flow vs. average flow

It is necessary to point out that all the approaches listed above are based on standard averaging principles (Lewis and Schrefler, 2000). Such approach is valid for manmade geotechnical structures, such as earth dams, and for natural subsoil, when homogeneity is confirmed by detailed geophysical survey, during the initial phase of internal erosion with reasonably small hydraulic gradients. According to our experiments that are described below, the soil creates small caverns when subjected to high hydraulic gradient. The change in the overall porosity during this process is very small but the flow inside the caverns cannot be simulated as flux through porous materials especially when it comes to interconnection of the caverns and creation of the preferential flow paths. Such type of flow is closer to flux through fractured rock with very high matric flux rather than Darcy's flux. One possibility of modelling such combined flux is to use 2D elements for flow through the "matric" and 1D channel element for assumed flow paths. Further evaluation of this approach is still under consideration. Stochastic models using random spatial fields with high correlation for adjacent elements could prove to be potentially very successful (Duchan, 2012).

Chapter 4

EXPERIMENTAL ANALYSIS

In order to study the processes influencing the behaviour of the soil when groundwater is present, several experiments have been designed. For this purpose we divide the processes into two categories. The final affection of the soil behaviour could certainly be a combination of all acting processes from both categories.

First category involves all changes in the pore pressure, including pore pressure change in saturated soils. However, a unique position belongs to the process of suction cancellation in unsaturated soils. Although this process is not of the same importance for sandy soils as for clays, in this chapter we show that it still has an indispensable influence on the soil behaviour even for coarse grained soils. More experimental results are then available in Appendix B for poorly graded gravel, in Appendix C for silt loam and in Appendix D for undisturbed samples of sands.

The second category covers all possible ways of losing particles. As in the case of first category one process has special position. It is the piping process sometimes called wash out process. Obtained results on undisturbed samples are in general commented in this chapter together with the principles of the experiment while all measured values are summarized in Appendix E.

Requirements for all of the proposed experiments are simplicity; repeatability; transparency of results and their interpretation and boundary conditions being close to in-situ boundary conditions, with the exception of small scale experiments with undisturbed samples. Aims of the experiments coincide with goals of the thesis and follow the proposed path, i.e. observation of the phenomena and quantification of the impact on selected soils while leaving general recommendation for more extensive experimental research, which would provide results for all soil classes. Tested soils were also subjected to standard tests, such as hydraulic conductivity test, Proctor Standard test, etc. to gain more information about the tested soils. Grain distributions of all the tested soils were also obtained together with grain distribution of washed out particles in case of high gradient internal erosion experiments. The density of the large soil samples was calculated from the known total weight before the compaction and volume after compaction. It was measured after all experiments were carried out with the help of rubber balloon density meter.

The full scale experiments were carried out on soil samples built in the laboratory from excavated soils. The soil was inserted into the model stand by layers 200 mm thick. First layer was placed on nonwoven geotextile (200 g/m^2) protecting the outlets from pipelines. Each layer was compacted by vibrating plate. The time over which was the vibrating plate acting on each layer was estimated by compacting experiment carried out in advance. The soil contained natural amount of moisture as it was kept in plastic covers after being removed from the site. The time of storage was kept as short as possible. The moisture content was monitored in selected intervals during the time of storage.

All small scale experiments, on the other hand, are carried out on undisrupted specimens taken from the selected sites. The soil samples were obtained by pushing the standard hollow steel cylinder into the soil in selected depth. The surrounding soil had to be excavated to allow the cylinder to be removed without disrupting the sample. The cylinder has inner diameter equal to 0.120m and height equal to 0.100m.

4.1. Tested soils

1) Poorly graded gravel - compacted large sample

The soil specimens were classified according to CSN 731001 as G2 – GP, i.e. poorly graded gravel and as saGr with medium content of cobbles according to EN ISO 14688. Fig. 6 shows the grain distribution of the soil sample. It is important however, that the portion of particles larger than 63 mm was 17.3% of the weight. The optimal moisture content and maximal dry soil density was evaluated using standard Proctor test and the compacting experiment prescribed 25 minutes duration of compaction with vibrating plate for each layer.

The soil was obtained from deep excavation in the central area of the Prague city. This soil class is typical for one layer of the Prague area, which can be divided into 5 nearly horizontal layers - terraces. In this part of the city the soil is experiencing large groundwater movement especially due to engineering activity linked with lowering water table for foundation works.

Tab. 4. Characteristics of tested soil

Characteristic	Value
Optimal water content from PS (%)	11
Original water content (%)	4
Maximum dry density PS (kg/m^3)	1950
Measured dry density (kg/m^3)	2217

This soil has also proved its predisposition for internal erosion and collapse when exposed to high hydraulic gradient or flow pressure. Several road and building accidents were reported regarding this matter.

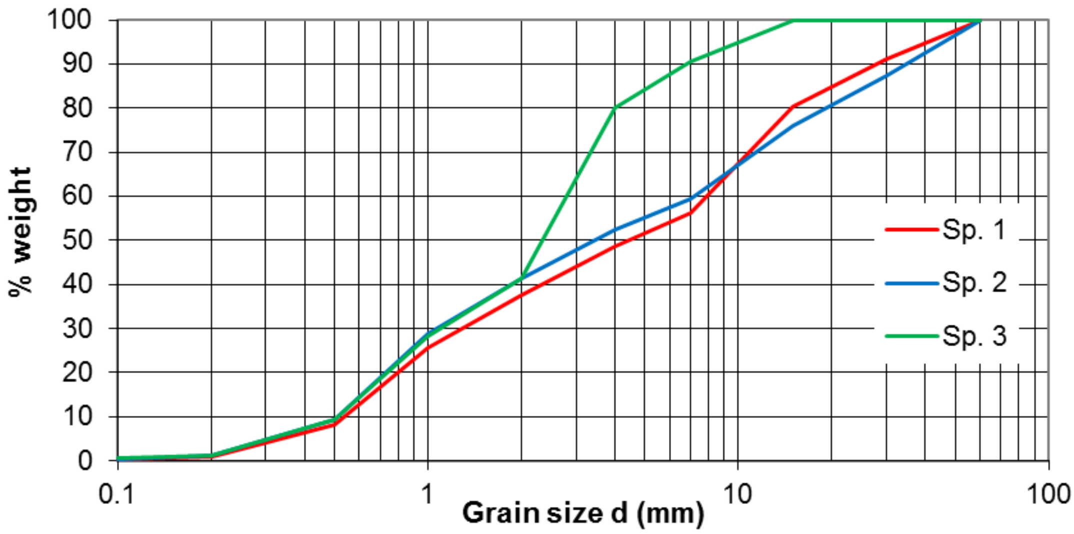

Fig. 6. Grain distribution of poorly graded gravel (three specimens)

2) Silt loam - compacted large sample

The soil specimens were barely classified as F5 – F, i.e. silt loam according to CSN 731001 or saSi according to to EN ISO 14688. Grain distribution of the soil samples is shown in Fig. 7 from which is also clear that the portion of fine particles is very close to F3 - FS class. The optimal moisture content and maximal dry soil density were evaluated using standard Proctor test.

This particular soil was obtained from excavation in the Prague city district near Prague Castle (Kings Park) and built in the model with natural moisture content being close to 7%. Compacting experiment prescribed 19 minutes duration of compaction with vibrating plate for each 200 mm thick layer while achieving soil density approximately 1550 kgm^{-3}. Without consolidation, although compaction also helps, this soil is considered highly collapsible and moisture sensitive with high volumetric deformations due to swelling and shrinkage.

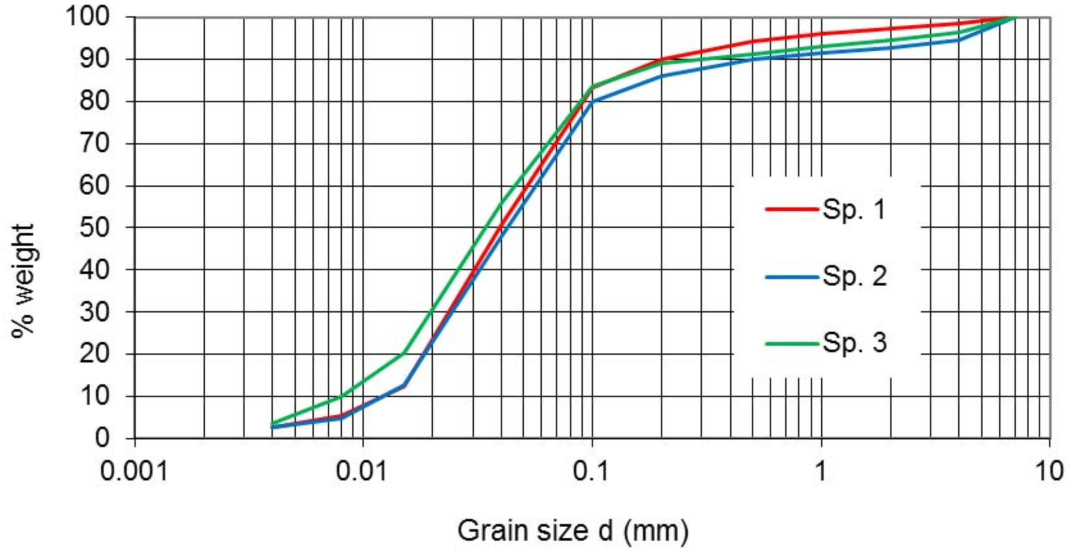

Fig. 7. Grain distribution of silt loam (three specimens)

3) Small samples – sand; silty sand; sandy silt

All of the small soil specimens were obtained from the Veseli nad Luznici town which suffered severe losses during 2002 and 2006 floods. The samples were taken from several different sites after approximately 1.0 m of topsoil was removed, i.e. the depth from which the samples were collected corresponds with the most common depth of foundation base of houses in this town. The sites were particularly selected to as be as close to the earlier demolished buildings as possible without the subsoil being influenced by the former structure. All the samples were classified according to Czech Standard (CSN 73 1001) and the EN ISO 14688. Number of samples of different classes is clear from following table.

Tab. 5. Classification of small scale specimens

Class	Symbol CSN 73 1001	Symbol EN ISO 14688	Number of samples
Poorly graded sand	SP	Sa	10
Silty sand	SM	siSa	8
Sandy silt	MS	saSi	5

The grain distributions of original specimens were back analysed after the experiments from the grain distributions of eroded and remained soils. Examples of grain distributions are shown in the following figures.

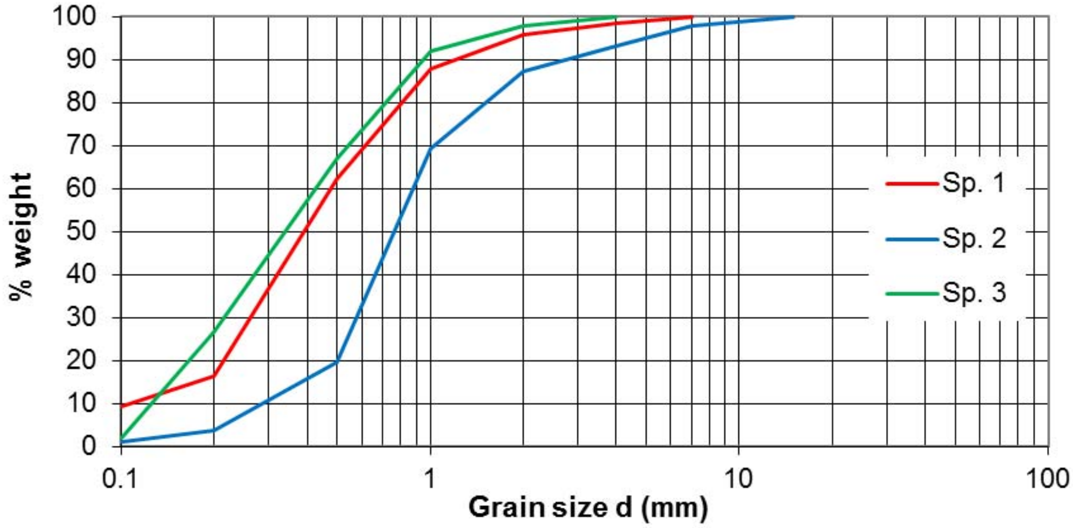

Fig. 8. Grain distribution of poorly graded sand (three specimens)

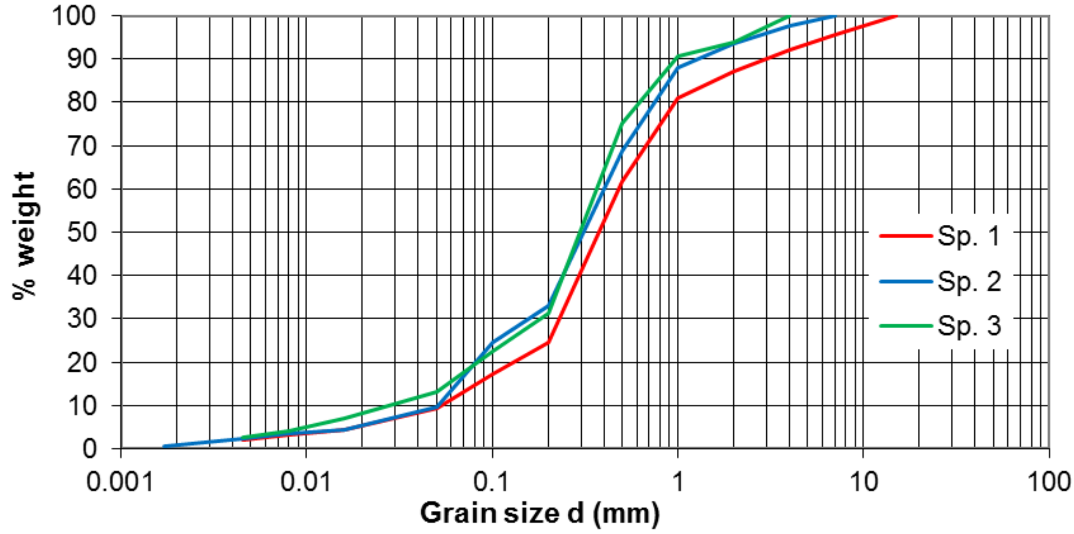

Fig. 9. Grain distribution of silty sand (three specimens)

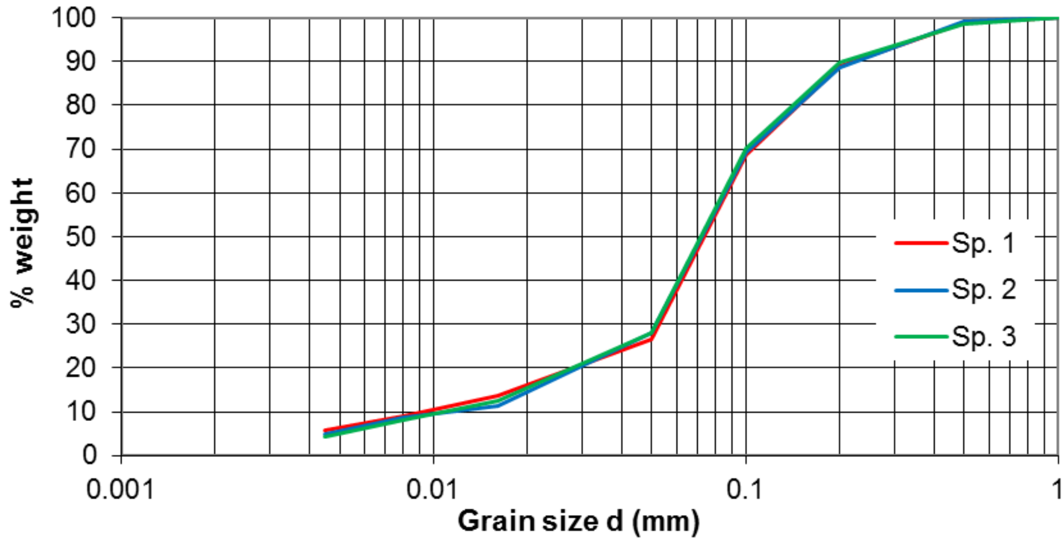

Fig. 10. Grain distribution of sandy silt (three specimens)

4.2. Static plate load test – full scale

Governing idea of this test is to provide experimental results easily comparable with in-situ measured values. With similar loading / unloading behaviour measured on unsaturated soils in-situ and in laboratory appropriate analogy could be used to predict the effect of wetting, suction cancellation or groundwater table variations. Obtained results can also be used for calibration and confirmation of numerical models as shown in relevant parts of this thesis.

The stand for tested soil sample is a massive reinforced concrete box without the top covering part. The bottom part contains a system of pipes 12.5 mm in diameter and is connected to the large water storage tank. The side walls are 200 mm thick and the box is constricted by steel beams in two levels. A steel frame is attached to the box to take the reaction force and additional small frame presents an inertial body to which the deformations are measured. The internal dimensions of the box are 1.0 x 1.0 x 1.0 m. The stand was designed and constructed strictly for this purpose while taking into account the effect of vibrations during the soil sample compaction as well as the impact of the load and water. Although the stand served well with respect to the needs of this thesis, adjustments recommended regarding the water tightness and pore pressure measurements are presented at the end of this chapter.

Load is applied through a hydraulic jack to the steel plate 20 mm thick and 300 mm in diameter ($70.685.10^3$ mm^2 surface area). As the maximum safe load for the reaction frame was 80 kN, the plate is assumed rigid within the load interval for analytical and numerical purpose. The applied load is measured in the hydraulic system, which means oil pressure in the system is measured by calibrated manometer and is converted to force induced by the piston, and once more in the pressure cell bellow the reaction frame. The pressure cell was removed after several experiments as the differences between measured forces were negligible when considering the accuracy of the pressure probe equal 5 kN, see Fig. 13. Fig. 11 shows the scheme of the experiment, while Fig. 12 shows the completely built model ready for lunching the very first experiment.

Settlement was measured by two dial gauges installed on the plate with guaranteed accuracy 0.01 mm.

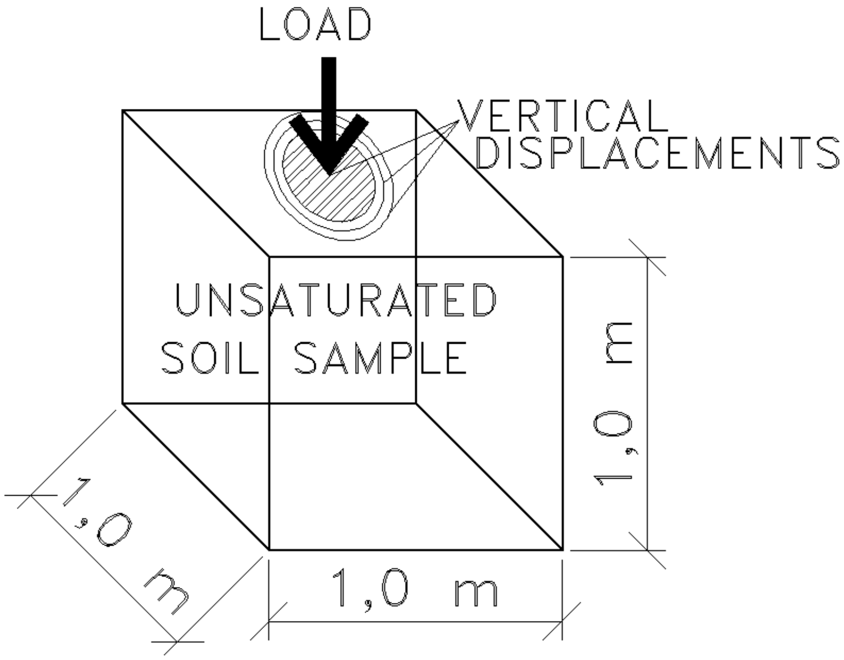

Fig. 11. Static plate load experiment – scheme

Fig. 12. Full scale plate load test on the soil specimen

The experiment involves several loading and unloading cycles on the sample with natural moisture content or better with moisture content measured during compaction.

After several „dry“ loading cycles, the specimen was subjected to wetting from the bottom as described further. During the experimental period, after first results were discussed, the need for lateral pressure on the vertical wall of the stand and also the shear zone evolution measurement emerged. The stand was therefore improved with added lateral pressure probe and two more settlement sensor with guaranteed accuracy 0.01 mm installed 50 mm, and 100 mm, from the edge of the plate, respectively. In the part 4.3. Fig. 24 shows scheme of the improved experiment setup while Fig. 25 presents the overall picture of the experiment and Fig. 26 detailed view on the plate with measuring devices.

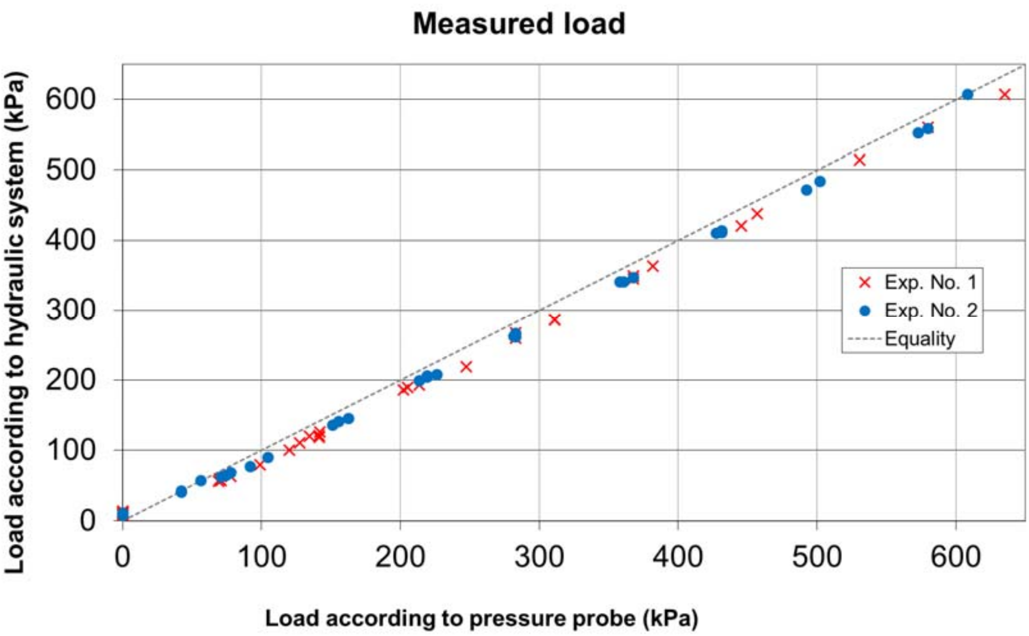

Fig. 13. Full scale plate load test on the soil specimen

It is easy to gain an impression that the proposed static plate load experiment represents merely enlarged oedometer. It is therefore important to stress that it is not the case. Distances to the rigid boundaries, either to the sides or to the bottom, are large enough to prevent the boundary condition from significantly influencing the response of the specimen. Part 4.11 of the EN 1997-2 (Eurocode 7), which focuses on plate load tests, requires the rigid bottom boundary condition to be distant minimum 2 times the diameter of the plate. So from the point of view boundary condition the experiment is designed in agreement with standing standards. Size or depth of an influence zone is discussed in chapter 5 and 6.

The Czech standard CSN 72 1006 focused on testing of soil compaction requires in the Appendix A, which describes the plate load test for roads and pavements and is considered as a Principle (EC7 definition), requires the every loading step to be no shorter than 120 seconds. The Appendixes B and E of the same standard, which are also focused on plate load tests for railway embankments and other constructions respectively, however, require each loading step to be measured when the settlement within last three minutes is smaller than 0.05 mm. The proposed experiments either on dry or wet soil respect both of these requirements

4.2.1. Selected commented results for G2 specimens

Three facts can be nicely observed in the Fig. 14., which shows results from first experiment on G2 specimen. First it is the unloading/reloading path that has different slope than primary loading path. This phenomenon of structural strength vs. void ratio which was described in the past (Terzaghi et al. 1996) was could be observed in all load-displacement curves from all experiments.

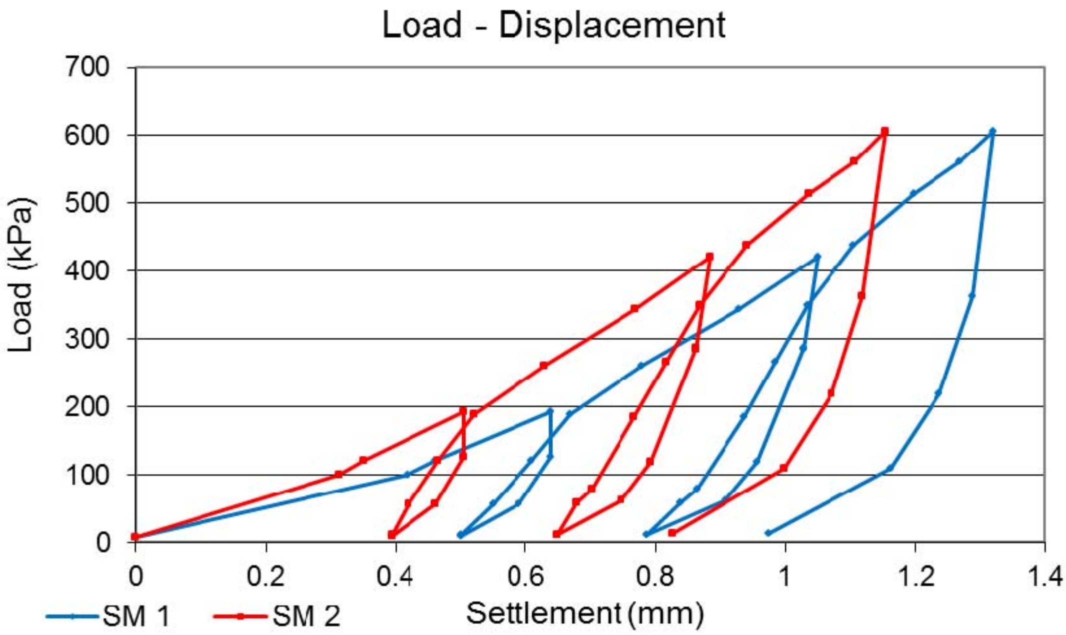

Fig. 14. Results from first experiment on dry but compacted (dense) G2-GP specimen (SM1 and SM2 stands for dial gauge no. one and two)

Second fact to be observed is the characteristic loop in the unloading/reloading path. As the elastic hysteresis is generally load rate dependant it is quite interesting observation when the load steps were no shorter than 5 minutes each. Hysteretic unloading/reloading behaviour can also be found in the literature even for isotropic compression e.g. (Matyas and Radhakrisna, 1968) or (Fredlund and Rahardjo, 1993).

Third important fact observed is small hardening of the material which can hardly be attributed to the rigid boundary condition on the bottom of the layer. This type of behaviour is rather soil type related but at first it was attributed to delayed shear zone activation. Once was the displacement of the top of the shear zone obtained, see Fig. 15, showing immediate response to the applied loading, the above mentioned assumption was abandoned.

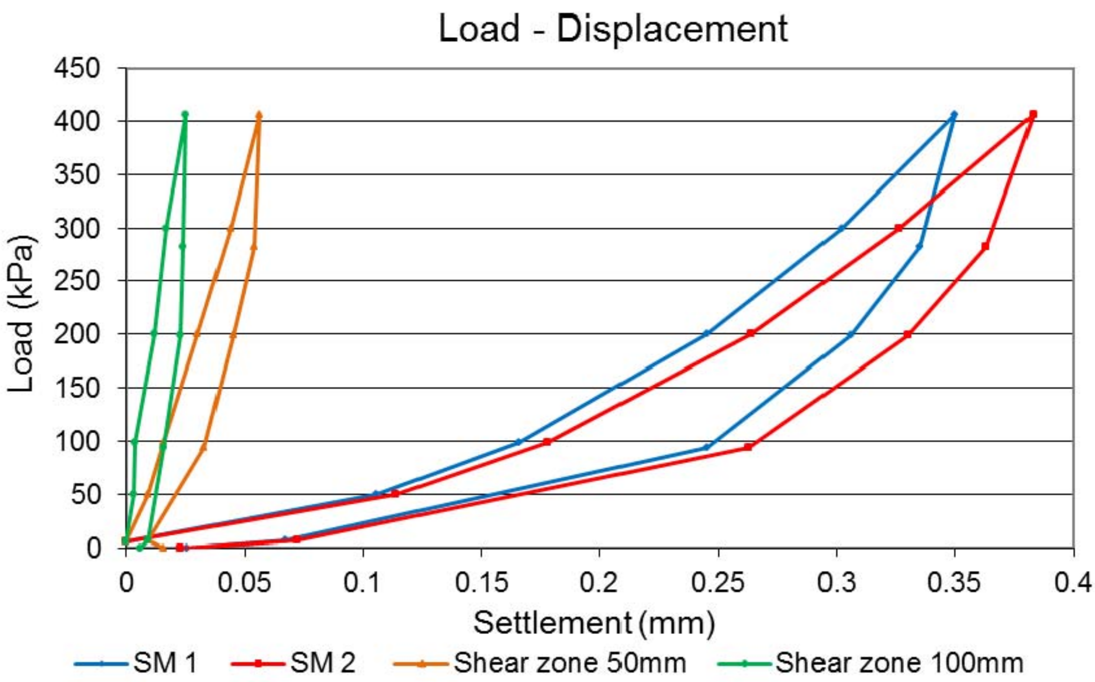

Fig. 15. Results from experiment on dry but compacted (dense) G2-GP specimen with shear zone displacement (immediate response can be observed; SM1 and SM2 stands for dial gauge no. one and two)

The second test proved creep behaviour of the soil even without the presence of water. Creep was observed in sandy soils in the past (Hsiung, 2008). The important aspects are the magnitude of the creep and the duration. The whole creep behaviour last approximately 1 hour but more than 80% of the creep deformation was reached after first 15 minutes, see Fig. 17.

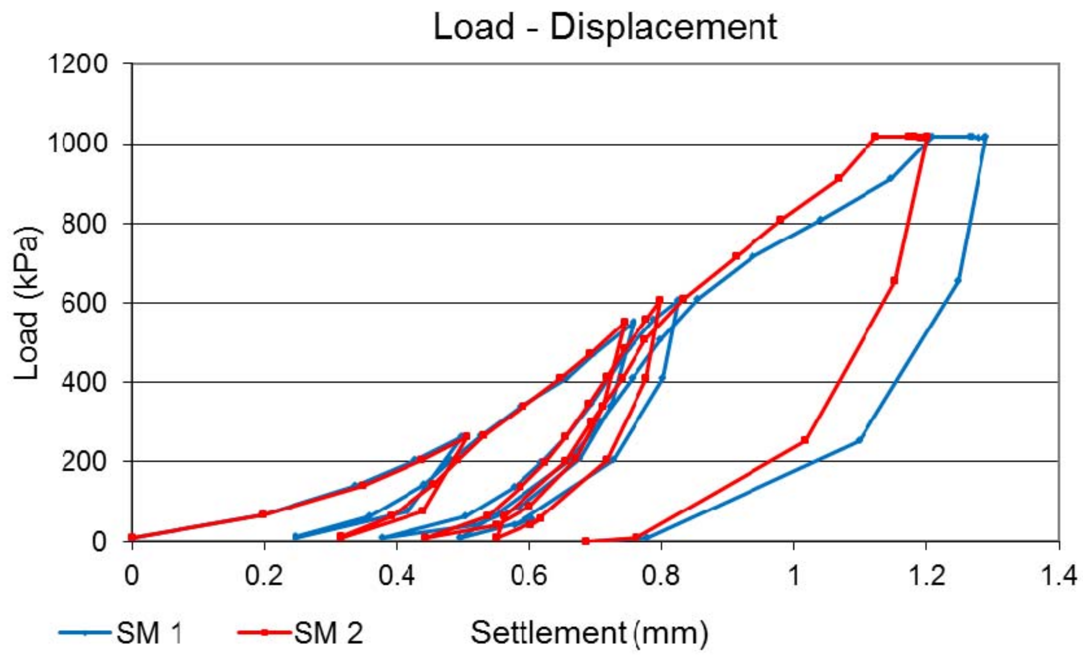

Fig. 16. Results from experiment on dry but compacted (dense) G2-GP specimen with creep behaviour at 1015 kPa (SM1 and SM2 stands for dial gauge no. one and two)

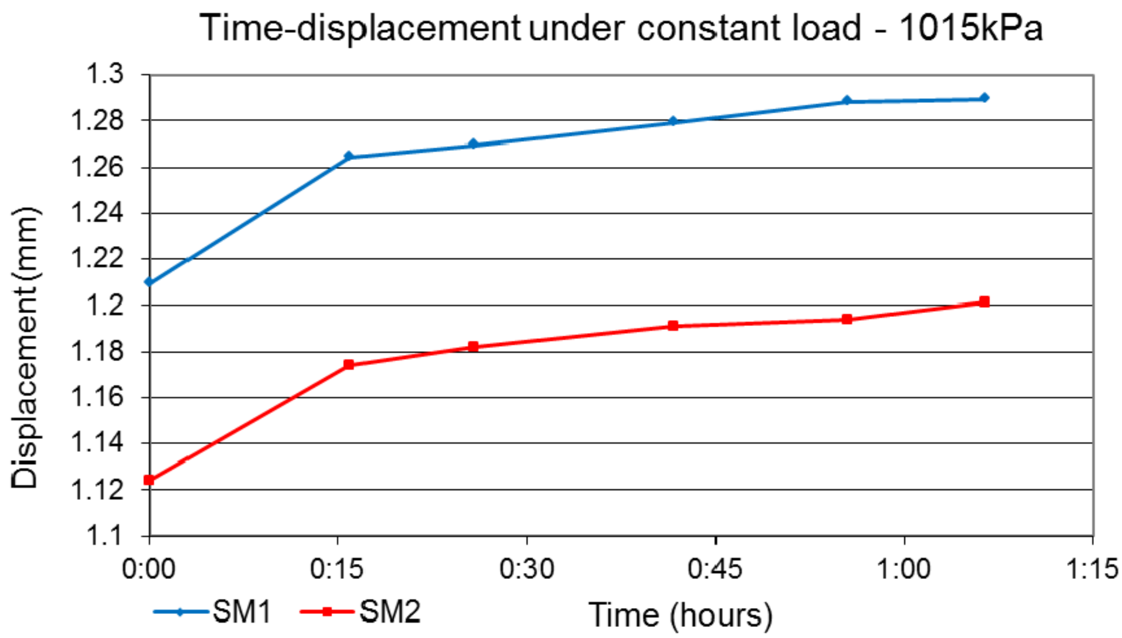

Fig. 17. Creep behaviour at 1015 kPa for G2 specimen (SM1 and SM2 stands for dial gauge no. one and two)

Small consolidation/compaction observed in Figs. 18 and 19 is a result of cyclic dry loading, which in fact represents compaction, with longer pauses between cycles – experiments. It can be observed that even though the response in the following experiments is stiffer, the loading path has not the same slope as previous experiments unloading path as in the case of silt loam, see Fig. 21. After every time some permanent deformation remains even after completely unloaded. Groundwater influence on this phenomenon is commented in the next part of this chapter.

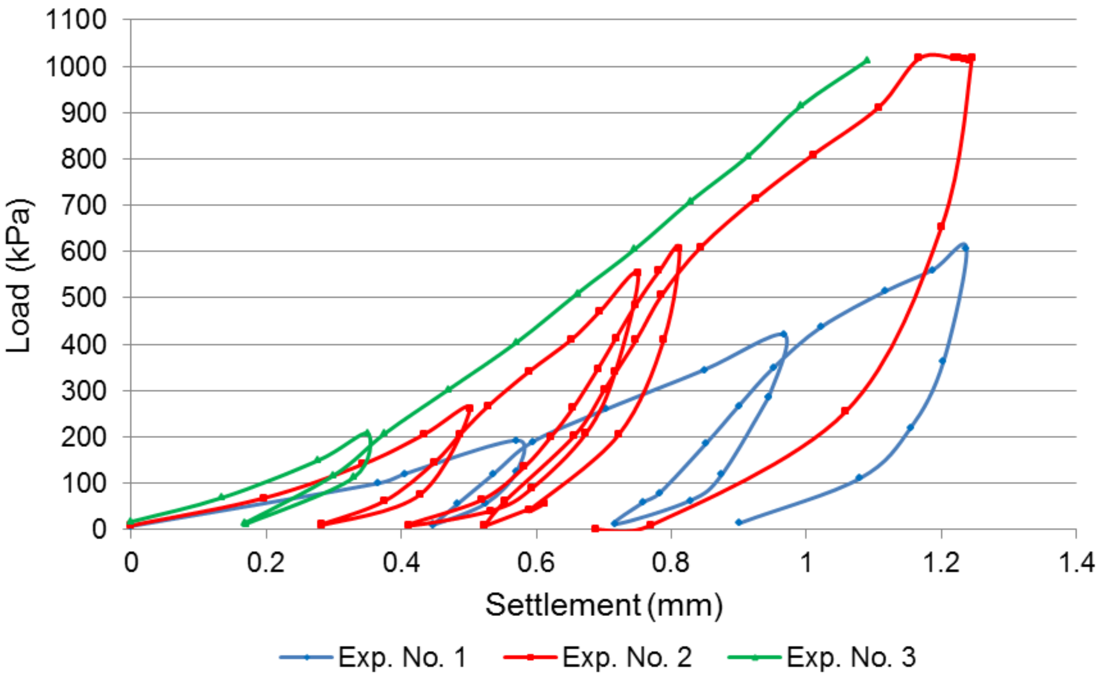

Fig. 18. Three consecutive dry experiments – the permanent deformation cleared

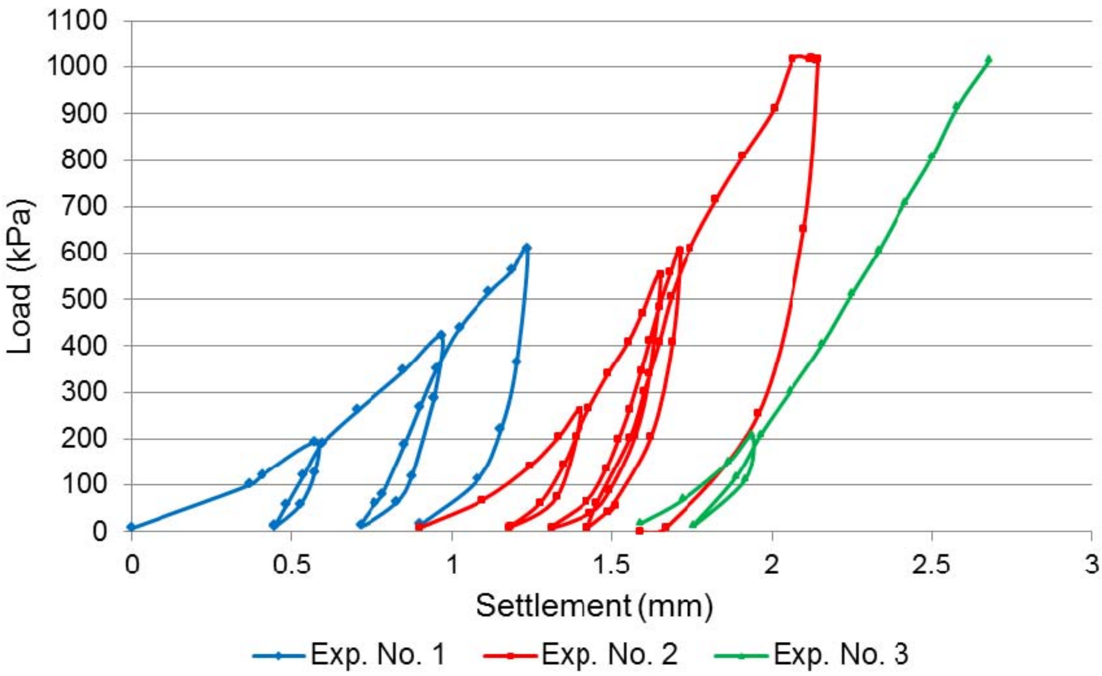

Fig. 19. Three consecutive dry experiments – the permanent deformation kept

Total settlement of the plate, acting on well compacted (dense) G2 soil specimen, was, as expected, of very small magnitude even for applied loading exceeding 1000 kPa. Such stiff response, using classical approach for evaluation of E_{def} we obtain values around 200 MPa, makes this soil an ideal subsoil material.

4.2.2. Selected commented results for F5 specimens

The difference between slopes of loading and unloading/reloading paths as well as the hysteresis on the unloading/reloading commented in the above section for the case of cohesionless coarsely grained soils can be also observed in experimental results measured on cohesive fine grained soils.

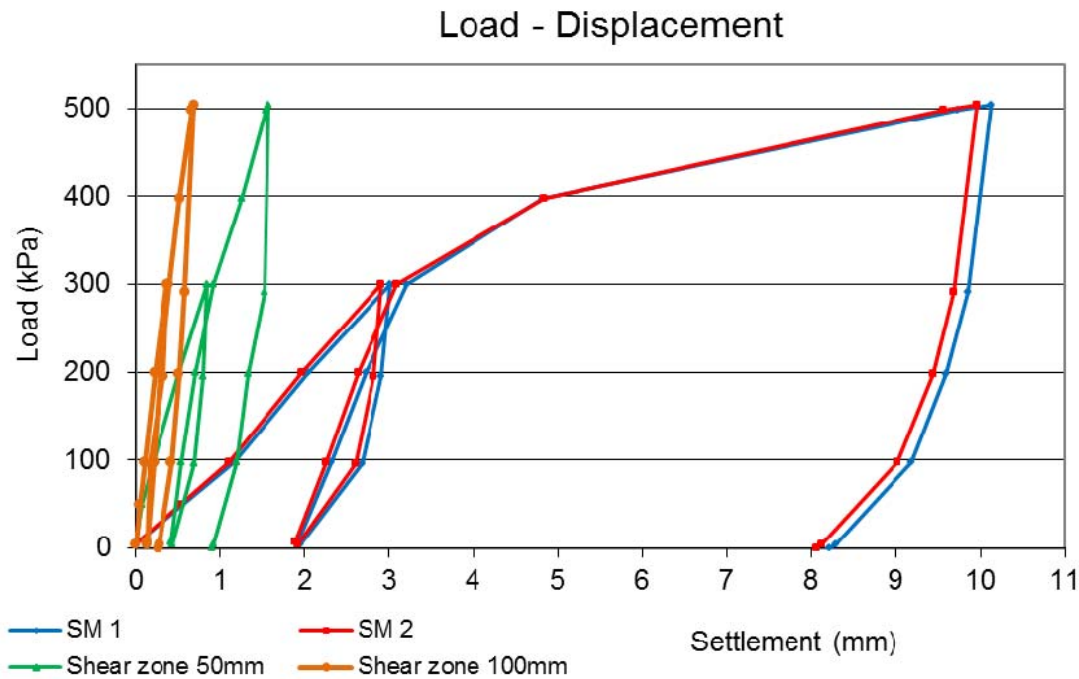

Fig. 20. Results from experiment on unsaturated F5 specimen under constant suction condition (SM1 and SM2 stands for dial gauge no. one and two)

Immediate response of the surrounding soil indicating activation of the shear zone from the very beginning of the experiment, even for very small loads, can also be observed in the following figure.

In contrast to G2 specimen plastic yielding was observed in the behaviour of the sample for load values higher than 400 kPa.

It can be also observed that unlike coarsely grained soil in previous example the loam was able to “memorize” the previous loading and even after 2 months (time lag between Exp. No. 1 and Exp. No. 2) still the slope of the loading path roughly copies the slope of previous unloading path.

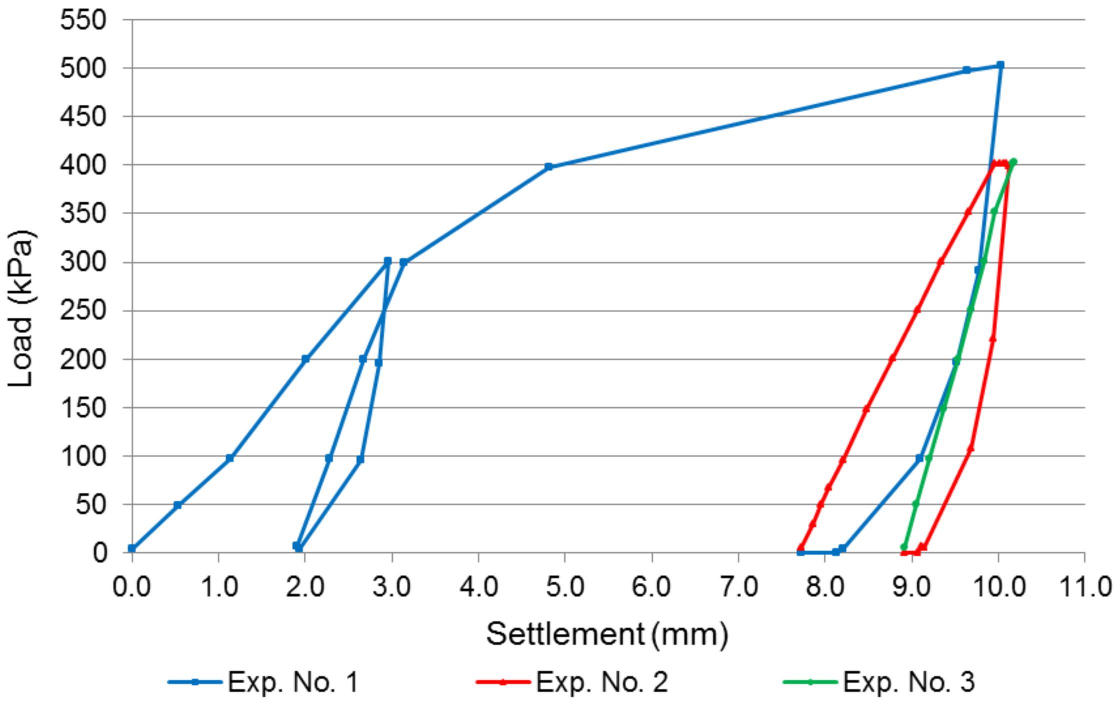

Fig. 21. Three consecutive dry experiments – the permanent deformation kept

The following figure shows the evolution of lateral pressure on the side wall when the load is applied. The hysteretic behaviour can be also clearly seen from this chart however it is to be pointed out that the lateral pressures are related to the beginning of the experiment, it means the probe was resented before. The lateral pressure which remained after the specimen was placed into the stand and compacted equalled 33,1 kPa. The measured values are used for confirmation of the numerical models.

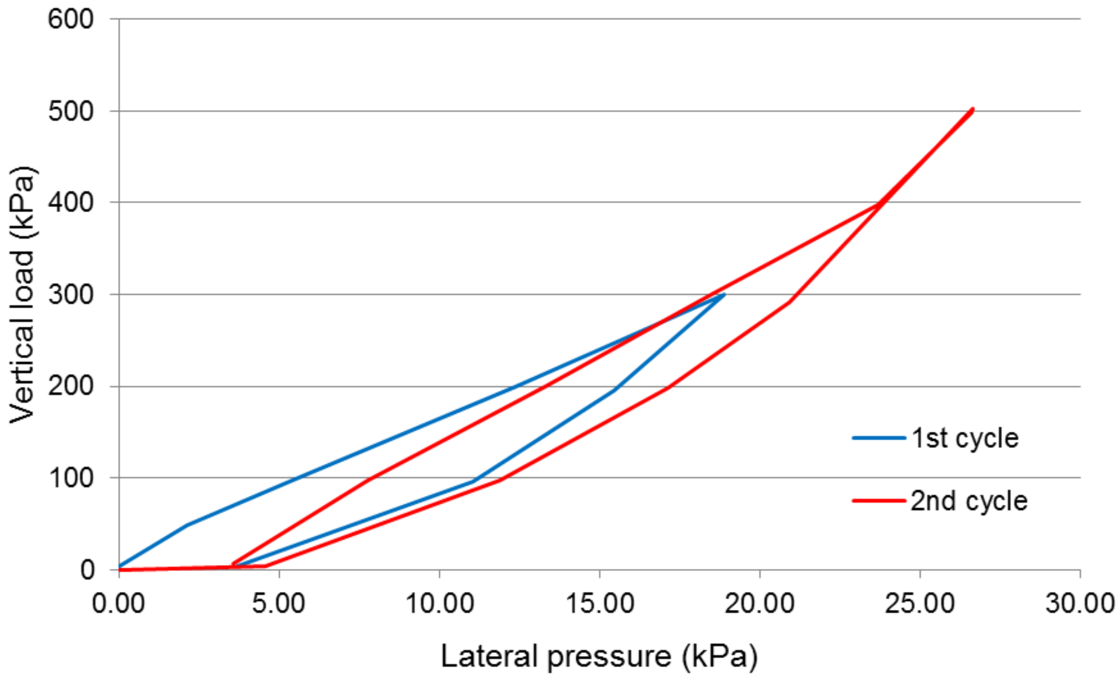

Fig. 22. Vertical load vs. lateral pressure induced on the side wall

Creep behaviour of the soil in unsaturated state was also examined. The whole creep behaviour lasted approximately 3 hours but more than 90% of the creep deformation was reached after first 70 minutes, see Fig. 23.

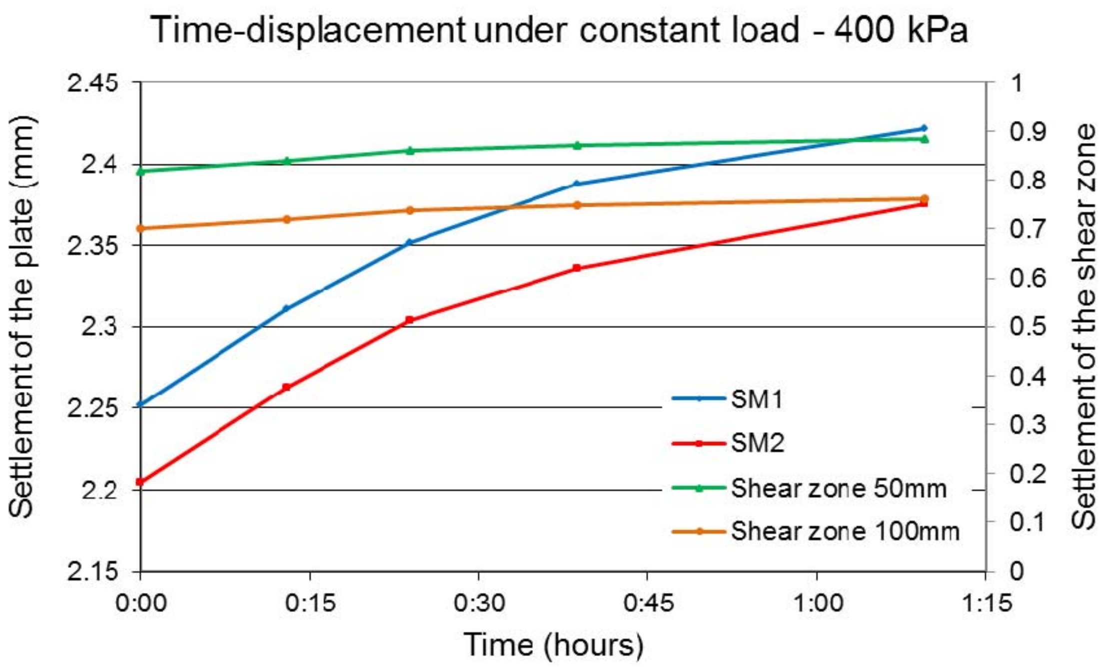

Fig. 23. First determining hour of the creep behaviour of F5 specimen (SM1 and SM2 stands for dial gauge no. one and two)

4.3. Suction cancellation under constant load – full scale

The wetting experiment commenced after the maximum or full load was applied on the specimen and kept constant for some time. After that the valve was opened and the water started to flow very slowly into the soil specimen. Even though the gross hydraulic head was nearly 1,5 m, due to local hydraulic losses the overall flow rate dropped to approximately 0,01 l/s even for empty stand, i.e. without the soil sample. Therefor any theories suggesting the influence was caused by flow pressures can be rejected. As the water table rise in the sample the settlement is measured under constant load applied on the rigid plate.

After the prescribed position of the water table is reached, the soil is slowly drained. Next experiment is performed on the same sample in a short period of time, but for completely drained sample to prove the ability of soil to memorize the load after structure collapse. Another reason for the unloading and stopping the experiment is excessive settlement which would pass the limit of measuring devices (approximately 10-15 mm). The scheme for the suction cancelation experiment is clear from Fig. 24., while the real model and details of the plate and measuring devices are in Fig. 25 and 26 respectively.

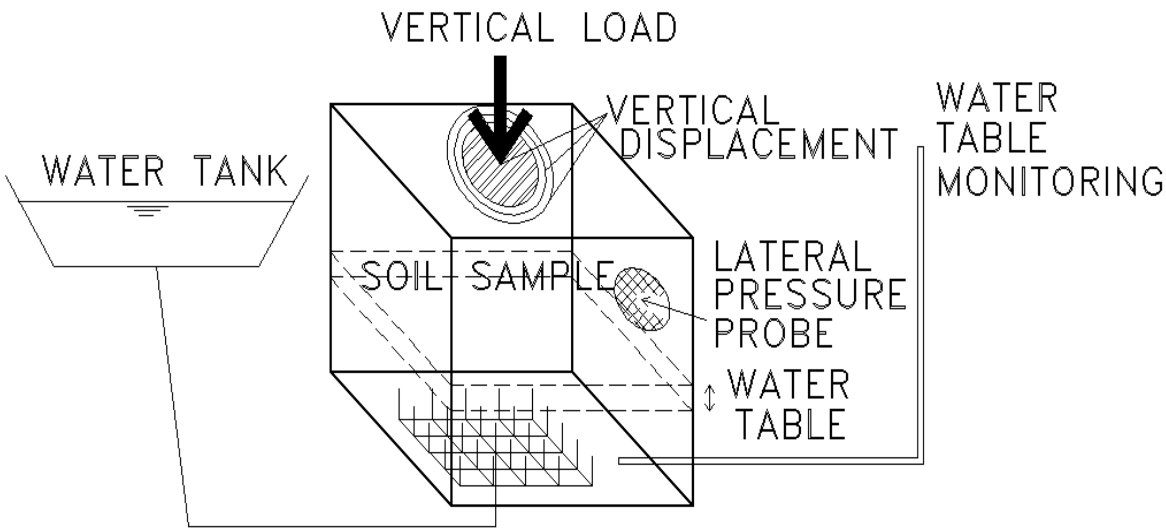

Fig. 24. Improved stand for plate load test experiment including groundwater table variation – scheme

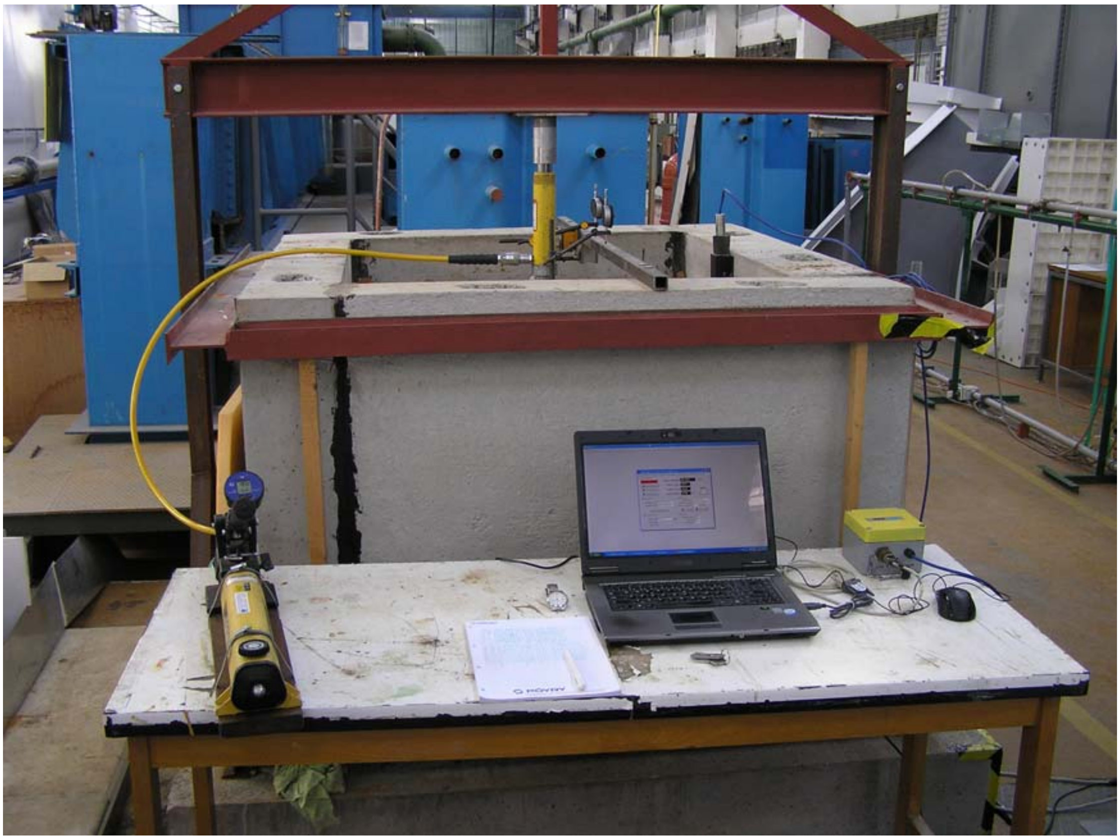

Fig. 25. Fully equipped stand for plate load test with shear zone and lateral pressure measurement

Fig. 26. Detail view on the analogue settlement measuring devices (later on digital)

4.3.1. Selected commented results for G2 specimen

General opinion about coarse grained soils and suction is that the influence is negligible and therefore the first wetting experiment on G2 soils exceeded the expected increase in settlement when it reached nearly 18.5% of the total settlement after creep effect diminished. The following figures show the entire course of the experiment in terms of settlement of the plate and applied load in case of Fig. 27, and detail of the settlement during the time of wetting in case of Fig. 28.

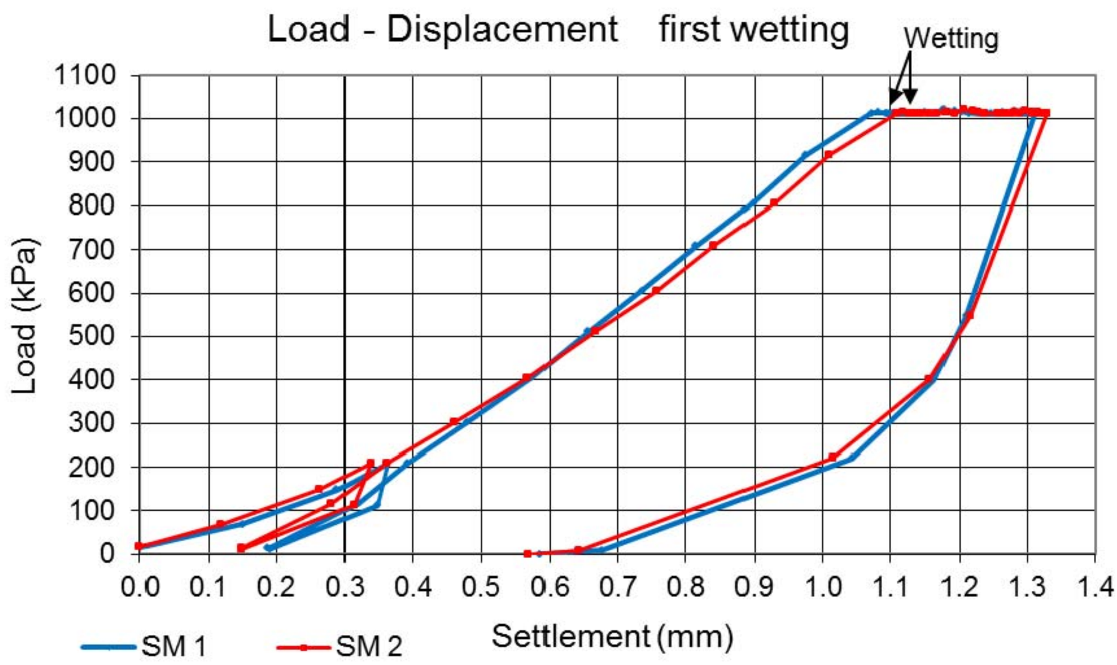

Fig. 27. Full scale wetting under constant load experiment (SM1 and SM2 stands for dial gauge no. one and two)

Subsequent wetting experiments on the same specimen shown decreasing contribution to the settlement when compared to the settlement due to external load. Table 6 summarizes the increase of the total average settlement due to wetting in four consecutive experiments on the same specimen.

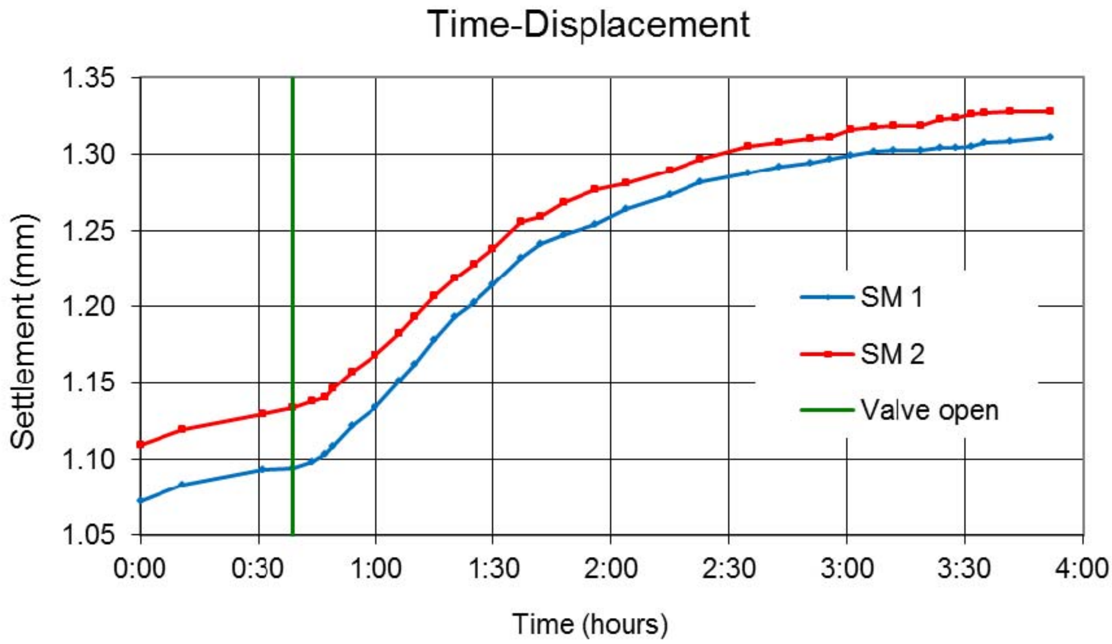

Fig. 28. Full scale wetting under constant load experiment - time factor (SM1 and SM2 stands for dial gauge no. one and two)

Tab. 6 Settlement increase due to repeated wetting

Exp. No.	Max. load (kPa)	Max. settlement due to load (mm)	Settlement due to wetting (mm)	Increase in settlement (%)
1	1010	1,114	0,206	18,5
2	710	0,562	0,081	14,5
3	1010	0,844	0,039	4,6
4	910	1,053	0,040	3,8

(Max. settlement due to load includes settlement from creep)

It is important to point out that part of the settlement due to wetting can be observed even in distant parts of the shear zone leading to expected conclusion that the whole specimen has subsided. However the increase in settlement of the plate was more than double the overall subsidence even for the fourth experiment in a row.

The influence of the suction cancellation on the consolidation process can be best observed in the following figure showing only the loading paths of all subsequent experiments while highlighting the wetting experiments.

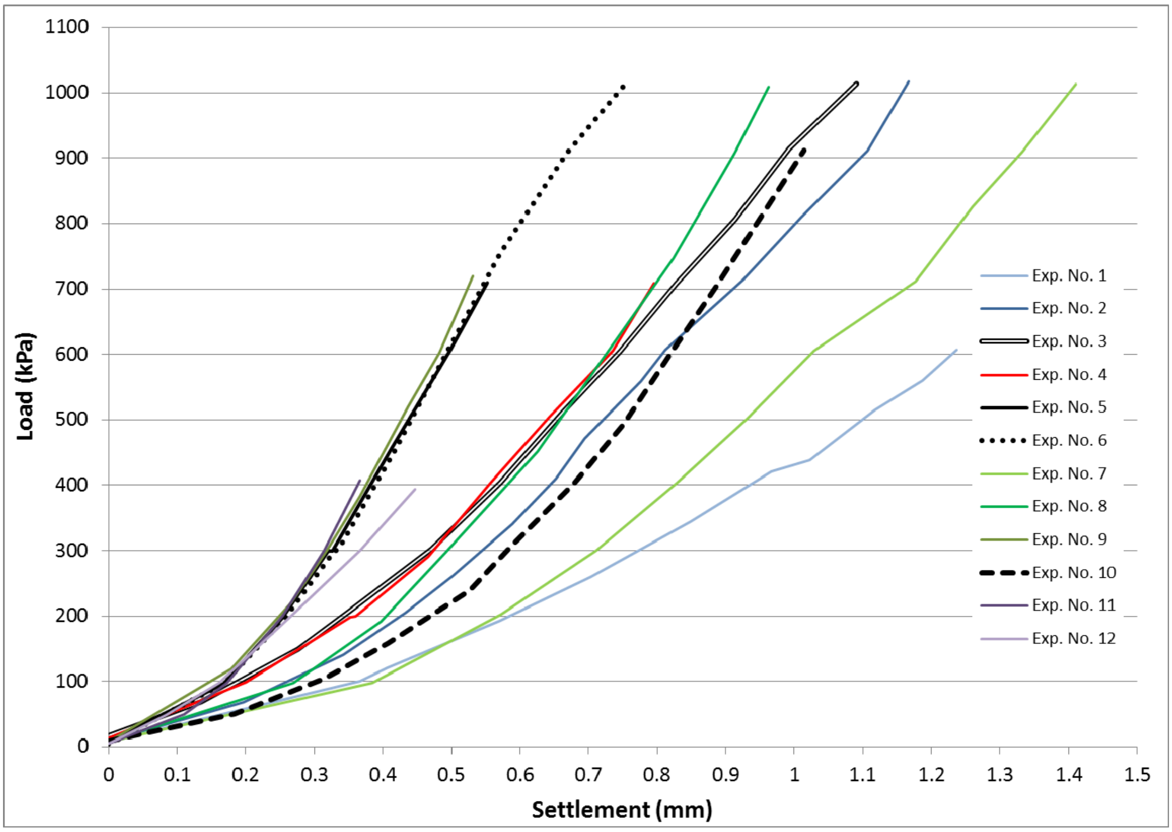

Fig. 29. Loading paths of subsequent experiments on the same specimen

At this point it is necessary to emphasize that full saturation of the entire specimen was not achieved due to excessive leakage which exceeded the inflow when certain level of water table in the specimen was reached. More results can be found in the Appendix B.

4.3.2. Selected commented results for F5 specimen

As the silt loams are generally considered as collapsible, dramatic increase in settlement due to wetting was expected, however the rate of settlement was rather high than expected. Also the settlements of the shear zone were extremely high when compared to the settlement due to external load. Fig. 30 shows entire course of the suction cancellation experiment. It can be observed that settlement due to wetting of the sample was more than 4 times higher than settlement caused by the load and as can be seen from Fig. 31, this increase took place within three hours.

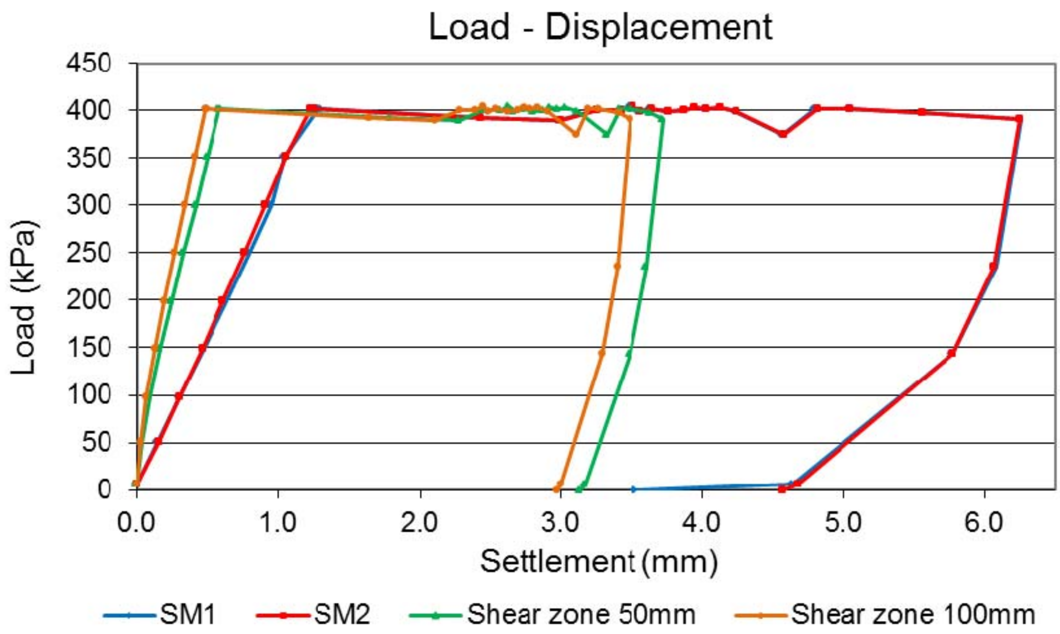

Fig. 30. Full scale wetting under constant load experiment (SM1 and SM2 stands for dial gauge no. one and two)

The problem of any numerical model as well as physical interpretation is when to stop the wetting and for how long will the load act, i.e. the suction cancelation as the external loading should be considered as permanent. To explain this statement it is necessary to describe more in detail the time after the experiment and the state of the specimen the following days.

After the valve controlling the water supply pipeline was closed, water from the tank was drained within one day and the valve was reopened to allow the specimen to drain as well. However the soil started to swell significantly. The next day the shear zone heaved 4,5 and 6,0 mm above the original surface (the settlement was negative) and the soil bearing capacity was dramatically decreased.

After leaving the soil sample to dry for three months, the moisture was still very high and dry load experiment was proposed to confirm the actual bearing capacity of the soil. From the following figures it can be see that the soil was unable to sustain loads above 70 kPa. The whole process took place without any water supply except for the water during the experiment. We must conclude that repeated wetting would be impossible to test unless only very small loads are applied. Such approach would however disqualify the results from having any practical use for engineering purposes.

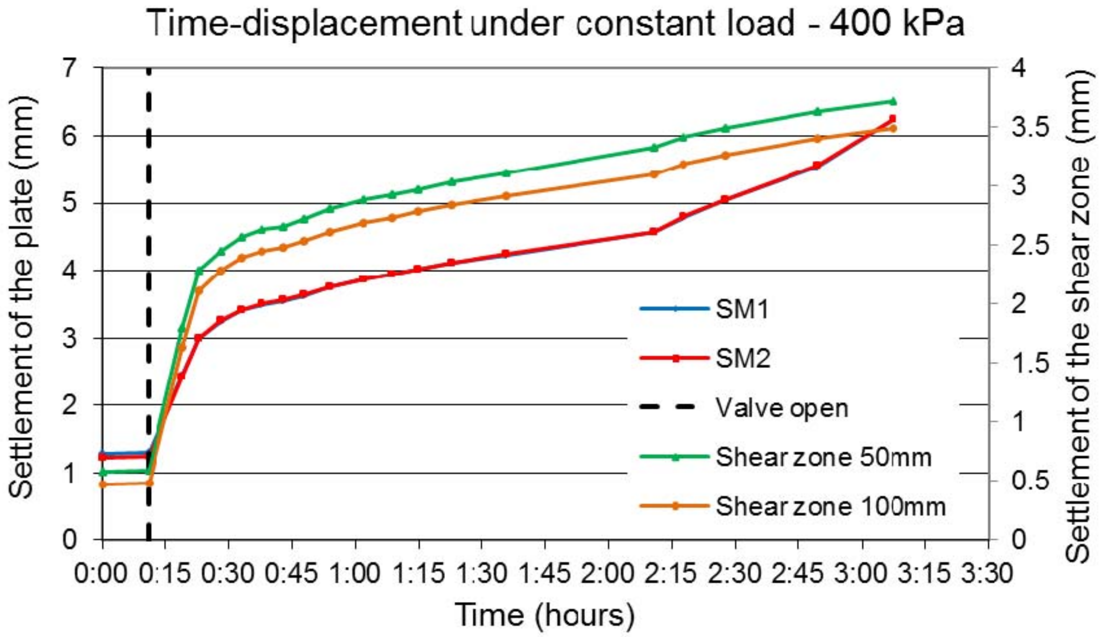

Fig. 31. Full scale wetting under constant load experiment – time factor (SM1 and SM2 stands for dial gauge no. one and two)

The short time of access to water followed by significant change in parameter can also lead to conclusion that even small variation or more precisely increase in groundwater table above long term maximum could lead to large settlement and potential damage to the upper structures.

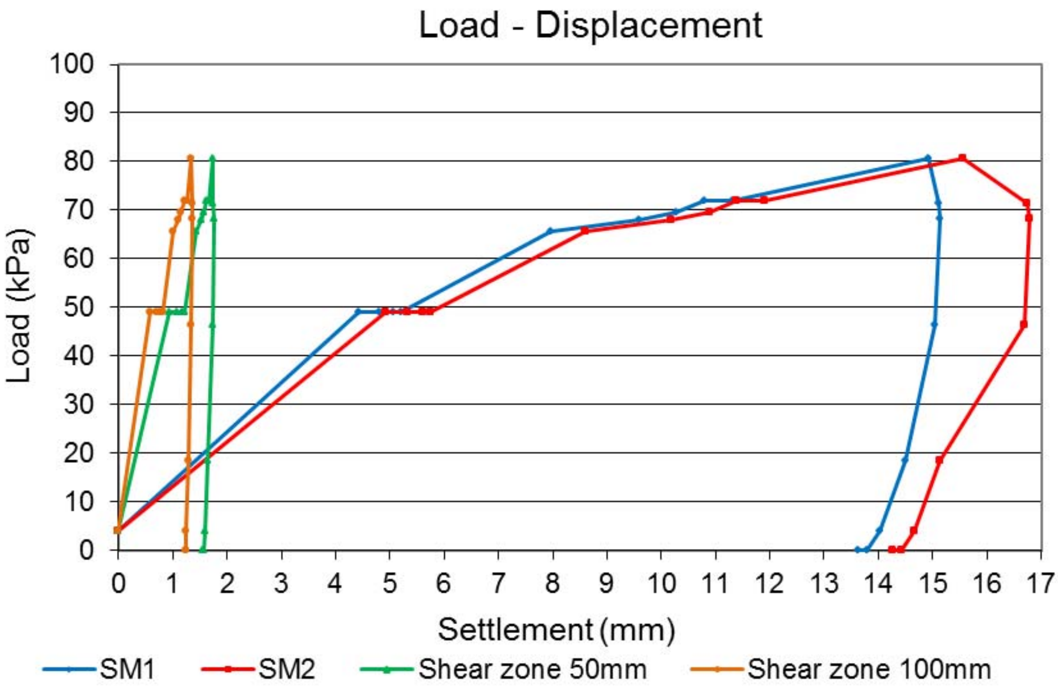

Fig. 32. Full scale dry experiment 3 months after wetting

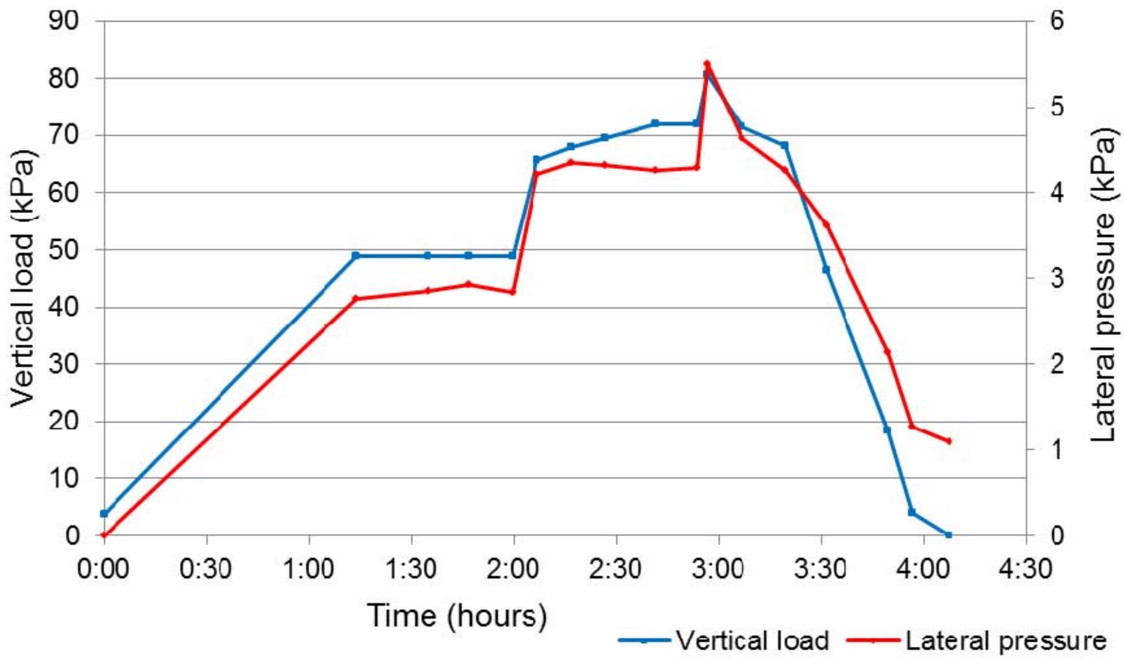

Fig. 33. Full scale dry experiment 3 months after wetting – time factor and lateral pressures

4.4. Wetting under constant load – small scale

The small scale experiments were designed to confirm the governing idea and results obtained from full scale experiments on undisturbed samples as the large specimens must always be considered as reconstituted. The undisturbed specimen was set into the bottom part of the standard equipment for measuring hydraulic conductivity without the constraining brass cylinder being removed. Load and measuring device were applied and the specimen was wetted from the bottom. The experiment setup is clear from Fig. 34.

At the time t + 0 hours the water is in the water basin at the bottom of the specimen. The water level rise continuously but stops immediately the moisture is observed at the top of the specimen. This part of the experiment is called phase 1. The water level is kept constant as long as the settlement increase – phase 2. After that is the specimen completely flooded which cause additional settlement - phase 3. The time period for the phase 1 and 2 is dependent on the soil type. Phase 3 is carried out long enough to keep the complete time of the experiment at least 5 days – i.e. 120hours.

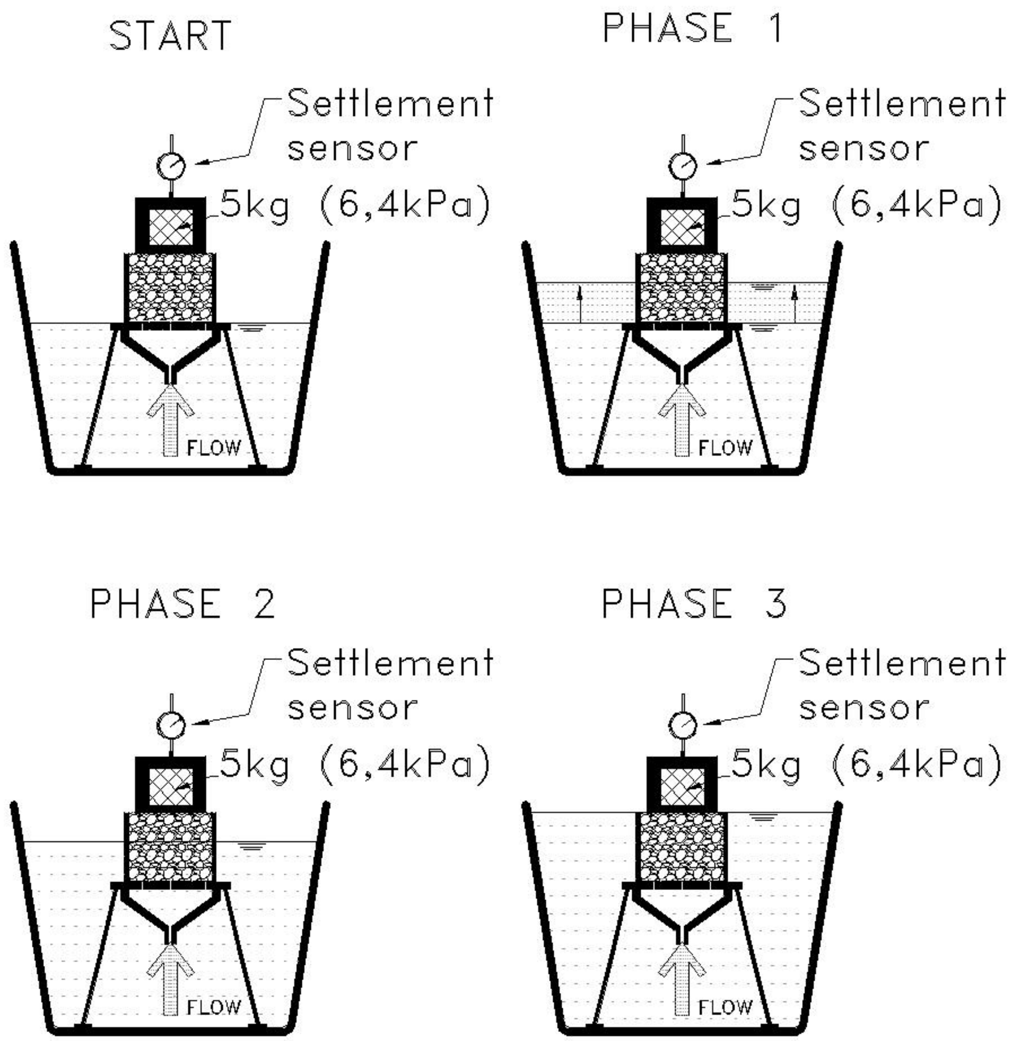

Fig. 34. Small scale wetting under constant load experiment – scheme

Such timing of the experiment allows us to separate the effects of suction in capillaries from the effect of larger pores. Alternative approach using connection to the water tank and higher hydraulic head significantly reduces the time necessary for the experiment but brings difficulties in the results interpretation procedure. The typical result from wetting experiment is shown on the following Fig. 35. The observed additional settlement is compared with the calculated settlement.

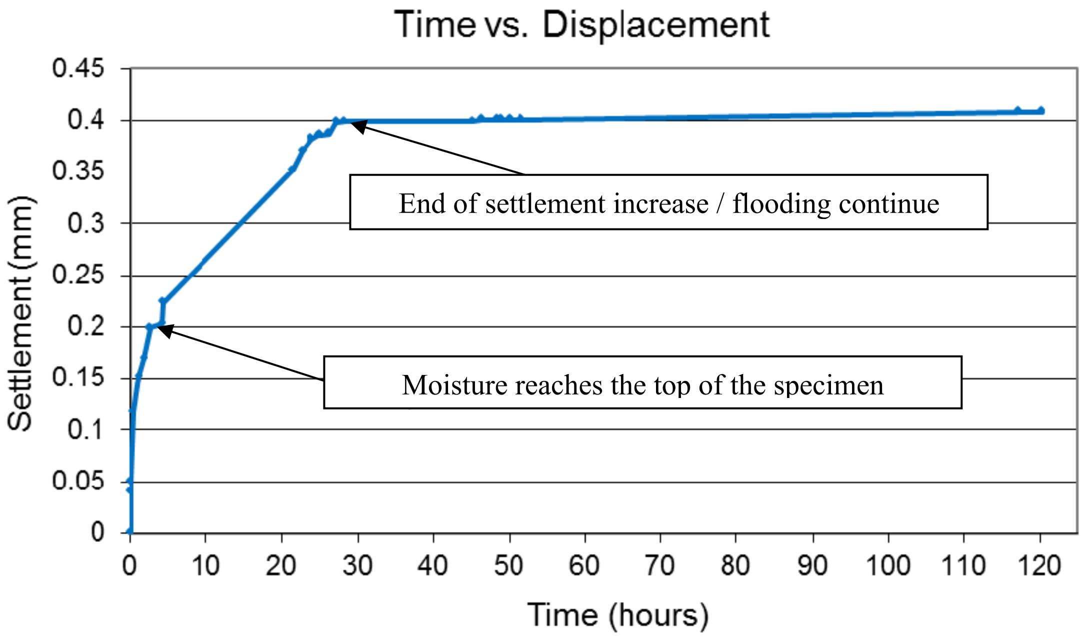

Fig. 35. Small scale wetting under constant load experiment – example of results for silty sand (siSa)

In addition to the goals mentioned above the results obtained were particularly useful for evaluating the time necessary for the specimen to be completely saturated as the internal erosion experiments show different results for specimens saturated in advance. This observation can be confirmed by works of other authors e.g. (Wan and Fell, 2002, 2004a and 2004b), (Lim, 2006) and (Lim and Khalili, 2010) who also found that most clay soils when saturated have significantly higher erosion rate than at the partially saturated compaction condition.

4.5. Erosion under extremely high gradients

This experiment was designed for evaluation of soil stability under extremely high hydraulic gradients acting over limited time. Although generally accepted ultimate value of vertical hydraulic gradients in practice does not exceed the range 0,5 – 1,0 and the proposed experiment induced gradients over 8 even for the smallest hydraulic head applied, the experiment simulates well the unsteady situation occurring during fast raise in water table in stream. Comparable flow velocities can also serve for extrapolation of the results towards specific internal erosion problems around preferential paths, cut-off walls and grout holes failures or wrong design of position of drains and sheet piles etc. The experiment also allows for study the initiating process of the internal erosion.

In order to stabilize the soil sample with respect to uplift forces, external load was placed on the top increasing the total pressure. The experiment setup is clear from Fig. 36. Small specimen is set into the bottom part of the standard equipment for measuring hydraulic conductivity. Load represented by a lead weight and measuring device were applied on the specimen that was afterwards subjected to water flow under pressure from the bottom. The washed out particles are collected in the tank bellow the specimen.

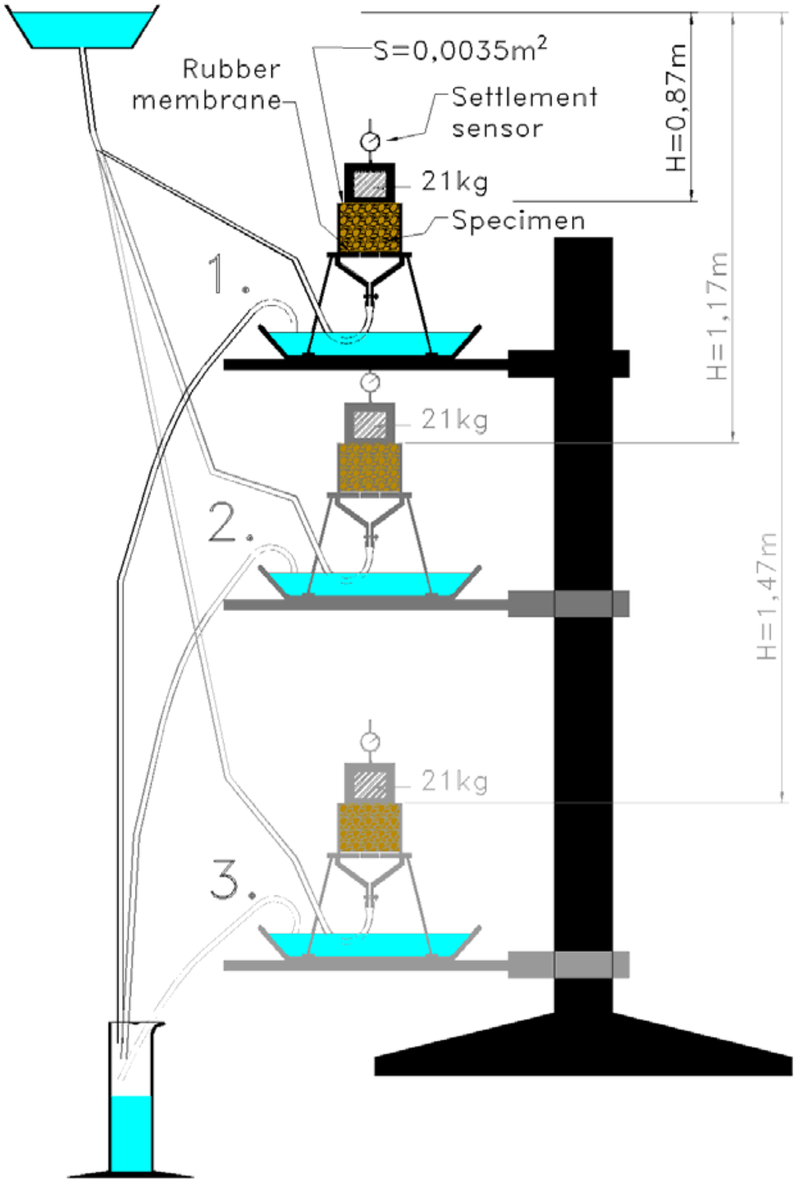

Fig. 36. Internal erosion experiment – scheme

The experiment has three phases, each one represented by different value of hydraulic gradient. Changes between the phases were sudden and the exact time of the change depends on the soil behaviour. The end of the experiment is when the specimen collapses, see Fig. 37, or/and the settlement of the lead and flow rate extremely rise or after 25 hours in 3rd phase of the experiment.

Fig. 37. Example of collapse of the specimen

Before the collapse some specimens behave normally and do not show any sign of the approaching end of an experiment. Other specimens show increased flow several hours before collapse. In the following charts the vertical lines presents the change between the stages of the experiment i.e. between the applied hydraulic gradients.

Fig. 38 shows typical results obtained from experiments with specimen that collapses after the gradient exceeds certain value. Quite important is also the duration of the action of the flow loading. The following figure (Fig. 39) shows that when the action of the drag forces is interrupted and restored again the specimen can sustain even higher gradient. It can be observed that this specimen will likely collapse in the second stage but due to the interruption of the flow the specimen sustained another increase in hydraulic gradient.

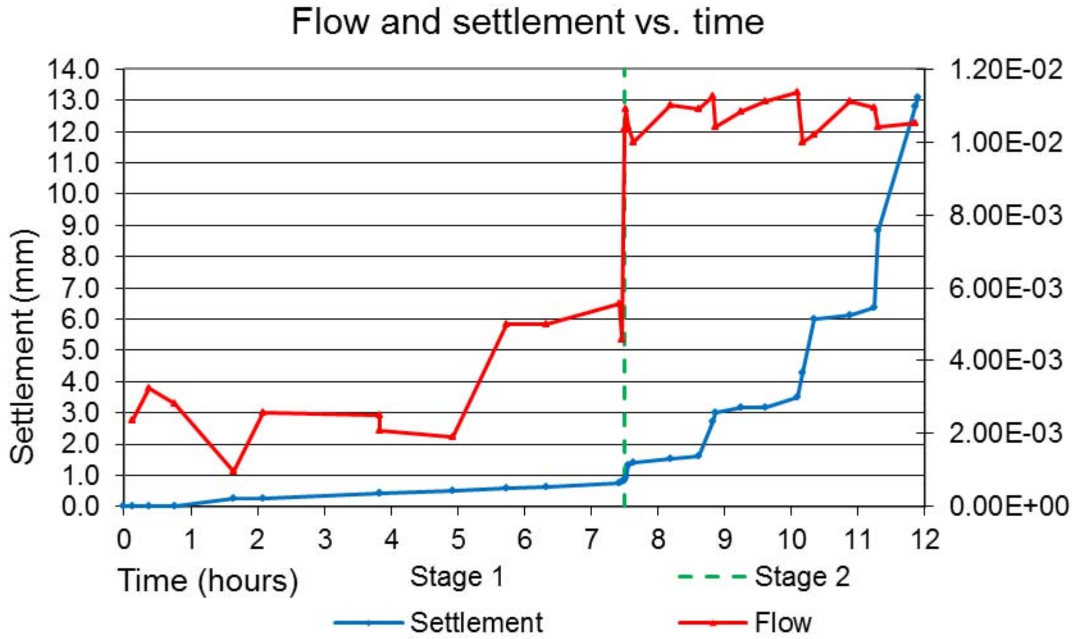

Fig. 38. Flow and settlement before collapse during the second stage

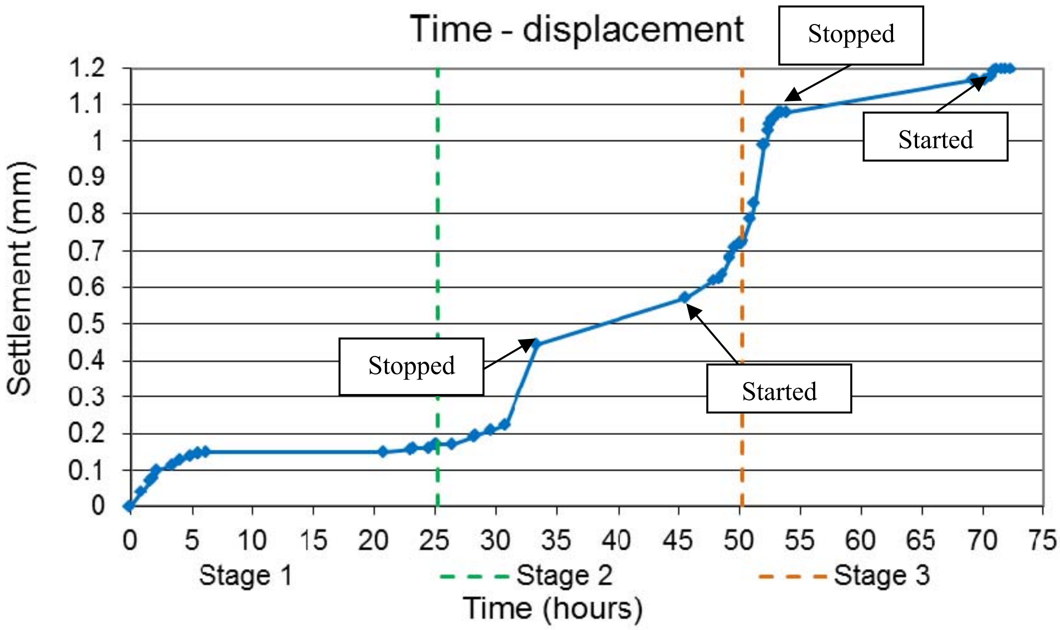

Fig. 39. Settlement of the weight for the internal erosion experiment with interruptions

It is necessary to point out that the increase in flow during the experiment does not always correspond to the settlement of the lead. This phenomenon can be seen in Fig. 40. This flow-time chart belongs to the same experiment as Fig. 39. The rapid increase in flow rate occurs in the third stage of the experiment but form the settlement chart is clear that the specimen will collapse already in second stage if the flow was not stopped. In the flow-time diagram the pauses are removed, as the flow can be only measured when the experiment is running.

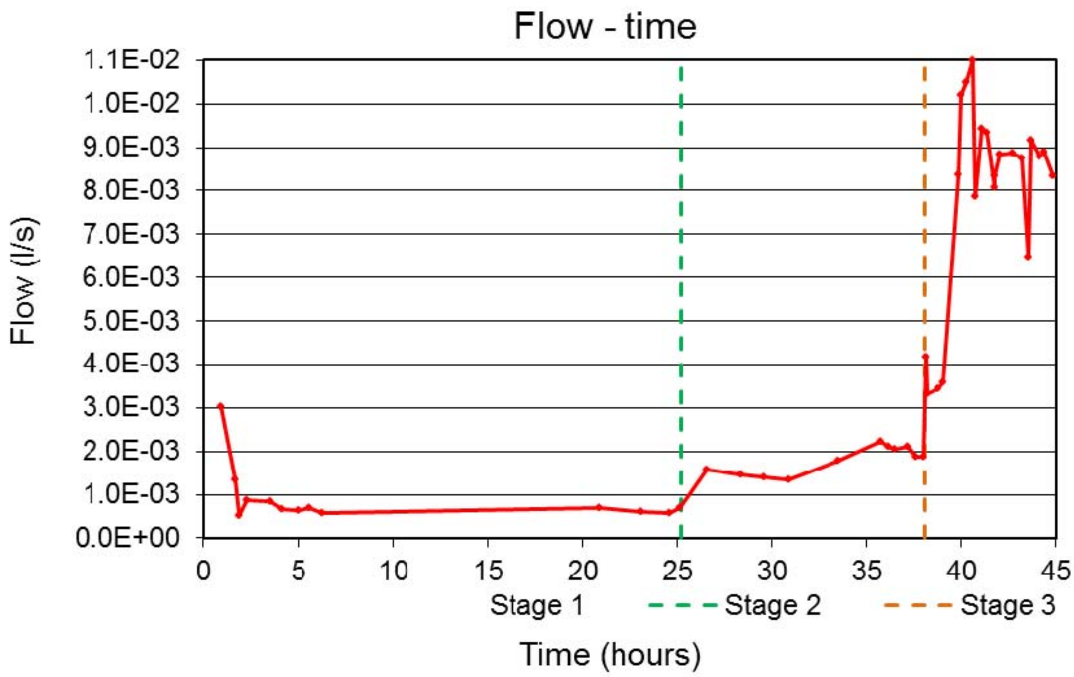

Fig. 40. Flow-time graph for the internal erosion experiment form Fig. 39

The grain distribution of the specimen before and after the experiment as well as the grain distribution of the washed out particles is also part of the procedure and can be seen in Fig. 41.

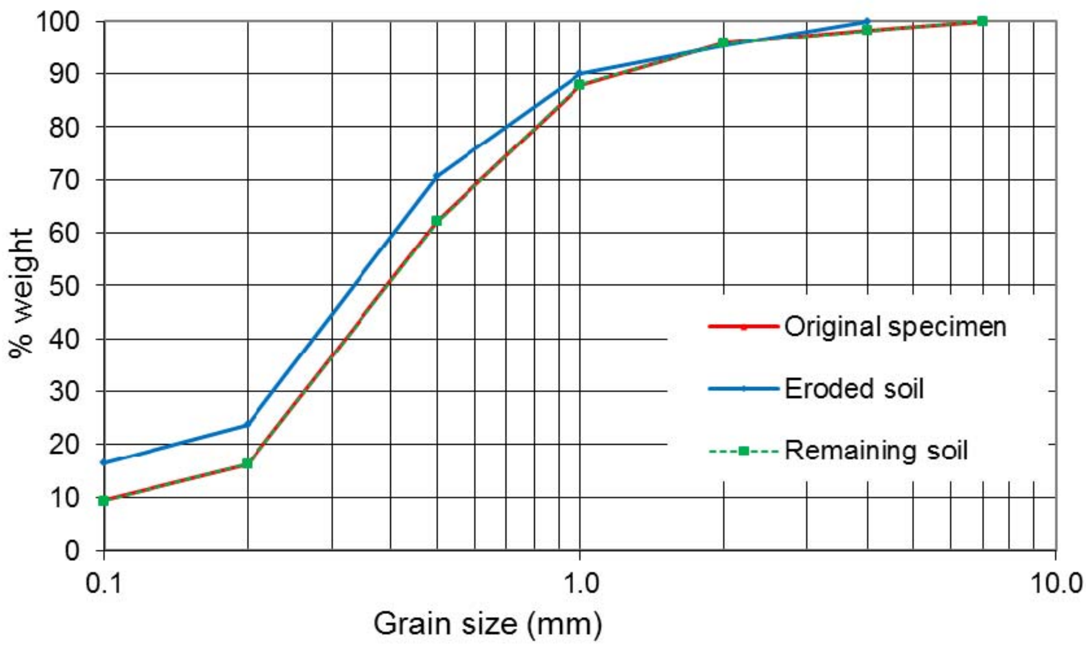

Fig. 41. Internal erosion experiment – typical result SP (grain distribution)

The grain distributions of the particles that have been eroded were very close to the original specimen grain distributions. For some specimens the washed out part has the distribution moved to the left i.e. it contained finer particles than the original specimen. But as this is not the case of all tested specimen and as the washed out parts does not contain only fine particles it can be concluded that the amount of fine particle in the soil is not the most determinant parameter of the soil for the internal erosion under high gradients and limited time of action although it would seem that higher portions of fines makes the soil more stable over short time respectively. More important is the distribution itself and the density and size of the preferential ways present in the soil.

After the experiment is ended, the remaining part of the specimen is dried and cut in order to obtain the information about creation of preferential flow paths, see Fig. 42.

Fig. 42. Internal erosion experiments - cut through specimens after collapse

Last remark to the internal erosion experiments considers the change in porosity due to particle loss. It seems that the porosity change is not directly proportional to the amount of washed out particles. The water flow crates small caverns inside the specimen and the collapse of the specimen occurs when these caverns collapse. It can be before or after the caverns are connected together with channels. When created these preferential paths are responsible for the majority of the particle losses.

Obtained results have confirmed several hypotheses. First, there was question regarding the ability to withstand high hydraulic gradient loading for limited time and the influence of the portion of fine particles. Based on the experimental results it safe to assume that sandy silts and silty sands can withstand loading from hydraulic gradients as high as 14 for more than 25 hours while some of the poorly graded sand specimens collapsed after one hour when subjected do hydraulic gradient 8.7. Therefore we conclude that for limited time fine grained soils proved to be more stable when facing extremely high hydraulic gradient.

Second, the initial porosity is not necessary determining factor. The sandy silt samples had initial porosity approx.. 0.5 and yet sustained the highest gradient for more than 25 hours, while sands had porosity approx. 0.41 and their resistance varied significantly.

Third, fine grained samples wetted prior the experiment shown higher hydraulic conductivities while in case of sand samples the differences were not significant.

Tab. 7. Results summary

Class	Average initial porosity	Average porosity after experiment	Portion of samples without collapse
Sa	0.41	0.38*	20%
siSa	0.31	0.31	100%
saSi	0.50	0.44	100%

*results are influenced by the eroded particles

4.6. Full scale experiment enhancement

Although the designed experiment provided sufficient data to fulfil the partial goals of this thesis, experience gained during the testing can be used for future improvement of the model stand. Following suggestions are presented which would allow for easier interpretation of results and increase the amount of information gained about the soil state during the experiment.

- Two vibrating wire piezometers should be placed into the sample for change in pore pressures – the current open piezometer presents a barrier for homogeneous compaction of the specimen creating preferential paths for water; new measuring devices would also allow for continuous data logging over longer time period as well as observation of immediate response to changes in external load
- One total pressure cell should be installed for studying the stresses inside the sample over time
- One or two soil moisture sensors should be installed to allow for soil moisture measurement without the necessity of taking small soil samples from the specimen during longer experiments

- Digital gauges should be used instead of analogous one to gain all the data at once – in coarse grained soils are changes very fast
- The leakage problems would be best to solve with different stand material. Welded steel plates creating the inner part of the stand would ensure sufficiently high water tightness though the number of supporting beams would have to be increased.
- The compaction method should be changed. To allow for easier evaluation of pre-consolidation pressure, static load or standardized hammer weight and height of free fall should be used instead of vibrating plate. However it must be pointed out that vibrating plates and rollers are most common in practice.

Chapter 5

INFLUENCE ZONE THEORY

It is generally accepted that the effect of load applied on the soil will not propagate to infinite depth. The influence zone presents an area or more precisely a domain below the acting load. In this domain all the deformations due to the applied load take place. Below the influence zone all the deformations from the particular load are negligible.

It is easy to see that the depth of influence zone must depend on the size of the load, its magnitude and the characteristics of the soil. Standing standard for geotechnical design in Europe, the Eurocode 7, (EN 1997-1; part 2.4.5.2) requires the engineers to take into account "*the extent of the zone of ground governing the behaviour of the geotechnical structure at the limit state being considered*" when selecting the characteristic values for geotechnical parameters. It also recommends considering the influence of the supported structure on the zone that governs geotechnical behaviour. Therefore for every in-situ testing procedures, i.e. dilatometric and pressiometric measuring techniques, plate load tests, standards penetration test, etc., the depth of their influence zone should be evaluated and confronted with the expected depth of the designed structure. Also, when performing back analysis of in-situ experiments, the size of the influence zone is crucial parameter as shown in chapter 6.

Application of this theory in numerical modelling of shallow foundations leads to restriction of the model range especially in depth of the modelled area. In analytical solutions this theory leads to subsoil of finite depth, i.e. elastic layer theory. The main issue, however, is how to estimate the depth of the influence zone in practise and regarding the groundwater how the presence of groundwater or its flow can influence this depth.

Although more sophisticated numerical methods often require the parameters identification to be done by back analysis with the same method in order to ensure consistency of the results, hereafter presented fast analytical approach could be used to in practice for simple geotechnical problems as well for evaluation of the received data from in-situ tests. Successful application of semi-analytical method on tropical residual soils was earlier published by Cunha (Cunha et al., 2002), (Cunha and Kuklik, 2003).

5.1. Basic principles and governing idea

The governing idea for estimating the depth of influence zone is the pre-consolidation of the soil, which is generally caused by the excavation and the soil's ability to memorize the highest load it was subjected to. When the additional load is applied the vertical stress from the load is added to new (after excavation) geostatic stress and where the sum is equal to the original geostatic stress (before excavation) that is the depth of influence zone. It can be easily written as

$$\sigma_{zz}(0,H)=\gamma h \tag{5.1}$$

where H is the depth of influence zone, h represents the depth of excavation, γ stands for the unit weight of the soil and zero coordinate is placed at the surface of the excavated ground, i.e. where the load is applied.

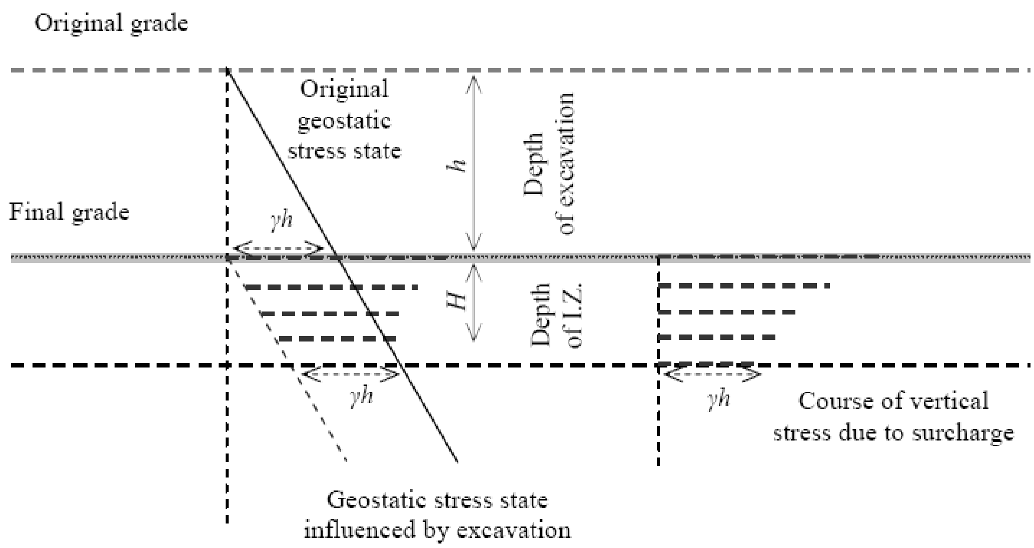

Fig. 43 The governing idea of the influence zone depth calculation (Kuklik, 2011)

The depth of excavation or pressure from soil excavated respectively can easily be replaced by known pre-consolidation pressure. This pressure can be estimated when soil improvement takes place or when new geotechnical structure is designed and the compaction is prescribed.

5.2. Influence zone depth estimation

The problem in estimating the influence zone depth, according to above mentioned assumptions, can be substituted by problem of calculating the vertical stress for complex geotechnical problems when it is dependent on the soil parameters which cannot be obtained before the estimation of the influence zone.

Instead of time consuming FEM analysis it was suggested the use of elastic layer solution in Westergard manner (Kuklik et al., 2009). For the back analysis of the static plate load test all the assumptions made are quite reasonable and the errors are usually much smaller than the spatial differences at the construction site. Similar theory can be applied even for non-vertical experiments such as dilatometric analysis in deep boreholes as shown in the chapter 6.

The maximum stress below the centre of the foundation structure in the depth H can be then expressed in following form

$$\sigma_z(0,0,H) = f_z F(\beta) = \gamma h \tag{5.2}$$

As the value of preconsolidation γh and the level of surcharge f_z are known, we can in inverse way explain the value β. The following formula describes this statement and the idea how to calculate the depth of influence zone when a represents half of characteristic dimension of the foundation structure (a represents radius for circular shape; a represents half of the strip width for strip foundation etc.)

$$\frac{\gamma h}{f_z} = F(\beta) \rightarrow \beta = \frac{a}{H}\sqrt{\frac{2-2\nu}{1-2\nu}} \rightarrow H \tag{5.3}$$

Using this method, see Appendix A, the estimation of the influence zone can be very fast as analytical solution is derived for different shapes of the footing based on values of the $F(\beta)$ function.

For instance in case of the circular load (plate load test) the $F_r(\beta)$ function can be introduced as:

$$F_r(\beta) = 1 - \beta \int_1^{+\infty} \frac{t}{\sqrt{t^2-1}\cosh\left(t\frac{\pi}{2}\beta\right)} dt \tag{5.4}$$

Fortunately it is possible to follow the basic idea of the influence zone and plot the pre-consolidation or "excavated" geostatic stress against β as shown in Fig. 44. From this chart the value of β can be obtained

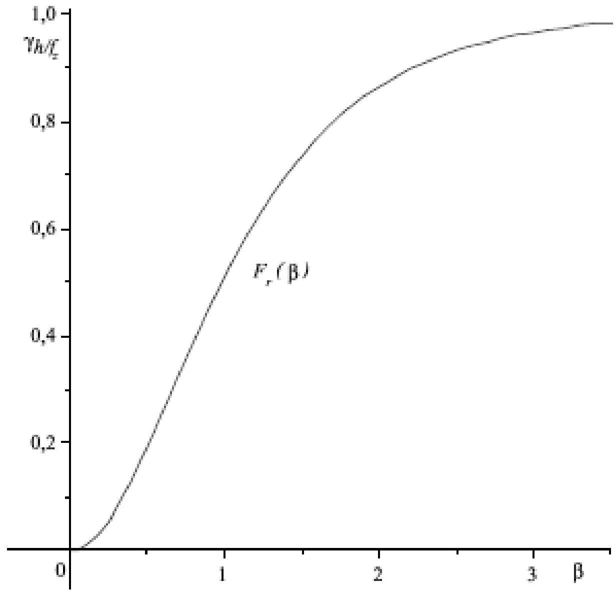

Fig. 44. $F_r(\beta)$ function for circular load area

And with the value of (β) we can immediately calculate the depth using Eq. 5.5

$$\beta = \frac{2\alpha r}{\pi} = \frac{r}{H}\sqrt{\frac{2-2\nu}{1-2\nu}} \tag{5.5}$$

The $F(\beta)$ function for different shapes of footing gain different form and different values for similar values of β, see Fig. 45. It is clear from presented formulas that the depth of the influence zone is not E dependent.

For selected shapes, the influence zone depth can be expressed in explicit form. For example for infinite strip footing the depth of the influence zone can be calculated as

$$H = 2a\frac{\pi}{4}\sqrt{\frac{2-2\nu}{1-2\nu}}\frac{1}{\ln\frac{\sin((\pi\gamma h)/2f_z)+1}{\cos((\pi\gamma h)/2f_z)}} \tag{5.6}$$

where a is a half of the strip width, f_z is the load magnitude, h represents the depth of excavation, γ stands for the unit weight of the soil and ν is the Poisson's ratio.

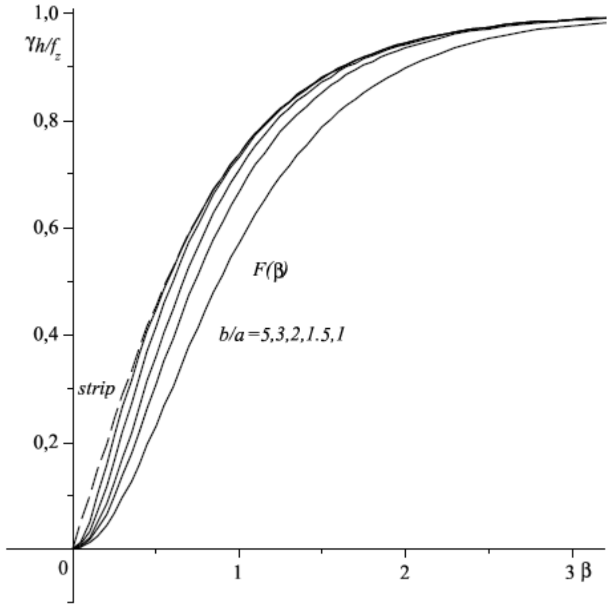

Fig. 45. *F (β)* function for rectangular load area and strip footing

Practical applications of the presented theory and principles can be found in following chapter.

5.3. Influence zone theory and groundwater table variations

For saturated soils is the change of groundwater table level directly proportional to the change of the depth of influence zone. As the groundwater table rises and soil increases its level of saturation or pore pressures the over consolidation ratio decreases and part of the load is carried by pore pressures. The shear zone contribution becomes smaller and the depth of the influence zone decreases. The subsoil behavior is getting closer to the Winkler's model. Assuming theoretical case for influence zone approaching zero depth, we obtain only Winkler's model.

This description, however, is not valid for unsaturated soil as it does not involve the suction cancellation effect and in practice it should be used for coarse grained soils such as gravel rather than for clay soil. On contrary in soils with a significant suction effect the rising level of saturation first cancel this effect. So at first the influence zone is getting deeper because of the lack of the negative pore pressures. This effect can be simulated with decrease in pre-consolidation pressures as shown in next chapter. Based on the experimental results and practical experience we suggest following approach for pre-consolidation pressure reduction:

a) Coarse grained soils

a1) First wetting after the soil was compacted or when groundwater table rises above long term maximal level – the effect depends highly on the present moisture content of the wetted soil but for rough estimation the reduction of pre-consolidation pressure by the portion which correspond with the portion of influence zone flooded seems to provide reasonably accurate results

a2) Repeated wetting cycles, i.e. groundwater table variation within normal positions – for small variation of the groundwater is the effect negligible and for larger variation (such as due to draining deep foundation pit) the effect should be taken into account by increasing the value of *F(β)*

$$\frac{\gamma h + \gamma_w h_w}{f_z} = F(\beta) \qquad (5.7)$$

b) Fine grained soils

b1) Short term action of water or limited water access (e.g. infiltration trenches or galleries) – – the effect depends highly on the present moisture content of the wetted soil but for rough estimation the cancellation of pre-consolidation pressure seems to provide reasonably accurate results

b2) Long term groundwater table rise – experimental investigation necessary

Chapter 6

PRACTICAL APPLICATIONS AND NUMERICAL MODELLING

This chapter is focused on practical examples of use of the above described approaches and theories. At first we concentrate on application of the influence zone (IZ) theory on back analysis of in-situ plate load tests and full scale laboratory experiments, and on back analysis of in-situ dilatometric measurements in deep boreholes carried out for Brenner base tunnel excavations.

Next part focuses on application of general knowledge of unsaturated soils behaviour on current practical issues regarding infiltration policy for new structures and groundwater table shift due to reconstruction of hydraulic structures.

Description of risk analysis for floods and proposed enhancement of the losses on buildings and structures is presented in the third part of this chapter.

Last part deals with numerical modelling of the full scale experiments presented in chapter 4. Difficulties with calibration of material parameters of the used models as well as the accepted assumptions are commented.

6.1. Influence zone change and elastic layer theory

6.1.1. Static plate load tests

It was experimentally confirmed that by using plates with different diameters and loading forces and employing generally used Bousinesq formula (Eq. 5.2) to obtain secant modulus of the subsoil, very different results can be achieved for the same soil. (Kuklik et al. 2008a).

$$E_0 = \frac{\pi}{2}\left(1-\nu^2\right)\left(\frac{f_z r}{s_{tot}}\right) \tag{6.1}$$

where r is the radius of the plate, s_{tot} represents final settlement, f_z is the load magnitude and ν is the Poisson's ratio.

As the formula was originally derived under the infinite half-space assumption, which is very useful as it allows for explicit estimation of secant modulus but also limiting as it neglect the phenomenon of soil's memory, it should be use only, when the depth of the influence zone exceeds approximately 2 times the diameter. For shallow influence zones the resulting secant moduli obtained from the formula will be overestimated, i.e. the subsoil would seem to be stiffer than it is.

This could be demonstrated on static plate load tests carried out in-situ on construction site in Prague, which was prepared for foundation slab construction. Two plates with diameters r_1 = 0.399 m (contact area S = 0.5 m^2) and r_2 = 0.1785 m (contact area S = 0.1 m^2). Due to limited possibilities for reaction force constriction, which were represented by the heaviest machinery available on construction site, the applied load in term of stress were insufficient for the larger plate reaching only to 366 kPa in contrast to 1200 kPa for the smaller plate (Kuklik, 2006). The Poisson's ration for the soil was assumed equal 0.25 and the depth of the influence zone for both cases was calculated to be approximately 0.6 m. Following table summarizes the measured data and calculated secant moduli from three in-situ experiments.

Tab. 8. Summary of experimental data and calculated secant moduli

Test No.	Applied load (kPa)	Measured settlement (mm)	Calculated secant modulus (MPa)
1 (larger plate)	366	1.27	169.3
2 (smaller plate)	1200	3.93	80.3
3 (smaller plate)	1000	2.49	105.6

Employing professional FEM code ADINA v. 8.1 results of the plate load tests were obtained numerically for the larger plate. The settlement was calculated 0.97 mm for secant modulus E_0 = 100 MPa and 1.21 mm for E_0 = 80 MPa yielding the average settlement 1.09 mm. Comparing with measured data the numerical results (1.09 vs. 1.27 mm) seem acceptable. Small discrepancy can be explained as follows. The first overestimation of the secant modulus is due to back analysis using Boussinesq formula, secondly there is a shear lack inside the soil on boundary the rigid plate, which was not simulated.

In order to confirm applicability of theory and recommendations introduced in chapter 5, it was applied on the results from full scale experiments presented in chapter 4.

For the influence zone depth estimation software DEPTH or TPS Overconsolidation was used while for settlement calculations the subsoil reaction was described according to known Winkler-Pasternak model, see Eq. 6.2

$$C_1 w - C_2 \Delta w = f_z \tag{6.2}$$

where parameters C_1 and C_2 are calculated in agreement with the influence zone theory, and while assuming elastic layer instead of original parameters, by using identity between compliance matrixes, see Appendix A. This solution is incorporated into many software packages. For this thesis purposes we used Geo 5 Beam on elastic foundation.

Tab. 9. Static plate load test on G2 soil in a view of elastic layer theory

Exp. No.*	3 BW	3 AW	4	5 BW	5 AW
Applied load (kPa)	1010	1010	710	710	710
Measured settlement (mm)	1.11	1.32	0.81	0.57	0.64
Measure water table from top of the specimen (m)	---	0.41	---	---	0.35
Calculated secant modulus (MPa)	200	200	200	290	290
Poisson's ration	0.2	0.2	0.2	0.2	0.2
Assumed pre-consolidation (kPa)	300	150	300	300	200
Depth of IZ (m)	0.79	1.63	0.53	0.53	0.83
C_1 (MNm^{-3})	351.6	210.4	487.1	706.3	493.9
C_2 (MNm^{-1})	8.6	11.8	7.1	10.3	12.8
Calculated settlement (mm)	1.0	1.3	0.8	0.5	0.7

*(BW stands for "before wetting" and AW for "after wetting")

Tab. 10. Static plate load test on F5 soil in a view of elastic layer theory

Exp. No.*	1	3 BW	3 BW adj.**	3AW
Applied load (kPa)	400	400	400	400
Measured settlement (mm)	4.82	1.25	1.25	6.25
Measure water table from top of the specimen (m)	---	---	---	0.6
Calculated secant modulus (MPa)	16	73	37	37
Poisson's ration	0.4	0.4	0.4	0.4
Assumed pre-consolidation	150	300	300	300

(kPa)				
Depth of IZ (m)	0.92	0.36	0.36	147
C_1 (MNm^{-3})	44.2	460.1	233.4	2.1
C_2 (MNm^{-1})	0.8	2.0	1.0	48.5
Calculated settlement (mm)	4.8	0.6	1.2	5.9

*(BW stands for "before wetting" and AW for "after wetting")

** Secant modulus was adjusted to represent the soil as the depth of the influence zone did not correspond with the idea of half space

Two facts can be observed in tables 9 and 10. First it is the already mentioned issue with using Boussinesq formula for calculation of secant modulus when the influence zone is not sufficiently deep compared to the loading plate.

Second, it is the increase in the depth of the influence zone after suction is cancelled. Even for G2 soils the depth of IZ exceeds the real depth of the specimen, which is approximately one meter. However as the aim is to describe the change in soils behaviour or response to suction cancellation respectively, such approach can be found justifiable though not physically sound.

6.1.2. Dilatometric measurements and analysis

Determination of geomechanical properties of rock massif presents difficulties due to the problems arising in sampling, specimen preparation and testing. Questionable is also the accuracy of the results for more complex formations since the tests are usually conducted on small specimens that cannot depict the structure. One of the methods used to directly evaluate the actual geomechanical properties of the rock mass is a dilatometer analysis.

The dilatometer determination of the rock mass mechanical properties is based on real time measurement of the applied pressure and change of the borehole diameter. The deformation is directly measured by three transducers installed in the metal body of the dilatometer probe.

A dilatometer test is usually performed in two, three or four cycles. The first testing cycle is preceded by, so called, base pressure inflation of the probe. The first cycle should guarantee a good contact between the probe and the borehole wall. The base pressure is typically a hydrostatic pressure plus 0,15 – 0,5 MPa.

While the first cycle consist of loading and subsequent unloading to the base pressure, in case of all other cycles the loading path consist of two parts. At first, the maximum pressure of the previous cycle is reached and then the loading continues to a higher level followed by unloading.

The common test evaluation is derived from three boundary conditions. Namely they are the zero displacement in the radial direction in infinity distance, the measured displacement on the probe-borehole interface and the known pressure in the same place.

The new formula introduced two new aspects (Kuklík et al., 2008b). First, it was the plastic zone around the borehole wall and secondly it was the phenomenon of influence zone presenting the assumption of zero displacement in the final distance from the borehole. The newly introduced formula is consistent with the common one and it can be shown that in limit case, where thickness of plastic zone is zero and influence zone is infinite, both formulas are equal.

$$E = \frac{\Delta p.(1+\nu)}{\frac{1}{2}\Delta d.\frac{\overline{R}_1}{R_2^2 - \overline{R}_1^2}\left(\frac{R_2^2}{\overline{R}_1^2} + \frac{1}{1-2\nu}\right)} \tag{6.3}$$

where Δp = pressure difference; Δd = change of borehole diameter; ν = Poisson's ratio; $\overline{R}_1$ = thickness of plastic zone; R_2 = thickness of influence zone.

In order to confirm the agreement between proposed formula based on influence zone theory and numerical simulation ADINA code was selected for numerical analysis. Due to the nature of the problem, the axisymmetric analysis was found to be most suitable. Using the appropriate time function, and with help of death element time it was possible to simulate the entire process of consolidation, material excavation and, finally, the dilatometer test, see Fig. 45 .

As an example was used dilatometer test from 986.5 m deep borehole in chlorite schist. The test was a part of a Brenner base tunnel geotechnical investigation project. Label of the tested borehole is Va-B-03/04. All necessary data were obtained from Kuklík et al. (2008b) and from Zalesky et al. (2006).

For the analysis purposes it was assumed that the borehole along the dilatometer packer sleeve and in close surroundings has constant diameter d = 92 mm. The total average displacement of the borehole wall was Δd_t = 80.10-6 m, while the unloading /elastic path reaches $\Delta d_e = 30.10^{-6}$ m. The entire test log can be seen on Fig. 47.

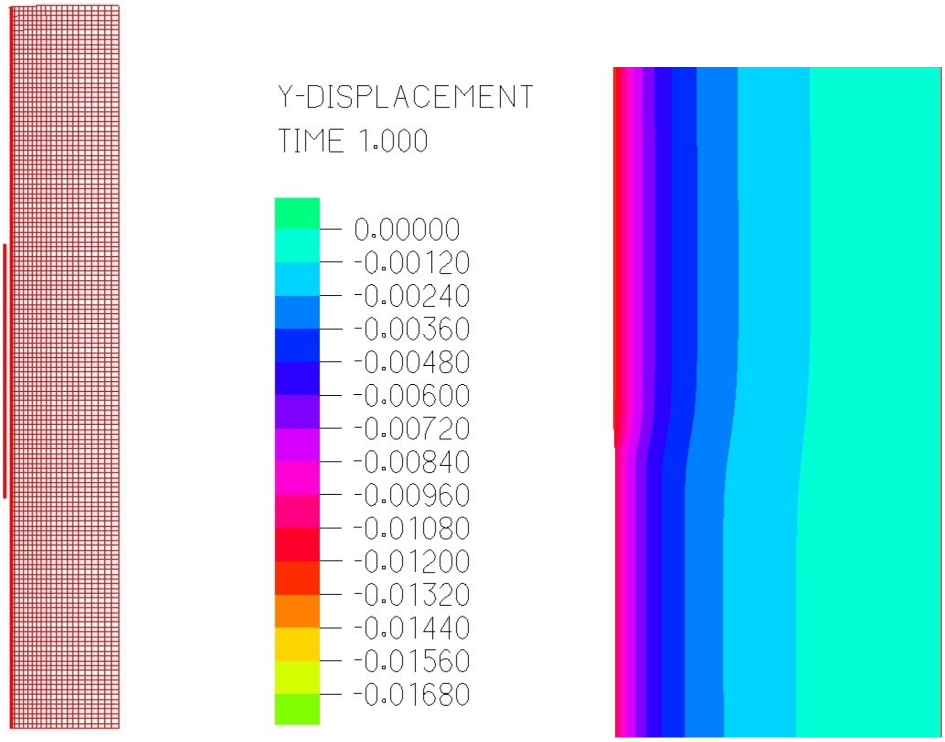

Fig. 46 Numerical simulation of dilatometric test – mesh before deformation and detail of the contact during loading

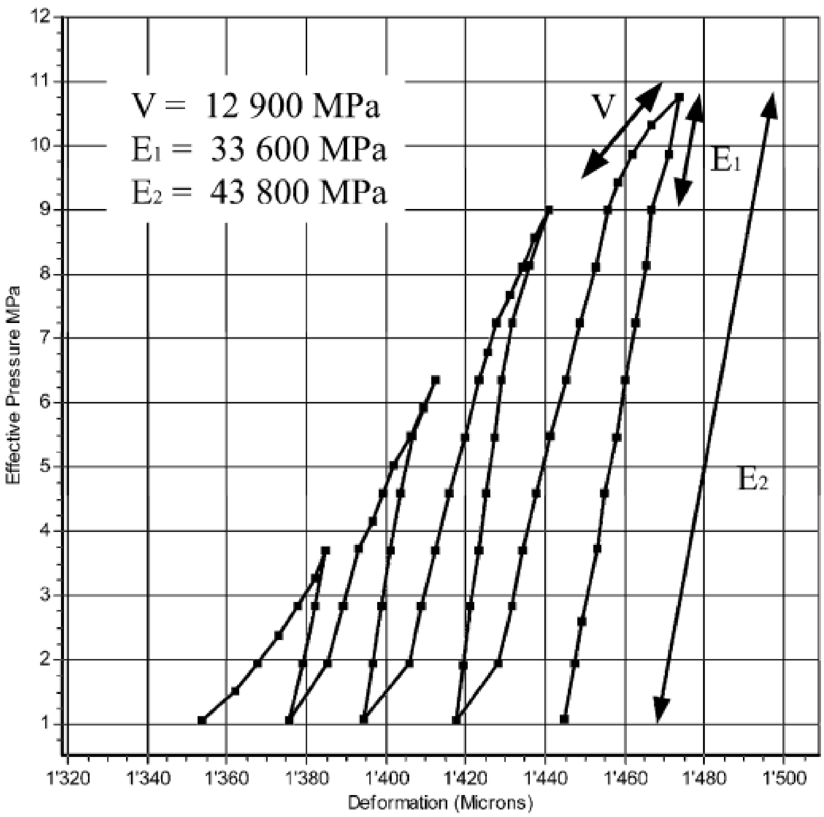

Fig. 47 Dilatometer test in borehole Va-B-03/04s, 986.5 m depth, chlorite schist. Graphical representation from the DilatoII software program: average from deformation measurements of all three extensometers (Zalesky et al., 2006)

Due to the lack of laboratory data Poisson ratio of the rock was assumed to be ν = 0.33. Results in the following table have been obtained for the same study case assuming $R_2 = 5\,\overline{R}_1$.

Tab. 11 Values of E according to new formula (Kuklik and Broucek, 2008)

$\overline{R}_1$	1,1R$_1$	1,2R$_1$	1,3R$_1$	1,4R$_1$	1,5R$_1$	1,6R$_1$	1,7R$_1$	1,9R$_1$	1,9R$_1$	Original formula
E (GPa)	41,6	45,4	49,2	53,0	56,8	60,4	64,3	68,1	71,9	43,8

Numerous calculations have been carried out to simulate the dilatometer test incorporating both elasticity and plasticity (Mohr – Coulomb) for rock and also various contact elements.

The initial stress state was either directly prescribed or reached by self-weight load with appropriate time function. It can be point out that both approaches lead to similar results. This cannot be stated for the different modelling approaches on the contact, as they tend to give slightly more variable results.

The results indicated that plastic zone around borehole is small and can be nearly neglected. So in the new formula borehole radius can be used instead of plastic zone radius with negligible loss of accuracy. The main reason for this simplification is the depth of the borehole or actually the depth in which the measurement took place. In case of shallow borehole analysis attention needs to be paid to the possible increase of plastic zone diameter.

The results also confirmed the improvement in accuracy when the influence zone theory is used for evaluation of rock mass parameters. When the characteristics evaluated from the original formula were used, the displacement (rock deformation) were either too small or the effective stress for the required deformation was nearly double than measured. Generally good results can be obtained for width of the influence zone in range from 2.R_1 to 5.R_1, where R_1 is borehole radius.

Unfortunately this range will presumably vary for different rocks and also for different testing depth, so proper numerical back analysis has to be carried out in order to secure the accuracy of interpretation of measured results.

Neglecting the idea of an influence zone and calculating the deformation parameters of the rock mass with the original formula tends to give higher values of deformation modulus and Young's modulus. If these values should be used further for numerical simulations of the geotechnical work (e.g. tunnel excavation) the loss in model accuracy can be very high. Optionally such numbers should be used only as an upper limit and the scale effect is considered.

6.2. General knowledge about unsaturated soils behaviour

Many examples of problems requiring application of general knowledge about unsaturated soils behaviour can be found even in the temperate climate in which is located Czech Republic. For the purpose of this part we select two current issues related to water management. At first we describe the debate concerning groundwater table position shift due to implementation of flood protection measures in the UNESCO listed town Cesky Krumlov. Second, the standing requirements of the civil service for infiltration of precipitation water from newly constructed buildings and impermeable areas is discussed from the point of view of potential damage to the adjacent construction when the steady state is disrupted.

6.2.1. Flood protection measures

All sorts of non-structural and structural flood protection measures were supported by EU adaptation and mitigation programs including channel improvements, generally widening and deepening of channels, and flood barriers with deep and impermeable foundation structures i.e. sheet piles, pile walls etc. In most cases, no serious estimations regarding the groundwater regime change and its possible impact to the upper structures in protected areas were made. And again, in most of the cases, no abnormal behaviour of upper structures was reported. In the Cesky Krlumlov town, however, cracks were reported in the walls of historical buildings, many of them dated back to Middle Ages. The town centre is UNESCO listed and it would seem that our cultural heritage is at stake due to flood protection structures and channel improvement.

As presented in this thesis, and by many other authors, the soil's ability to memorize a certain loading history, the highest level of loading respectively, which is mathematically represented by the over-consolidation ratio, and initial void ratio, can be seriously influenced by the saturation level of the soil in several ways. Furthermore the material parameters of soils and consequently the response to loading characterised as settlement are influenced by the groundwater. So in general, disruption of the long term steady state by construction works during building phase or structures itself may cause additional deformation of the subsoil and potentially cracks in upper structure. It should be noted, however, that for soils in saturated state the change in pore pressures needs to be significant with relation to the present stress state and in case of the unsaturated soils, which do not undergo excessive shrinkage during saturation level decrease, the deformation will only take place when the groundwater table rises above the long term maximum.

Based on all the presented arguments and theories and experimental results presented in this thesis we can conclude that lowering the groundwater table by several decimetres or one meter as in the case of Cesky Krumlov can hardly cause additional deformation of upper structures which would result in cracks development in walls of historical buildings.

It is to be emphasized, however, that every channel improvement or other protective measures should be considered from broader perspective carefully evaluating all possible impacts on the steady state of the hydrogeological regime in particular areas. In sensitive cases, such as historic town centres, passportisation of selected building and monitoring of the hydrogeological regime can prove to be extremely helpful.

6.2.2. Infiltration from large impermeable areas

Current policy of the civil service regarding the management of water from precipitation requires the owners of new properties to infiltrate, or use otherwise, all the whole amount of water without using sewer systems. This approach is very unfortunate when applied without the respect to the subsoil reaction on the large quantity of water and could be potentially dangerous to adjacent structures.

Nowadays, the infiltration capacity of subsoil and storativities of appropriate aquifers are estimated and analysed by field infiltration or pumping tests and numerical simulations based on models of flow through porous material. Such analysis presents sophisticated results and is perfectly suitable for the original purpose, i.e. to design the infiltration galleries or trenches and confirm that the infiltration is possible. The main issue is the absence of geotechnical analysis of the impact of estimated changes on the foundation and upper structures. Even if such analysis is carried out it usually neglects the so important differences between saturated and unsaturated soil behaviour assuming only deformation from positive pore pressure.

Data for the following example of newly designed block of flats were obtained from the field but due to on-going planning enquiry it was not yet published. The present situation involves several older buildings located on lands adjacent to the planned block. Subsoil can be described as silt loam and silty sand followed by weathered silty sandstones and sandstones. The neighbouring buildings which include family houses as well as tower block are founded on the silt loams or silty sands using strip foundations under the basement level. Results from numerical simulations of groundwater flow show permanent increase of groundwater table by 0.35 – 0.5 m and average maximum level would even touch the foundation base.

Applying the saturated soils (classical soil mechanics) approach would yield in variation of effective stress between 3.5 and 5 kPa which is negligible change when compared to present state. Applying the unsaturated approach, however, would yield in suction cancellation and dramatic increase in settlement for the silt loams case. Unfortunately, the understanding of unsaturated soils behaviour just only started to be recognized by the geotechnical engineers dealing most of the time with common saturated problems.

6.3. Risk analysis for flood events

The internal erosion problems as well as additional deformations caused by the change of mechanical behaviour of unsaturated soils when subjected to suction cancellation can fully emerge during flood events and be the decisive source of damage to the upper structures. The flood risk assessment became debated on national level as well as on European level in recent decades thanks to the concept or rather the obsession of risk evaluation and potential damage monetization, which is enabled and supported by massive extension of the numerical models and use of GIS software packages. Nevertheless, for evaluation of the impact of flood events and for the effect of flood protection schemes the risk analysis presents the most impartial tool. The definition of the risk due to flood is generally defined in the following form

$$R = \int_{0}^{+\infty} D(Q)\; f(Q)\; dQ \cong \int_{Q_a}^{Q_b} D(Q)\; f(Q)\; dQ \qquad (6.4)$$

where R is the average risk for 1 year (that is average potential loss in one year over a very long period), D is a damage caused by flow of magnitude Q, $f(Q)$ is the probability density function for flow of magnitude, Q_a is the magnitude of flow that starts inflicting damage (3rd flood activity degree) and Q_b is the flow magnitude which probability of occurrence is close to zero. The damage to the buildings is so far considered by using loss functions which are related to the depth of the water, and a type of the building (Satrapa, 1999), (Kang et al., 2005) or its purpose. Severe structural damage, which usually requires demolition of the building with appropriate losses, is not necessary directly proportional to the depth of the water or flow velocity or its combination.

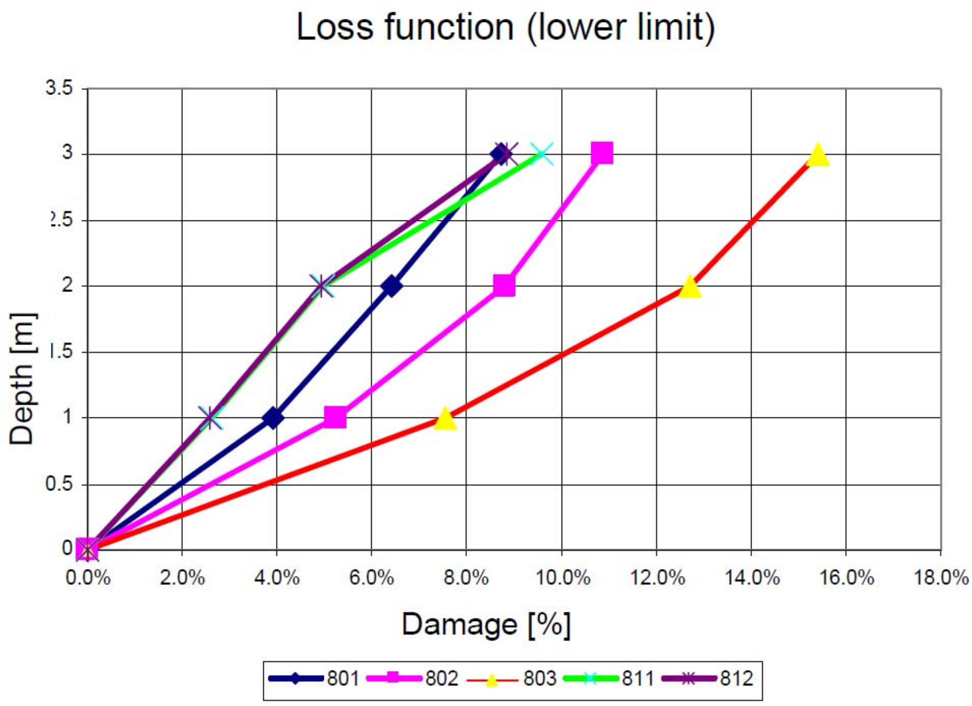

Fig. 48. Example of Loss functions for different categories of buildings (Satrapa et al., 2006)

As shown in the appropriate parts of this work, the subsoil is highly influenced by the groundwater flow, which is undoubtedly very variable during the natural flood events. Therefore, it does not come as a surprise that more rigorous approach reveals that the real losses must also depend on the subsoil type, foundation type and also the characteristics of the upper structure. These conclusions were made after the evaluation of the losses on buildings and structures after big flood events in the year 2002 (Valenta et al., 2006). Following recommendations and coefficients for loss functions enhancement resulted from the analysis of damaged buildings in the past two decades.

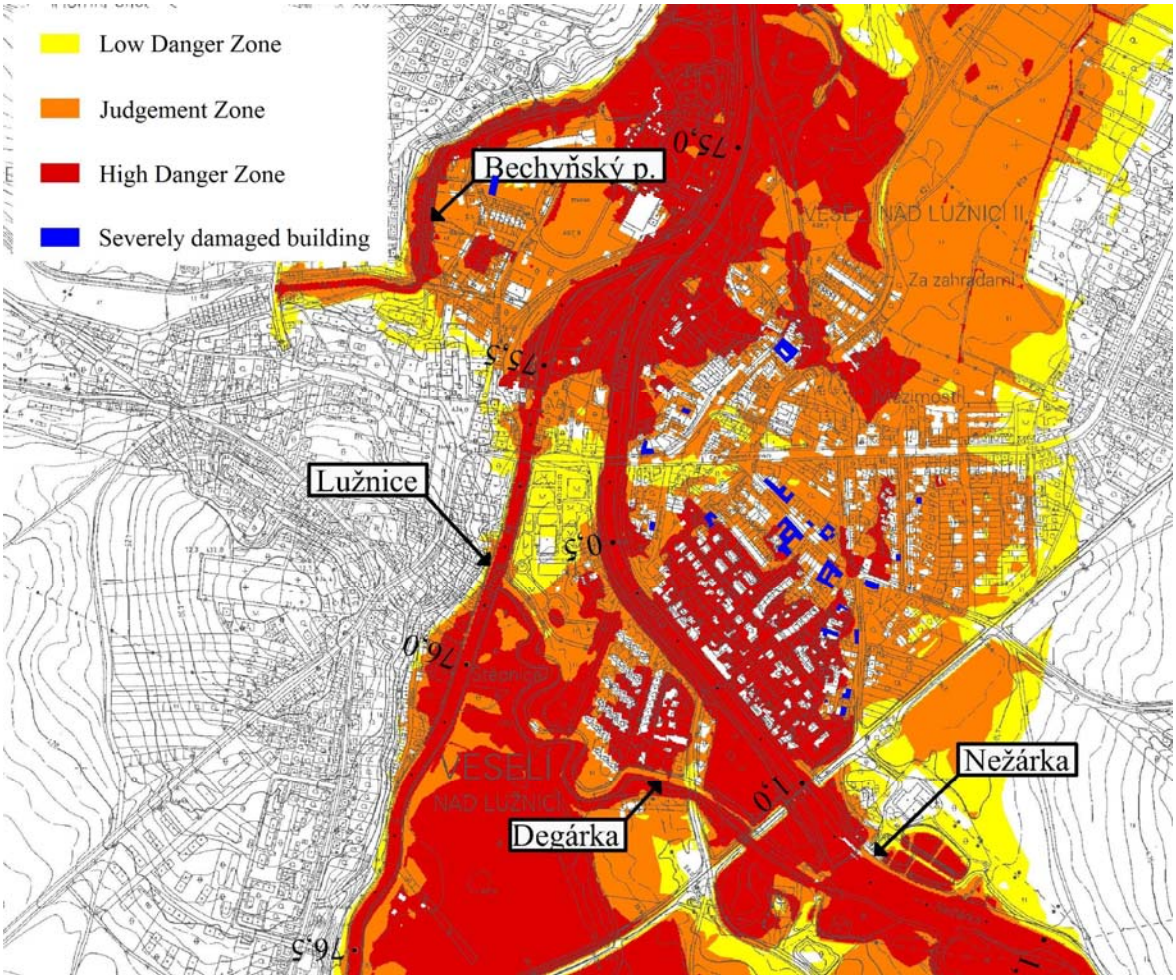

Fig. 49. Danger zones for buildings evaluated according to USBR (1988) for flood in the year 2002 in Veselí n. Lužnicí Town and locations of buildings with severe structural damage (Broucek and Kuklik, 2006)

In order to limit the increase in complexity of the problem we suggest that each loss function would be increased by only one number, i.e. for each building type, based only on the "flood structural hazard category". Even this single coefficient increases the time necessary for the assessment as every entity (building) needs to have three variables instead of only one (the type, and area). The categorisation is based on following assumptions:

- Structures of immense cultural or historical values are assessed separately.
- The urban areas have been flooded in the past (this assumption limits the possibility of full soils structure collapse and with respect to the history of majority of urban areas can be made without serious reduction of generality of the proposed approach).

- The area does not contain any backfilled trenches or channels (presence of this preferential flow paths localise the problem and require the relevant buildings to be assessed separately).
- The building should be attributed the lowest category it can qualify for.

Tab. 12. Flood structural hazard categories

Category no.	1
Foundation structure	piles, piled rafts or other deep foundations; slabs designed with respect to the possible groundwater table variations
Subsoil	solid rock
Upper structure material	welded steel
Category no.	2
Foundation structure	slabs designed without respect to the groundwater table variations; foundation strips below 2nd basement level
Subsoil	weathered rock
Upper structure material	cast-in place reinforced concrete
Category no.	3
Foundation structure	foundation strips below 1st basement level
Subsoil	coarse grained soils
Upper structure material	precast concrete; bricks and blocks with compressive strength higher than 5 MPa
Category no.	4
Foundation structure	other shallow foundations
Subsoil	fine grained soils
Upper structure material	adobe bricks; biodegradable materials

The proposed additional percentage of losses, as shown in the following table, is not water depth dependent and should be attributed when the water surface touches the buildings perimeter.

Tab. 13. Additional losses to buildings

Flood structural hazard category	Influence of the subsoil – flood reaction	Additional losses (%)*
1	negligible	0
2	small	1
3	significant	5
4	determining	15

*This value should be added to original loss function

Although application of the above described principles presents more rigorous approach an argument can be raised stating the actual values of losses, i.e. real collected data about monetized losses after flood events, possess the capacity and in fact nowadays include the heavy structural damage using averaging principles. Therefore the use of suggested categories and principles has low chance to be incorporated into EU methodologies in the near future.

6.4. Numerical modelling

Results from the full scale experiments presented in chapter 4 and in appendixes B and C were meant to be for calibration and confirmation of constitutive models as well as for estimation of the behaviour based on analogy. Following commented examples of application of constitutive models, which theoretical bases were presented in chapter 2, are included here to support the idea of laboratory full scale experiments.

6.4.1. Modified Cam Clay (SIFEL)

The implementation of the Modified Cam Clay (MCC) model prepared in the SIFEL package was not so far successfully used for simulation of the wetting experiments described. Therefore we concentrate on experiment with constant degree of saturation on silt loam, which can be simulated using classical approach. Regular mesh consisting of quadrilateral finite elements using linear interpolation functions was employed. Loading plate is assumed to be rigid and the problem is simplified due to axial symmetry. The unchanging initial tangential stiffness matrix limits the possibilities of the code but also stabilizes and accelerates the computations.

The necessary material parameters were obtained from engineering assessment (based on the compaction experiment – void ratios) and confronted with values presented in literature for similar soils. So, the calibration was done only for two parameters, i.e. elasticity modulus and pre-consolidation pressure by simple trial and error method when as initial values we used estimation based on the Boussinesq equation for E and on IZ theory for pre-consolidation p_{c0}.

The behaviour of the specimen before the first loading cycle is difficult to simulate as the overall pre-consolidation should be distributed in layer (due to compaction).

Therefore two different approaches were employed to simulate the experiment. First approach focuses on the good approximation of the loading path while the unloading path is not considered for the calibration.

Second approach neglects the initial loading cycle and focuses on calibration of the rest of the experiment. Table 14 summarizes the calibrated parameters, while following figures 50 – 52 present deformed mesh and plastic strains, horizontal and vertical stress and displacement for first approach at the maximal loading point and figures 53 –55 present the same for second approach. The load – displacement chart for the plate comparing measured and computed data is presented in Fig. 56.

Tab. 14. Material parameters of MCC model

Parameter	Approach no. 1	Approach no. 2
λ	0.148	0.148
κ	0.037	0.037
e_0	2	2
p_{c0} *(OCR)*	300 kPa	280
M	0.69	0.69
E	25 MPa	55
ν	0.4	0.4

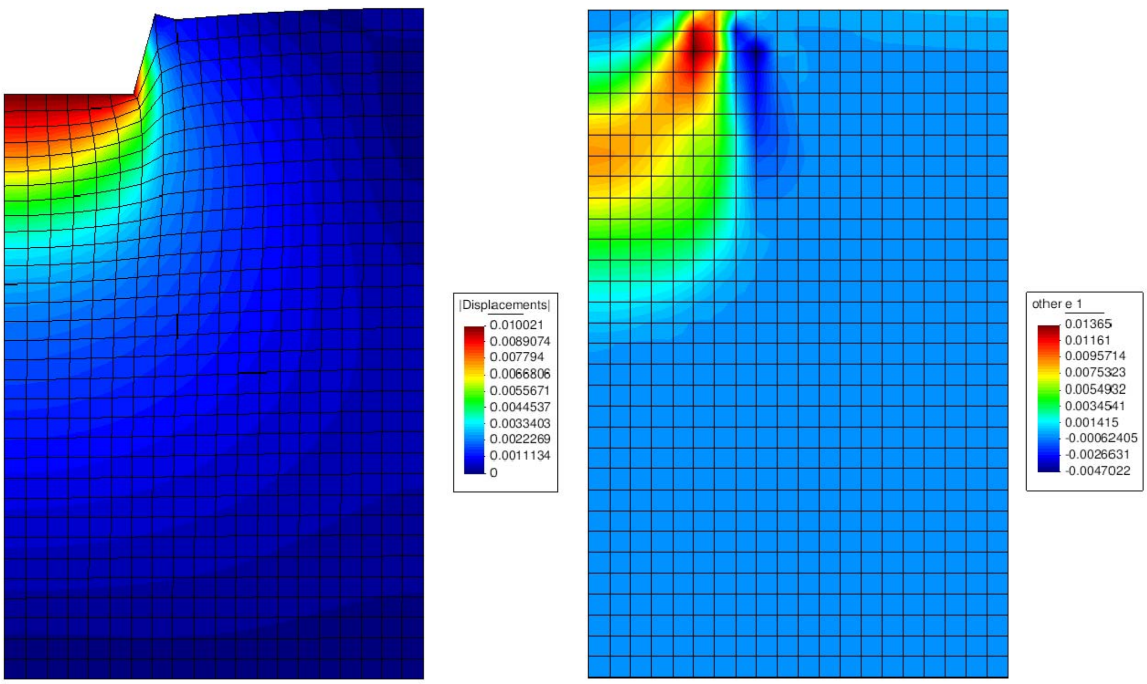

Fig. 50. Absolute value of displacement and deformed mesh (left – scaled 10x) and plastic strains (right) for the first approach and load 500 kPa

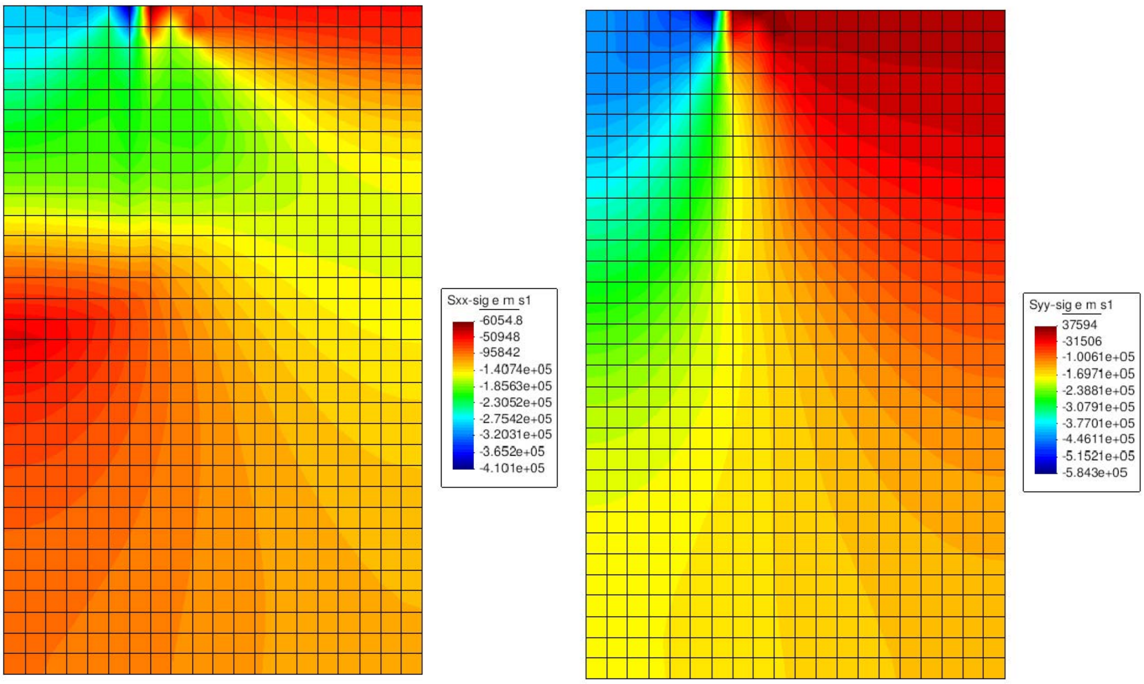

Fig. 51. Horizontal stress (left) and vertical stress (right) for the first approach and load 500 kPa

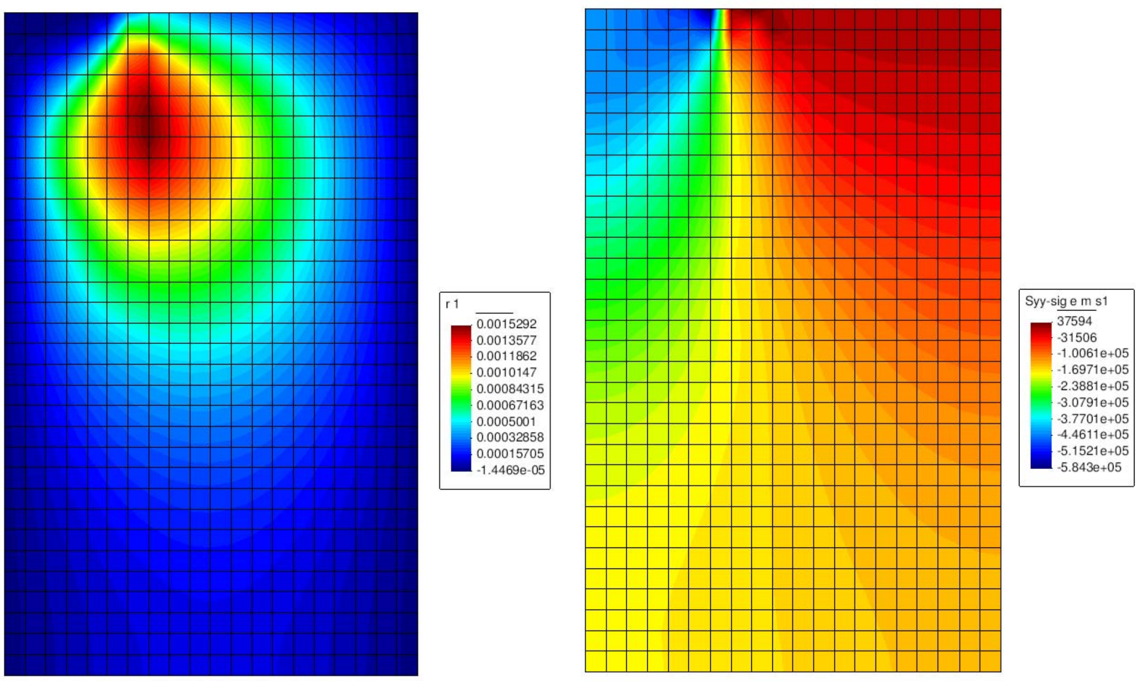

Fig. 52. Horizontal (left) and vertical (right) displacement for the first approach and load 500 kPa

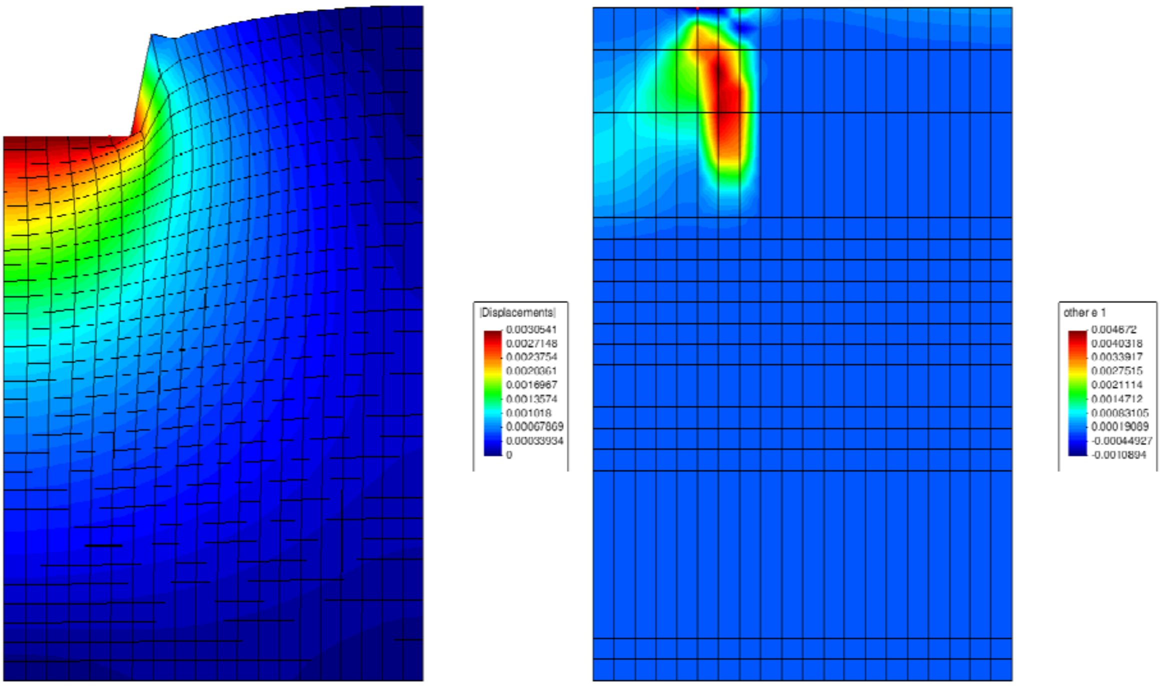

Fig. 53. Absolute value of displacement and deformed mesh (left – scaled 50x) and plastic strains (right) for the second approach and load 500 kPa

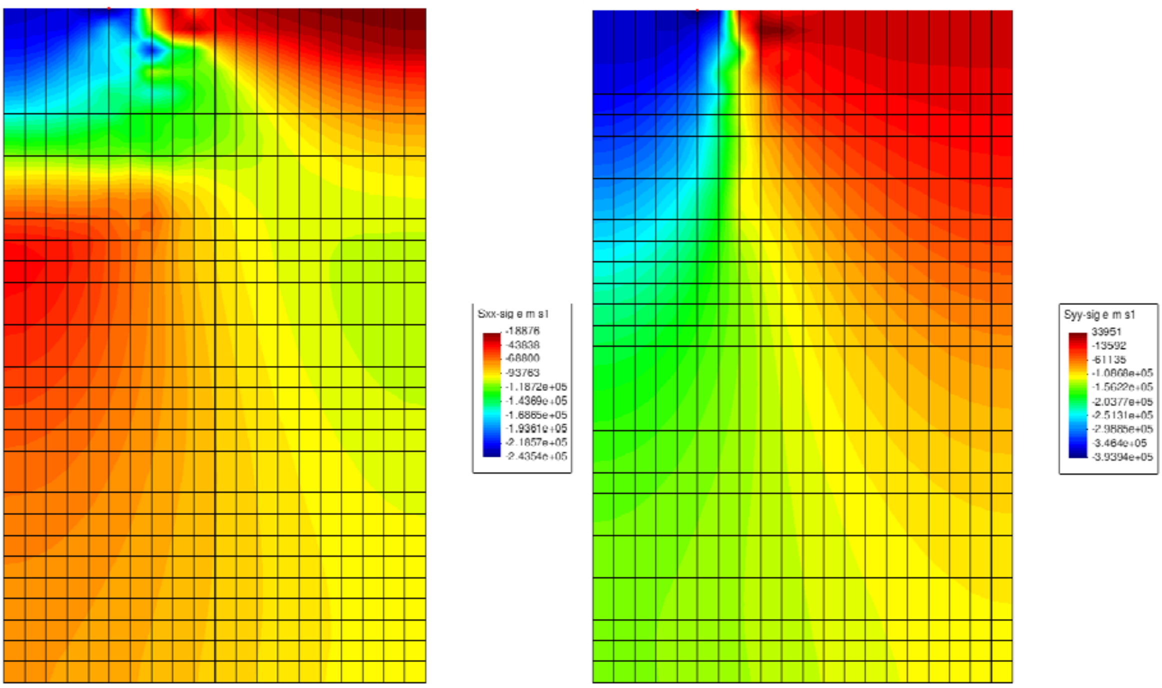

Fig. 54. Horizontal stress (left) and vertical stress (right) for the second approach and load 500 kPa

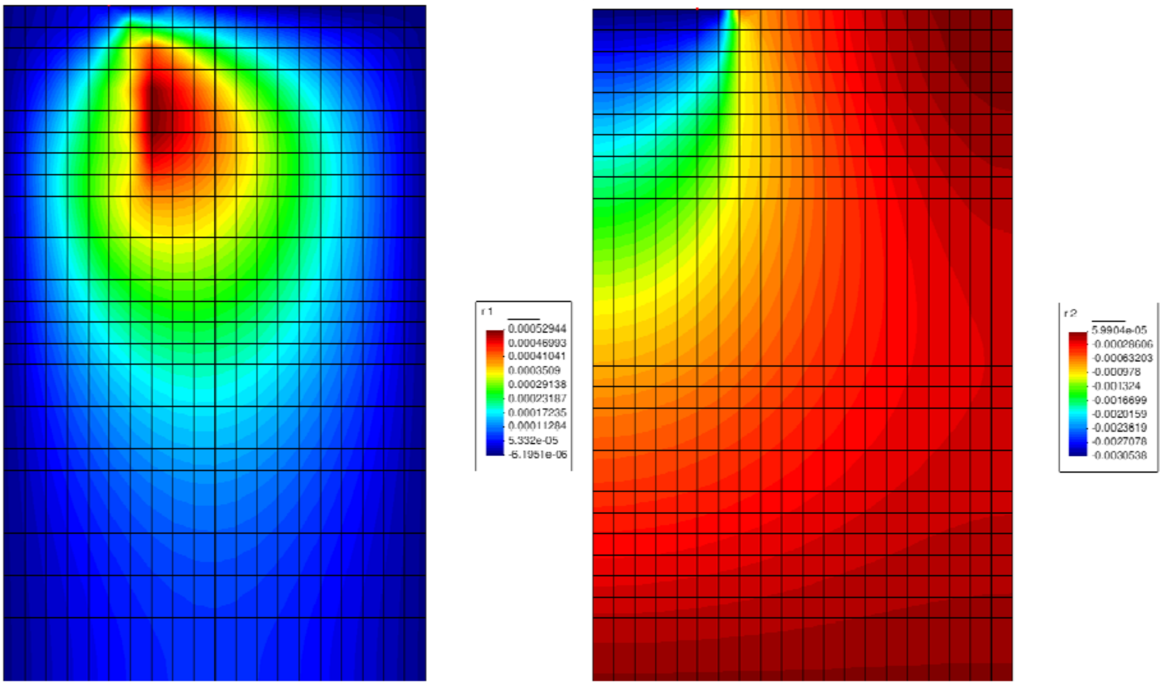

Fig. 55. Horizontal (left) and vertical (right) displacement for the second approach and load 500 kPa

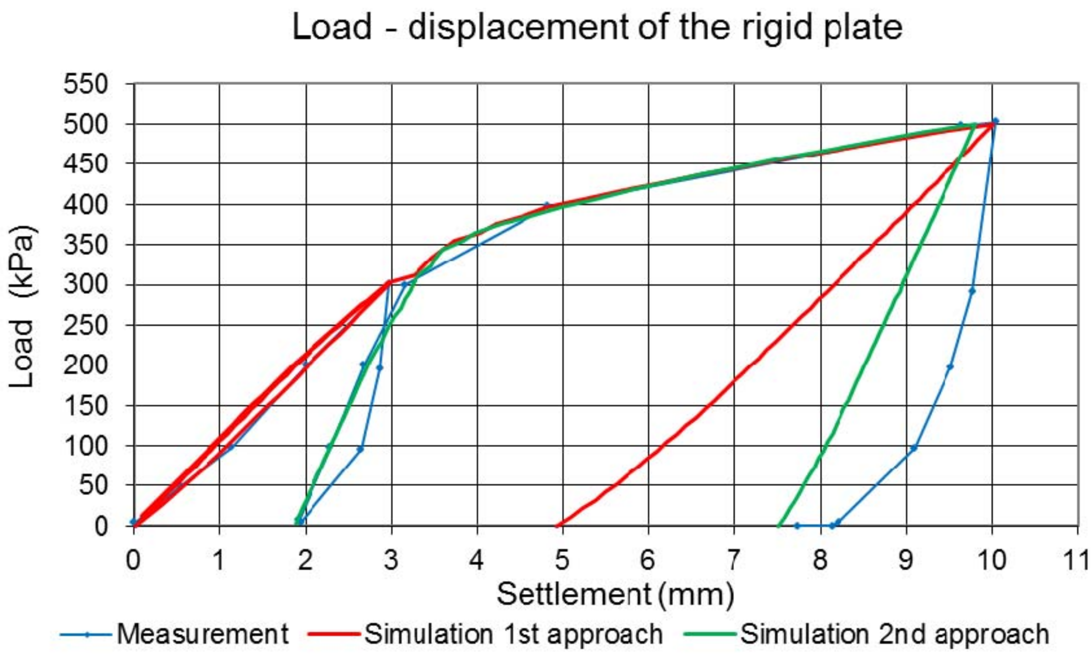

Fig. 56. Results comparison with full scale experiment

Even though both approaches are approximating well the part of the path they were meant to, we expect to gain better results when the tangential stiffness matrix is re-calculated after each loading step. The larges discrepancies can be observed in the horizontal stress as the values from numerical models near the position of lateral pressure probe are approximately 150 kPa while the measured maximal values are as low as 27 kPa.

6.4.1. Hypoplasticity for clays (GEO 5)

The hypoplastic constitutive model presented in chapter 2 was implemented in GEO 5 v. 16 software package. The model is suitable for description of behaviour of saturated or unsaturated fine grained soils, especially clays, under constant degree of saturation boundary conditions. For the purpose of this thesis we use the hypoplastic model to simulate the full scale experiment on silt loam as in case of Modified Cam Clay model (MCC). Finite element mesh was employed consisting of 6-nodes triangular finite elements with quadratic interpolation functions. Loading plate is assumed to be rigid and the problem is simplified due to axial symmetry. In contrast to the MCC model in SIFEL the tangential stiffness matrix was recalculated after every load step.

Material parameters were obtained partly from previous calculation from MCC model and partly from engineering assessment (based on the compaction experiment – void ratios) and confronted with values presented in literature for similar soils.

As in the case of MCC model, the behaviour of the specimen before the first loading cycle was found to be difficult to simulate as the overall pre-consolidation should be distributed in layer (due to compaction). This time only the second approach was applied, i.e. the initial loading cycle was neglected and calibration procedure focused only on of the rest of the experiment. Tab. 15 summarizes the calibrated parameters, while following Fig. 57 shows horizontal and vertical stresses (note that positive values are reserved for pressures and negative for tensions) and Fig. 58 presents horizontal and vertical displacement on deformed sample. The load – displacement chart for the plate comparing measured and computed data is presented in Fig. 59.

Tab. 15. Material parameters of hypoplastic model

Parameter	Value
λ^*	0.18
κ^*	0.003
N	1.4
φ_c	22°
r	0.01
e_{cur}	0.72

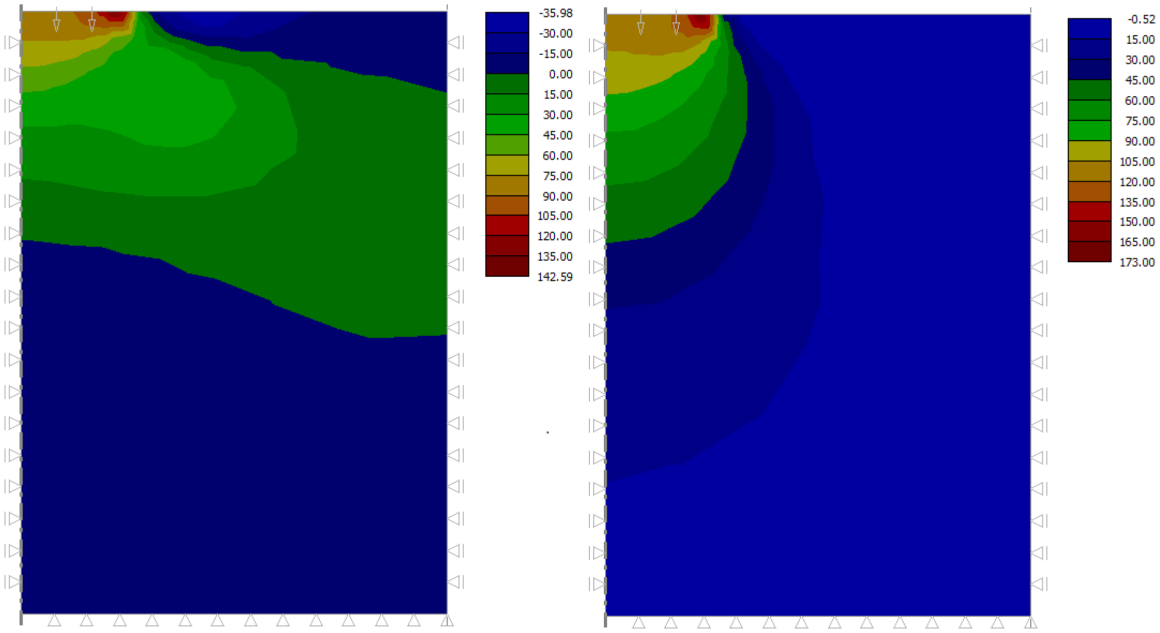

Fig. 57. Horizontal stress (left) and vertical stress (right) for the load 500 kPa

In contrast to MCC model calculated the horizontal stress and measured lateral pressure are very close. Calculated value is approximately 10 kPa while the measured value for vertical load 500 kPa is 27 kPa.

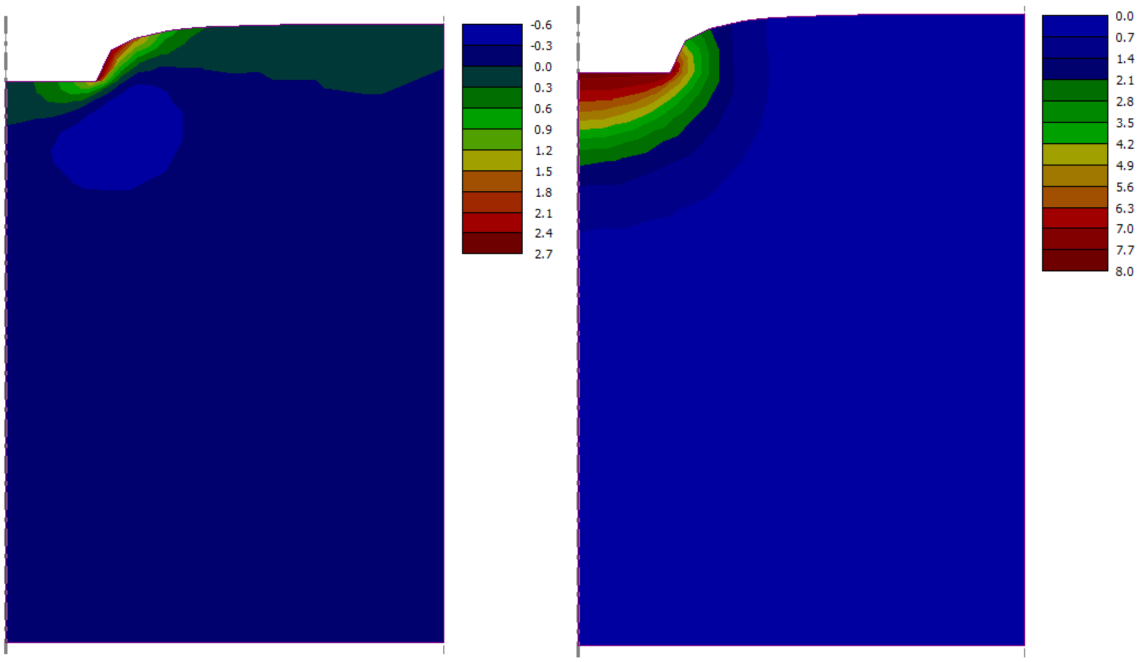

Fig. 58. Horizontal (left) and vertical (right) displacement on deformed specimen for the load 500 kPa

The shape of the shear zone from hypoplastic model approximates quite well the measured values, although some improvement could be achieved for the 50 mm distance. The only remaining issue is hysteretic behaviour on the unloading/reloading path which was not achieved for the full scale experiments even though it works when simulating the oedometric experiment.

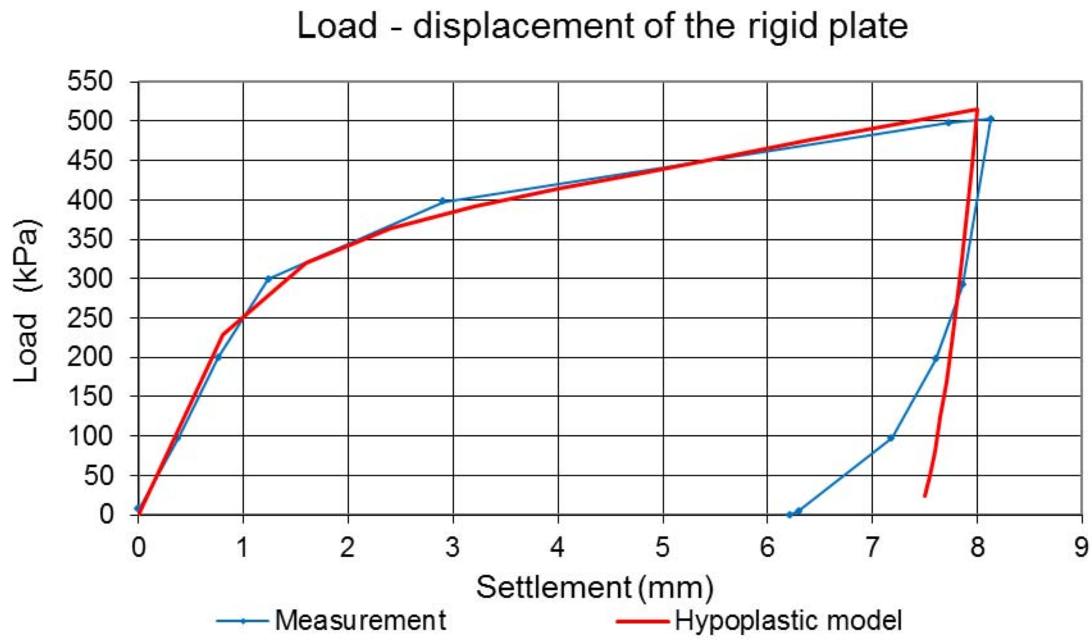

Fig. 59. Results comparison with full scale experiment

6.4.2. Hypoplasticity for unsaturated soils (PLAXIS)

The hypoplastic constitutive model for unsaturated soils presented in chapter 2 was implemented in PLAXIS software package. The model is suitable for description of behaviour of unsaturated fine grained soils under changing saturation boundary conditions, i.e. mainly the wetting induced collapse. The model was selected for simulation of 3rd full scale experiment on silt loam with suction cancellation. Finite element mesh was employed consisting of 15-nodes triangular finite elements. Loading plate was assumed to be rigid and the problem was simplified due to axial symmetry. Despite the successful application of the model for similar problem presented by Masin (2012) and the advantage of known material parameters of the soil for hypoplastic constitutive model from previous calculation in GEO 5, the obtained results were rather uncomplying. The matter is therefore still under consideration and subject of discussion with the author of the model.

Chapter 7

CONCLUSIONS AND FUTURE PERSPECTIVES

Understanding of the processes, which influence the behaviour of the subsoil and are caused by the presence or movement of the groundwater, can improve the design process and help to avoid unexpected and potentially damaging additional deformations of the upper structure. Although nowadays practice refers most of this influence to soils with large amount of fine particles the experiments proved that such influence is not negligible for sandy soils or gravel and is some cases it is even larger for coarse soils than for fine soils. The last part refers to weak performance of sands subjected to high hydraulic gradients.

Although, the theoretical base is very broad, it has been shown that it leaves enough space for improvement, especially in case of localized preferential flow and its coupling with mechanical behaviour but also on the field of unsaturated soils behaviour. Within the thesis we described the theoretical bases of the unsaturated poromechanics including different approaches to stress state variable and also the lack of consensus among leading authorities in the field. Several constitutive models approximating saturated and unsaturated behaviour were introduce including the criticism regarding their inconsistency with the physical elements of the system which comes partly due to widely used axis translation measuring technique for obtaining relevant data sets suction above cavitation limit. Description of the internal erosion and loss of particles was introduced together with its mathematical representation.

Due to the number of problems which could be solved with respect to the subsoil influenced by the groundwater it was necessary to concentrate the effort only selected parts of it. Even though highly sophisticated numerical models for unsaturated soils behaviour can often well simulate the real stress and strain behaviour for specified situations, their complexity, in terms of number of parameters and experiments for their identification, and demands, in terms of computational time and experienced individuals, excludes them from common practice towards rather unique problems and even there the spatial variability of the soils characteristics together with limited possibilities of geotechnical survey limits or decreases their accuracy. Slightly different situation can be observed around the "classical" saturated poromechanics models. Due to the possibility of using their assumptions and approaches even for soils with negative pore pressure but under suction steady state conditions these model have much wider area of possible application, however, hypoplastic or critical state constitutive models are not as widely used as Mohr-Coulomb or Drucker-Prager.

For the common engineering practice, however, it is necessary to search for a simple solution with large variety of use rather than increasing the overall complexity of the problem. That is why this thesis focuses on the experimental analysis and its evaluation followed by recommendations and sophisticated numerical models and their confirmation stand last in the line. Stand for full scale experiments with varying groundwater table was designed and constructed allowing for observation of all the phenomena and possibility of estimating the effects in situ due to selected measuring technique, i.e. static plate load test.

The results obtained from the full scale experiments proved to be very useful in understanding and evaluating of the processes through which the groundwater influence the behaviour of the subsoil leading to sets of recommendations in the influence zone theory and flood risk assessment. Some of the results obtained challenge the general assumptions, such as fine particle loss due to groundwater flow or negligibility of the effect of suction for coarse soils.

The results were also used to calibrate and confirm the ability of professional codes to approximate the soils behaviour during plate load tests and suction cancellation. The success of the last mentioned simulations was very limited despite the enormous computational time used.

All the presented information encourage further research activities in both major fields, i.e. internal erosion and unsaturated soils behaviour, with attention to both coarse and fine soils. Enhancements for the full scale experimental setup were presented in the thesis but large scale in-situ experiments are necessary to verify the suggested analogical approach followed by standard recommendations.

Use of random spatial fields with high correlation for adjacent elements could prove to be potentially very successful for evaluation of the risk of internal erosion for dam foundation and even for earth dam body with possible extension to unsteady state and estimation of effect of possible counter measures.

BIBLIOGRAPHY

Achmus, M., and K. Abdel-Rahman. (2003) The Influence of 'up-Scaling' on the Results of Particle Method Calculations of Non-Cohesive Soils *Numerical Modeling in Micromechanics Via Particle Methods*, Germany, 183-187

Aitchinson, G.D. (1965) Engineering Concepts of Moisture Equilibria and Moisture Changes in Soils, *Moisture Equilibria and Moisture Changes in Soils Beneath Covered Areas*, Australia, 7-21

Alonso, E.E, Gens, A. and Josa, A.(1990). A constitutive model for partially saturated soils. *Géotechnique*, 40(3), 405-430

Baker, R. and Frydman, S. (2009) Unsaturated soil mechanics, Critical review of physical foundations, *Eng. Geol.*, 106, 26-39

Bishop, A.W. (1959) The Principle of Effective Stress, *Teknisk Ukeblad*, 106(39), 859-863

Bittnar, Z. and Sejnoha, J. (1996) *Numerical Methods in Structural Mechanics*, ASCE Press, New York

Bligh, W.G. (1910). Dams, Barrages and Weirs on Porous Foundations. *Engineering News Record*, 64 , 708-710

Broucek, M., Kuklik, P. (2006) Důsledky změn hladiny podzemní vody v podloží a následné dopady na vrchní stavbu, In: *Staticko-konštrukčné a stavebno-fyzikálne problémy stavebných konštrukcií*, Košice (In Czech)

Buckingham, E. (1907) Studies of the Movement of Soil Moisture, *USDA Bur. of Soils, Bulletin No. 38*

Carman, P.C. (1937). Fluid Flow through Granular Beds. *Trans.Inst.Chem. Eng.*, 15,150

Caesar, G.J. (40BC) *De Bello Alexandrino*, (authorship debated since antiquity; release date estimated)

Cividini, A., Bonomi, S., Vignati, G.C., Gioda, G. (2009). Seepage-Induced Erosion in Granular Soils and Consequent Settlements. *Int. J. Geomech.*, 9(4), 187-194

Croney, D. and Coleman, J.D. (1961) Pore Pressure and Suction in Soils, *Proc. Conf. on Pore Pressure and Suction in Soils*, London, 31-37

Cui, Y.J., Sun, D.A. (2009) Constitutive modelling: from isothermal to non-isothermal behaviour of unsaturated soils, *Unsaturated soils – theoretical & numerical advances in unsaturated soil mechanics*, CRC Press, 493–506.

Cunha, R.P., Kuklik, P. and Laurin, J. (2002) Evaluation of Deep Foundations in Tropical Residual Soil by a Semi Analytical Mathematical Procedure Coded in Industrial Software, *Proc. Mecánica Computacional*, Santa Fe-Paraná, Argentina, vol. 21, 1045-1062

Cunha, R.P. and Kuklik, P. (2002) Experimental and Numerical Analyses of Bored Pile Foundations in a Tropical Soil, *Engineering Mechanics 2002*, 9(1), 91-98

Cunha, R.P. and Kuklik, P. (2003) Numerical Evaluation of Pile Foundations in Tropical Soils of the Federal District of Brazil by Means of a Semi-Analytical Mathematical Procedure, *Soils & Rocks*, 26(2), 167-182

Darcy, H. (1856) *Les fontaines publiques de la ville de Dijon*, Dalmont, Paris

Davies, L., Dollimore, D. (1980). Theoretical and experimental values for the parameter k of the Kozeny-Carman equation, as applied to sedimenting suspensions. *J. Phys. D: Appl. Phys.*, 13, 2013-2020

Donald, I.B. (1956) Shear Strength Measurements in Unsaturated Non-Cohesive Soils with Negative Pore Pressures, *Proc. 2nd Australia-New Zealand Conf. Soil Mech. Found. Eng.*, 200-205

Duchan, D. (2012) *Using Spatial Random Fields for Groundwater Modelling*, PhD Thesis, VUT Brno (in Czech).

Einstein, H.A. (1937). *Der Geshiebetrieb als Wahrsheinlichkeitsproblem*, Mitteilungen der Versuchsanstalt für Wasserbau, EHT Zürich

Fredlund, D.G., Morgenstern, N.R. (1977) Stress state variables for unsaturated soils. *J. Geotech. Eng. Div.*, ASCE 103(GT5), 447-466

Fredlund, D.G. and Rahardjo, H. (1993) *Soil mechanics for unsaturated soils*, Wiley-IEEE

Fredlund, D.G., Xing, A., Fredlund, M.D., Barbour, S.L. (1996) Relationship of the unsaturated soil shear strength to the soil-water characteristic curve. *Can. Geotech. J.*, 33, 440–448.

Fung, Y.C. (1965) *Foundations of Solid Mechanics*, Eagelwood Cliffs, NJ:Prentice-Hall

Gens, A. (1996) Constitutive modelling: application to compacted soils, *Unsaturated soils*, Rotterdam, vol. 3, 1179–1200

Gens, A., Guimarãs, L., Sánchez, M., Sheng, D. (2008) Developments in modelling the generalised behaviour of unsaturated soils. *Unsaturated soils: advances in geo-engineering*, CRC Press, 53–62

Gens, A. (2009) Some issues in constitutive modelling of unsaturated soils. *Unsaturated soils – theoretical & numerical advances in unsaturated soil mechanics,* CRC Press, 613–626.

Hogentogler, C.A. and Barber, E.S. (1941) Discussion in Soil Water Phenomena, *Proc. Hwy. Research Board*, 21, 452-465

Charlier, R., Radu, J.P., Collin, F. (2001) Numerical modelling of coupled transient phenomena, *Rev. Franc. G. Civ.*, 5(6)

Charlier, R., Laloui, L., Collin, F. (2006) Numerical modelling of coupled poromechanics processes, *Rev. Eur. G. Civ.*, 10(6-7), 669-701

International Commission on Large Dams (ICOLD), (1994). *Use of granular filters and drains in embankment dams*, Bulletin 95

International Commission on Large Dams (ICOLD), (2013). *Internal Erosion of Existing Dams, Levees, and Dikes, and Their Foundations - DRAFT*, Bulletin 1XX

Jones, D. E., and Holtz, W.G. (1973) Expansive Soils – The Hidden Disaster, *Proc. 6th Int. Conf. on Expansive Soils*, Delhi, vol. 2, 596-601

Kang, J-L., Su, M-D., Chang, L-F. (2005) Loss Functions and Framework for Regional Flood Damage Estimation in Residential Area, *J. Mar. Sci. Tech.*, 13(3), 193-199

Kayadelen C., Tekinsoy, M. A., Taşkıran, T. (2007) Influence of matric suction on shear strength behavior of a residual clayey soil, *Env. Geo.*, 53(4), 891-901

Kenney T.C. and Lau, D. (1985). Internal stability of granular filters, *Can. Geotech. J.*, 22, 215–225.

Khalili N and Khabbaz MH. (1998) A unique relationship for the determination of the shear strength of unsaturated soils, *Géotechnique,* 48, 681–687.

Kohgo, Y. (2003) Review of constitutive models for unsaturated soils and initialboundary value analyses. *Unsaturated soils – geotechnical and geoenvironmental issues*, 2nd Asian conf., 21–40.

Kozeny, J. (1927) Über Kapillare Leitung Des Wassers in Boden. *Sitzungsber Akad. Wiss.Wien Math.Naturwiss.Kl.*, Abt.2a, 136, 271-306 (In German).

Krahn, J. and Fredlund, D.G. (1972) On Total Matric and Osmotic Suction, *J. Soil Sci.*, 114(5), 339-348

Krohn, J.P. and Slosson, J.E. (1980) Assessment of Expansive Soils in the United States, *Proc. 1st Canadian Symposium in Microcomputer Application to Geotechnique*, Regina – Canada, vol. 1, 596-608

Kuklík P. (2006) Several Comments on Influence Zone Depth Progress in Deep Hole Foundations, *Underground Construction and Ground Movement,* Virginia ASCE, 355-362

Kuklik, P., Broucek, M., Kopackova, M (2008a) Fast estimation of the rectangular footings influence zone depth, *Contributions to numerical and experimental investigation of building materials and structures*. Prague

Kuklík, P., Záleský, M., Záleský, J. (2008b) Theory and comments on standard dilatometric back analysis, *Proceedings of the ICCES 08*, 7(2), 89-94

Kuklik, P., Kopackova, M., Broucek, M. (2009) *Elastic Layer Theory and Geomechanics* CTU Publishing House, Prague

Kuklik, P. (2011) Preconsolidation, Structural Strength of soil, and its effect on subsoil upper structure interaction. *Eng. Struc.*, 33(4), 1195-1204

Lane, E.W. (1935) Security from Under-Seepage Masonry Dams on Earth Foundations, *Transactions ASCE*, 100, 1919-1935

Lewis, R.W., Schrefler, B.A. (2000) *The Finite Element Method in the Static and Dynamic Deformation and Consolidation of Porous Media*, 2nd edition, John Wiley & Sons

Lim, S.S. (2006) *Experimental investigation of erosion in variably saturated clay soils*. PhD thesis, School of Civil and Environmental Engineering, University of New South Wales, Sydney, Australia

Lim, S.S. and Khalili, N.K. (2010) Laboratory measurement of erosion of clay soils using rotating cylinder test. Geotechnical Testing Journal, Vol.32, No 3.

Liu, B. and Li, H. (2008) A FLAC-based constitutive model for collapsible loess: analytical formulation and application, *Continuum and Distinct Element Numerical Modeling in Geo-Engineering*, Minneapolis

Lohani, T.N., Kato, S., Sakakibara, T., Shibuya, S. and Yoshimura, Y. (2008) Strength Parameters for Granular Soils Governed by Their Grain-Size Properties, *Continuum and Distinct Element Numerical Modeling in Geo-Engineering*, Minneapolis

Lu N. (2008) Is matric suction a stress variable?, *J. Geotech. Geoenviron. Eng.*, ASCE 134(7):899–905.

Masin, D. (2005) A hypoplastic constitutive model for clays, *Int. J. Numer. Anal. Meth. Geomech.*, 29(4), 311-336

Masin, D. and Khalili, N. (2008) A hypoplastic model for mechanical response of unsaturated soils, *Int. J. Numer. Anal. Meth. Geomech.*, 32(15), 1903-1926

Masin, D. (2010) *Hypoplasticity for practical applications - PhD course*. [calibration procedure available at http://web.natur.cuni.cz/uhigug/masin/hypocourse]

Masin, D. (2012) *PLAXIS implementation of hypoplasticity* [available at http://web.natur.cuni.cz/uhigug/masin/plaxumat/download/Hypo-Plaxis.pdf]

Matyas, E.L. and Radhakrisna, H.S. (1968) Volume Change Characteristics of Partially Saturated Soils, *Geotechnique*, 18(4), 432-448

Nuth, M. and Laloui, L. (2007) Effective stress concept in unsaturated soils: Clarification and validation of unified framework, *Int. J. Numer. Anal. Meth. Geomech*., 32, 771-801

Öberg A and Sällfors G. (1997) Determination of shear strength parameters of unsaturated silts and sands based on the water retention curve, *Geotech. Test. J.*, 20, 40–48.

Papamichos, E. (2006) Sand production. Physical and experimental evidence, *Rev. Eur. G. Civ.*, 10(6-7), 803-816

Papamichos, E., Vardoulakis, I. (2005) Sand erosion with a porosity diffusion law, *Comp. Geo.*, 32, 47-58

Pastor, M., Mira, P. (2002) Steady State Problems of Elliptic Type, *Numerical Modelling in Geomechanics*, Lavoisier and Hermes Science Publications, 1-22

Pastor, M. and Merodo, J.A.F. (2002) Transient Problems of Parabolic Type, *Numerical Modelling in Geomechanics*, Lavoisier and Hermes Science Publications, 23-39

de Pater, C. J. and Dong, Y. (2007) Experimental Study of Hydraulic Fracturing in Sand as a Function of Stress and Fluid Rheology, *SPE Hydraulic Fracturing Technology Conference*; Texas

Rees, J.M. (2010) *Reith Lectures 2010: Scientific Horizons – Lecture 3: What We'll Never Know*; BBC – Radio 4 [available online at http://www.bbc.co.uk/radio4/features/the-reith-lectures/transcripts/2010/]

Richards, L.A. (1928) The Usefulness of Capillary Potential to Soil Moisture and Plant Investigators, *J.Agric. Res*, 37, 719-742

Rodigues, R.A., Elis, V.R., Prado, R. and de Lollo, J.A. (2006) Laboratory tests and applied geophysical investigations in collapsible soil horizon definition, *Engineering geology for tomorrow's cities* (IAEG2006), Nottingham UK, 22 [on CD-ROM, Paper 115]

Sakthivadivel, R., Irmay, S. (1966) *A Review of Filtration Theories*, University of Claifornia, Berkeley

Satrapa, L. (1999) Disastrous Floods-Design of GIS Model for the Prediction of Flood Losses, *First International Conference on Advanced Engineering Design*, Prague, vol. A, p. 203-204

Satrapa, L., Fosumpaur, P. and Horsky, M. (2006) Možnosti a ekonomická efektivnost protipovodňových opatření, *Urbanismus a územní rozvoj*, 9(5), 25-30 (in Czech)

Sheng, D., Fredlund, D.G. (2008) Elastoplastic modelling of unsaturated soils: an overview. Keynote lecture, *12th Int. conf. int. assoc. comp. methods & advances in geomechanics (IACMAG)*, Goa, India, 2084–105.

Sheng, D., Gens, A., Fredlund, D.G., Sloan, S.W. (2008a) Unsaturated soils: from constitutive modelling to numerical algorithms. *Com. Geotech.,* 35, 810–824.

Sheng, D., Fredlund, D.G., Gens, A. (2008b) A new modelling approach for unsaturated soils using independent stress variables. *Can. Geotech. J.,* 45, 511–534.

Sheng, D. (2011) Review of fundamental principles in modelling unsaturated soil behaviour, *Com. Geotech.,* 38, 757–776

Sherard, J.L., Dunnigan, L.P. and Talbot, J.R. (1984). Basic properties of sand and gravel filters, *ASCE J. Geotech. Eng.*, 110(6), 684–700

Shroff, A.V., Shah, D.L. (2003) *Soil Mechanics and Geotechnical Engineering*, Taylor & Francis

Schrefler, B.A. (1984) *The Finite Element Method in Soil Consolidation (with applications to surface subsidence)*. Ph.D.Thesis. University College of Swansea.

Speedy, R.J. (1982) Stability-limit conjecture: an interpretation of the properties of water, *J. Phys. Chem*., 86, 982-991

Sun, D.A., Matsuoka, H., Yao, Y.P., Ichihara, W. (2000) An elastoplastic model for unsaturated soil in three-dimensional stresses. *Soils Found.*, 40, 17–28.

Tadepalli, R., Rahardjo, H., Fredlund, D.G. (1992) Measurements of matric suction and volume changes during inundation of collapsible soils. *Geotechnical Testing Journal*, ASTM, 15(2): 115–122

Terzaghi, K. (1936) The Shear Resistance of Saturated Soils, *Proc. 1st Int. Conf. Soil Mech. Found. Eng.*, Cambridge, MA, 1, 54-56

Terzaghi, K. (1943) *Theoretical soil mechanics*, Wiley, New York

Terzaghi, K., Peck, R.B., Mesri, G. (1996) *Soil Mechanics in Engineering Practice*, Wiley-Interscience

Thomson, W. (1871) Hydrokinetic solutions and observations, *Phil. Mag.,* 42, 362–377

Thu T.M., Rahardjo H. and Leong E.C. (2007) Critical state behaviour of a compacted silt specimen, *Soils Found.*, (47),749–755.

Toll, D.G. (1990) A framework for unsaturated soil behaviour. *Geotechnique*, 40, 31–44.

Turska, E., Schrefler, B.A. (1993) On convergence conditions of partitioned solution procedures for consolidation problems, *Comp. Meth. App. Mech. Eng.*, 106, 51-63

USBR (1988). *Downstream Hazard Classification Guidelines*. ACER Technical Memorandum No. 11, U.S. Department of the Interior, Bureau of Reclamation, Denver

Valenta, P., Valentova, J., Horsky, M. and Satrapa, L. (2006) *FLAMIS Project, Stage III, Final Report*, Czech Technical University in Prague

Vanapalli, S.K. and Fredlund, D.G. (1997) Interpretation of undrained shear strength of unsaturated soils in terms of stress state variables, *Proc. 3rd Brazilian Symposium on Unsaturated Soils*, 35-45

Vanapalli, S.K., Fredlund D.G., Pufahl, D.E., Clifton, A.W. (1996) Model for the prediction of shear strength with respect to soil suction, *Can. Geotech. J.*, 33, 379–392.

Vardoulakis, I., Sulem, J. (1995) *Bifuraction Analysis in Geomechanics*, Blackie Academic & Professional

Vardoulakis, I. (2006) Sand production. Mathematical modeling, *Rev. Eur. G. Civ.*, 10(6-7), 817-828

Wan, C.F. and Fell, R. (2002). Investigation of internal erosion and piping of soils in embankment dams by the slot erosion test and the hole erosion test. *UNICIV Report No. R-412, ISBN: 85841 379 5, School of Civil and Environmental Engineering,* The University of New South Wales

Wan, C.F. and Fell, R. (2004a). Investigation of rate of erosion of soils in embankment dams. *ASCE Journal of Geotechnical and GeoEnvironmental Engineering*, 130 (4), 373-380

Wan, C.F. and Fell, R. (2004b). Laboratory tests on the rate of piping erosion of soils in embankment dams. *Geotechnical Testing Journal*, 27(3), 295-303

Weng, L.K., Partzsch, S. and Daramalinggam, J. (2009) Comprehensive Site Investigation and Construction Monitoring for Tank Farms on Improved Ground, *Ground Improvement Technologies and Case Histories*, Singapore, 647-654

Wheeler, S.J., Karube, D. (1996) Constitutive modelling, *Proc. 1st Int. Conf. on Unsaturated soils*, vol. 3. Rotterdam, 1323–1356.

Zalesky, M., Buhler, Ch., Burger, U. and John, M. (2006): Dilatometer Tests in Deep Boreholes in Investigation for Brenner Base Tunnel, *Proceedings of World Tunelling Congress 2007 in Prague*, A. Balkema, Rotterdam.

Zienckiewicz, O.C., Paul, D.K., Chan, A.H.C. (1988) Unconditionally stable staggered solution procedure for soil-pore fluid interaction problems, *Int. J. Num. Meth. Eng.*, 26, 1039-1055

LIST OF AUTHOR'S PUBLICATIONS

Year 2012

Satrapa, L., Brouček, M. and Pechar, J. (2012) Study on measures to increase the capacity of protective structures on Orlik dam, *Twenty-Fourth International Congress on Large Dams - Kyoto 2012*, p. 1-10

Brouček, M., Jirsák, V., Králík, M., Nowak, P., Satrapa, L. and Zukal, M. (2012) Flow Based Vibrations of Sluice Gates - Physical and Numerical Modelling, *Engineering Mechanics 2012*. Prague: Institute of Theoretical and Applied Mechanics Academy of Sciences of the Czech Republic

Šejnoha, M., Brouček, M., Novotná, E., Lehký, D., Frantík, P. and Keršner, Z. (2012) Material Parameters of Cement and Alkali Activated Fly Ash Concrete Mixtures Laboratory Measurements and Numerical Simulation. In: *Engineering Mechanics 2012,* Prague: Institute of Theoretical and Applied Mechanics Academy of Sciences of the Czech Republic

Šejnoha, M., Brouček, M., Novotná, E. and Sýkora, J. (2012) Resistance of Concrete with Fly Ash Content under the RWS Curve Fire Loading, In: *Engineering Mechanics 2012,* Prague: Institute of Theoretical and Applied Mechanics Academy of Sciences of the Czech Republic

Brouček, M. (2012) The Impact of Groundwater Change Due to Channel Improvement on Soil-Structure Interaction. In: *Zborník príspevkov 11. konferencia mladých vodohospodárov*. Bratislava: SHMÚ, 2012, p. 1-10

Brouček, M., Jirsák, V., Králík, M., Nowak, P., Satrapa, L. and Zukal, M. (2012) Physical and Numerical Modelling of Vibration of Spillway Gates. In *Vodní toky 2012*. Kostelec nad Černými Lesy: Lesnická práce,1, p. 150-155 (in Czech).

Brouček, M., Králík, M., Satrapa, L. and Zukal, M. (2012) Reliability of Flood Gates Installed on Emergency Spillways under Extreme Hydrologic Conditions, In: *Workshop Adolfa Patery - extrémní hydrologické jevy v povodích*. Praha: Česká vědeckotechnická vodohospodářská společnost, p. 15-20 (in Czech).

Králík, M., Brouček, M., Satrapa, L. and Zukal, M. (2012) Hydraulic research of the Strakonice weir. In: *Vodní toky 2012*, Kostelec nad Černými Lesy: Lesnická práce, 1, p. 156-161 (in Czech).

Kuklík, P. - Brouček, M. (2012) Derived Analytical Formula for the Fast Estimation of the Influence Zone Depth in the Subsoil Beneath the Footings. In: *Spolehlivost, optimalizace a trvanlivost stavebních konstrukcí*, p. 84-90.

Kuklík, P., Brouček, M. and Blažek, V. (2012) Experimental Analysis of the Behaviour of Soils Subjected to Wetting. In: *Spolehlivost, optimalizace a trvanlivost stavebních konstrukcí*, p. 91-96. (in Czech).

Year 2011

Kuklík, P., Brouček, M. and Kopáčková, M.K. (2011) Two-Parameterical Model of Subsoil, Theory, Standards and Free Codes, In: *Stavební obzor*, 20(1), p. 2-6. (in Czech).

Brouček, M. and Satrapa, L. (2011) Reliability assessment of the sluice gates - possible approaches. In *Sympózium hydrotechnikov 2011*, Bratislava: Stavebna fakulta STU, 1, (in Czech).

Brouček, M. and Satrapa, L. (2011) Reliability of Manipulation Objects on Water Structures – Lock Gates, In: *Manažment povodí a povodňových rizík: zborník príspevkov,* Bratislava: Výskumný ústav vodného hospodárstva, (in Czech).

Fošumpaur, P., Satrapa, L., Horský, M., Brouček, M. and Nešvarová Chvojková, P. (2011) Assessment of the flood protection impacts due to rehabilitation of fishponds, small dams and landscape adjustments in the Czech Republic In: M*anažment povodí a povodňových rizík: zborník príspevkov*, Bratislava: Výskumný ústav vodného hospodárstva (in Czech).

Fošumpaur, P., Satrapa, L., Horský, M., Brouček, M. and Nešvarová Chvojková, P. (2011) Assessing the effectiveness of flood protection activities in the work of expert strategic program Flood Prevention in the CR. In: *Manažment povodí a povodňových rizík: zborník príspevkov*, Bratislava: Výskumný ústav vodného hospodárstva (in Czech).

Satrapa, L., Fošumpaur, P., Horský, M., Zukal, M., Brouček, M. and Broža, V. (2011) The relationship of global climate change to the assessment of dams and the solution reservoirs in the Czech Republic. In: *Sympózium hydrotechnikov 2011, zborník prednášok*, Bratislava: Stavebna fakulta STU, 2011, 1, p. 180-184 (in Czech).

Brouček, M. (2011) The Influence of Time during High Hydraulic Gradients Loading - Experimental Analysis, In: *Revitalizace vodního systému krajiny a měst zatíženého významnými antropogenními změnami*. Prague: CTU in Prague, Faculty of Civil Engineering, p. 24-29 (in Czech).

Brouček, M. (2011) Internal Erosion and Changes in Subsoil in Sands and Sandy Soils, In: *Revitalizace vodního systému krajina a měst zatíženého významnými antropogenními změnami*, Prague: CTU in Prague, Faculty of Civil Engineering, p. 7-13. (in Czech).

Brouček, M. and Kuklík, P. (2011) The Impact of Groundwater ton Artificially Compacted Soils. In: *Engineering Mechanics 2011*. Prague: Institute of Thermomechanics AS CR, 1, p. 63-66

Valenta, P., Satrapa, L., Brouček, M. and Horský, M. (2011) *The study of effectiveness of Srnčí reservoir*. [Technical report]. Prague: CTU in Prague, Faculty of Civil Engineering, 11142032110. (in Czech).

Year 2010

Krejčí, T., Koudelka, T. and Brouček, M. (2010) Modelling of Coupled Heat and Moisture Transfer in Soils. In: *ESCO 2010 Book of Abstracts,* Pilsen: University of West Bohemia, p. 59.

Brouček, M.,Kuklík, P. and Sýkora, J. (2010) The Causes of Construction Failures - Structural Analysis. *In Workshop 2010,* Prague: CTU in Prague, p. 366-367

Kuklík, P. and Brouček, M. (2010) Phenomenon of preconsolidation and simple tools for the influence zone depth estimation. In: *Konštrukčné a fyzikálne aspekty stavebného inžinierstva 2010,* Košice: Technická univerzita v Košiciach, 1, p. 120-127

Brouček, M. - Kuklík, P. (2010) The Impact of Groundwater to Artificially Compacted Soils – Experimental Analysis, In: *Proceedings of Twin International Conferences on Geotechnical and Geo-Environmental Engineering cum 7th Ground Improvement Techniques*. Singapore: CI-PREMIERE PTE LTD, 1, p. 187-192

Králík, M., Brouček, M., Zukal, M., Satrapa, L. and Kučerová, J. (2010) Hydraulic models: Orlík Dam, Koryčany Dam, Harcov Dam. In: *XXXII. Priehradné dni 2010 - zborník príspevkov*. Banská Štiavnica: Slovenský vodohospodárský podnik, p. 349-356. (in Czech).

Valentová, J., Valenta, P., Brouček, M. and Gvoždík, L. (2010) *Aktualizace záplavového území Berounky v ř. km 9,800 až 83,500, Úsek Beroun - Zvíkovec*. [Technical report]. Prague: CTU in Prague, Faculty of Civil Engineering, 83046/2. 26 p. (in Czech).

Valentová, J., Valenta, P., Brouček, M. and Gvoždík, L. (2010) *Aktualizace záplavového území Berounky v ř. km 9,800 až 83,500, Úsek Kazín - Beroun.* [Technical report]. Prague: CTU in Prague, Faculty of Civil Engineering, 83046/1. 25 p. (in Czech).

Year 2009:

Kuklík, P., Brouček, M. and Kopáčková, M. (2009) Fast analytical estimation of the influence zone depth, its numerical verification and FEM accuracy testing, *Structural Engineering and Mechanics*, 33(5), 635-647

Brouček, M. and Kuklík, P. (2009) The Impact of the Groundwater Table Level on the Influence Zone Depth – Experimental Analysis. In: *62nd Canadian Geotechnical Conference GeoHalifax 2009*, X-CD Technologies

Kuklík, P., Zálesky, M. and Brouček, M. (2009) New Extended Approach to Borehole Dilatometer Tests Back Analysis. In: *Computational Methods in Tunneling EURO:TUN 2009*, Aedificatio Publishers

Kuklík, P. and Brouček, M. (2009) Vliv biotických činitelů na stabilitu barokního krovu sv. Barbory v Otovicích, In: *Střechy, fasády, izolace*. vol. 16 (1) 34-37 (in Czech).

Kuklík, P., Kopáčková, M. and Brouček, M. (2009) *Elastic Layer Theory and Geomechanics* 1. ed. CTU Publishing House, Prague

Year 2008

Brouček, M. and Kuklík, P. (2008) Processes Identification of Changes of Mechanical Properties of Soils Due to Groundwater Flow In: *Proceedings of Workshop 2008*. Czech Technical University in Prague

Brouček, M. and Kuklík, P. (2008) Sandy Soils Influenced by Groundwater Flow In: *Proceedings of GEO - CHIANGMAI 2008: An international Conference on Geotechnical Engineering*. Singapore: CI-PREMIERE PTE LTD

Cordeiro, A.F., Cunha, R.P., Brouček, M. and Sales, M.M. (2008) Piled Rafts with Defective Piles: Influence of Reinforcement Systems In: *Proceedings of the Second British Geotechnical Association International Conference on Foundations, ICOF 2008.* Bracknell: IHS BRE Press

Cordeiro, A.F., Cunha, R.P., Sales, M.M., Kuklík, P. and Brouček, M. Influence of Interaction Factors and Defective Piles on Piled Raft Behaviour In: *Proceedings of the Second British Geotechnical Association International Conference on Foundations, ICOF 2008.* Bracknell: IHS BRE Press

Kuklík, P. and Brouček, M. (2008) Plastic and influence zone numerical evaluation for dilatometric back analysis In: *Engineering Mechanics 2008*. Institute of Thermomechanics AS CR

Kuklík, P., Brouček, M. and Kopačkova, M. (2008) Fast estimation of the rectangular footings influence zone depth In: *Contributions to numerical and experimental investigation of building materials and structures.* Prague, CTU in Prague

Year 2007

Brouček, M. and Kuklík, P. (2007) Experimentální vyšetřování zemin vystavených zvýšeným hydraulickým gradientům In: *Spolehlivost, optimalizace a trvanlivost stavebních materiálů a konstrukcí*. CTU in Prague, (in Czech)

Brouček, M. and Kuklík, P. (2007) Changes of Mechanical Parameters of Soils Due to Groundwater Flow - Processes Identification In: *Computational Plasticity IX.* Barcelona: University of Catalunya

Brouček, M. and Kuklík, P. (2007) Identifikace procesů změn mechanických vlastností zemin vlivem proudění podzemní vody In: *Engineering Mechanics 2007.* Institute of Thermomechanics, AS CR, (in Czech)

Kuklík, P., Blažek, V. and Brouček, M. (2007) Zpětná analýza poruchy základové desky In: *Spolehlivost, optimalizace a trvanlivost stavebních materiálů a konstrukcí*. Praha: CTU in Prague, (in Czech)

Kuklík, P., Blažek, V., Brouček, M. and Kopáčková, M. (2007) Application of the Semi-analytical Method and the Finite Element Method to the Analysis of Bored Piles In: *Recent Developments in Structural Engineering, Mechanics and Computation*. Rotterdam: Millpress Science Publisher

Year 2006

Anjos, G.J.M., Cunha, R.P., Kuklík, P. and Brouček, M. (2006) Numerical Evaluation of Bored Piles in Tropical Soils by Means of the Geotechnical Engineering "GEO4" Fine Software In: *Proceedings of III. European Conference on Computational Mechanics* Lisboa: Technical University of Lisabon

Brouček, M. and Kuklík, P. (2006) Důsledky změn hladiny podzemní vody v podloží a následné dopady na vrchní stavbu In: *Staticko-konštrukčné a stavebno-fyzikálne problémy stavebných konštrukcií* Košice: CPRESS, (in Czech)

Brouček, M. and Kuklík, P. (2006) Změny hladiny podzemní vody a jejich dopady na vrchní stavbu In: *Sanace a rekonstrukce staveb 2006*. Prague: WTA CZ, 2006, (in Czech)

Kuklík, P. and Brouček, M. (2006) Dopady extrémních povodní na podloží a možné preventivní přístupy In: *Zpravodaj WTAcz. 2006*, vol. 6(1-2), 19-22 (in Czech)

Kuklík, P. and Brouček, M. (2006) Soil Additionally Affected by Non Force Loading and Its Influence on Upper Structure In: *Proceedings EPMESC X*. Beijing: Tsinghua University Press/Springer

Kuklík, P. and Brouček, M. (2006) Tvorba výpočtových modelů v zeminách ovlivněných povodní s využitím projektu FLAMIS In: *Spolehlivost, optimalizace a trvanlivost stavebních konstrukcí*. CTU Publishing House, Prague (in Czech)

Valenta, P., Valentová, J. and Brouček, M. Numerical Modelling and Analysis of Extreme Flood Events on the Lužnice River In: *Advanced Engineering Design*. Prague

Year 2005

Broucek, M. (2005) *Numerické modelování povodňových situací na řece Lužnici v oblasti Veselí nad Lužnicí*, Master thesis, CTU in Prague, (in Czech)

Kuklík, P. and Brouček, M. (2005) Vliv překonsolidace na chování pilot pod deskami v hlubinných jamách In: *Zakládání staveb Brno 2005*, Brno: Academic publishing house CERM, (in Czech)

Appendix A

INFLUENCE ZONE – SOFTWARE SOLUTIONS

Softwares DEPTH, Strength-IZ and TPS-overconsolidation, which are issued under the GNU General Public License, were introduced as a free tool for fast estimation of the influence zone depth, coefficient of structural strength (in older Czech standard 73 1001 denoted as *m*) and two parameters of the subsoil C_1 and C_2. Following pages explain the theory behind these software tools which do not have to be installed and are available in Czech language at http://www.stavarina.cz/depth/depth.htm together with the manuals and full official version of the GNU General Public License.

Winkler – Pasternak model

The problem of elastic layer displacement assuming Westergard's solution is governed by the balance equation in the direction of gravity, i.e. in the vertical axis direction *z*:

$$j^2 C_1 w_j - C_2 \Delta w_j = (-1)^{\frac{j-1}{2}} f_z + \int_0^{2H} \frac{\sqrt{H}}{2} \rho g \psi_j dz \quad . \tag{A.1}$$

Where:

$j = 1,3,5,....;$

E_{oed} is oedometric modulus, G je elastic shear modulus;

Δ is Laplace operator;

f_z is uniform loading of the layer;

H is thickness or depth of the layer;

ρ is soils density;

g is acceleration of gravity.

$$C_1 = \frac{\sqrt{H}.\pi^2}{8H^2} E_{oed} \ , \quad C_2 = \frac{\sqrt{H}}{2} G \ . \tag{A.2}$$

When calculating the influence of surcharge, the balance equation neglects the influence of forces acting within the volume of the layer:

$$j^2 C_1 w_j - C_2 \Delta w_j = (-1)^{\frac{j-1}{2}} f_z \ . \tag{A.3}$$

Where C_1 represents the classical stiffness of an elastic spring in the direction of its axis (here vertical), which is often called "soil reaction modulus" or "modulus of subgrade reaction", and C_2 represents shear connection between adjacent springs C_1. In hypothetical case of $C_2 = 0$ (generally unreal) the subsoil can be substituted with vertical springs. For better understanding the Eq. A.3 is further presented for different indexes:

$$C_1 w_1 - \frac{C_2}{1} \Delta w_1 = \frac{f_z}{1} \ ,$$

$$C_1 w_3 - \frac{C_2}{9} \Delta w_3 = -\frac{f_z}{9} \ , \tag{A.4}$$

$$C_1 w_5 - \frac{C_2}{25} \Delta w_5 = \frac{f_z}{25} \ ,$$

$$C_1 w_7 - \frac{C_2}{49} \Delta w_7 = -\frac{f_z}{49} \ ,$$

An arbitrary level of accuracy can be achieved by using sufficient number of members of the Eq. A.4 which describes the balance within the layer. When only the first member is used, the accuracy level for standard soils can be approximately twenty per cent. With increasing thickness of the layer the accuracy level increases. However, it is necessary to keep in mind, that thickness of the layer is limited by the phenomenon of structural strength or pre-consolidation of the soil.

The Winkler - Pasternak model is widely used in practice. In this model, sometimes called as Filoněnkov-Borodič model assumes the balance equation in vertical direction as

$$C_{1\,WP}\, w - C_{2\,WP}\, \Delta w = f_z \quad . \tag{A.5}$$

As mentioned before this model only approximates the elastic layer solution and should the parameters described within Eq. A.2 be applied the shear stiffness of the subsoil would be overestimated while soil reaction modulus would be underestimated. Confirmation of this statement lies within the Eq. A.4. It is therefore important to introduce such parameters of Winkler – Pasternak model C_{1WP} (subgrade reaction modulus) a C_{2WP} (shear stiffness modulus), which are bounded with the elastic layer solution with identity of compliance matrixes for rigid footing.

Compliance matrix for Winkler – Pasternak model is as folows:

$$[\mathbf{C}] = \begin{bmatrix} \dfrac{1}{2\left[\sqrt{C_{1WP}C_{2WP}} + bC_{1WP}\right]} & 0 \\ 0 & \dfrac{1}{2\left[b^2\sqrt{C_{1WP}C_{2WP}} + bC_{2WP} + \dfrac{b^3}{3}C_{1WP}\right]} \end{bmatrix} . \tag{A.6}$$

For elastic layer solution following identities can be assumed. For displacement and rotation, see Eq. A.7 and subsequently for compliance matrix see Eq. A.8.

$$\begin{aligned} w_O &= \sum_{n=0}^{\infty} {}^{2n+1}\overline{K}_2 . \psi_{2n+1} = \sum_{n=0}^{\infty} \frac{f}{2\sqrt{H}\left[(2n+1)\sqrt{C_1C_2} + (2n+1)^2 bC_1\right]} , \\ \varphi_O &= \sum_{n=0}^{\infty} - {}^{2n+1}\overline{K}_1 . \psi_{2n+1} = \sum_{n=0}^{\infty} \frac{m}{2\sqrt{H}\left[(2n+1)b^2\sqrt{C_1C_2} + bC_2 + (2n+1)^2 \dfrac{b^3}{3} C_1\right]} . \end{aligned} \tag{A.7}$$

$$\begin{bmatrix} \sum_{n=0}^{\infty} \frac{1}{2\sqrt{H}\left[(2n+1)\sqrt{C_1C_2} + (2n+1)^2 bC_1\right]} & 0 \\ 0 & \sum_{n=0}^{\infty} \frac{1}{2\sqrt{H}\left[(2n+1)b^2\sqrt{C_1C_2} + bC_2 + (2n+1)^2 \frac{b^3}{3} C_1\right]} \end{bmatrix}$$

(A.8)

Following Fig. A1 allows for better understanding of the Winkler – Pasternak model and the above described identities.

The influence of the rigid subgrade below the layer and Poisson's ratio on the vertical stress within the layer is described in Fig. A2. The last part of the figure then compares the vertical stress in the elastic layer and elastic half space which is represented by Boussinesq's solution.

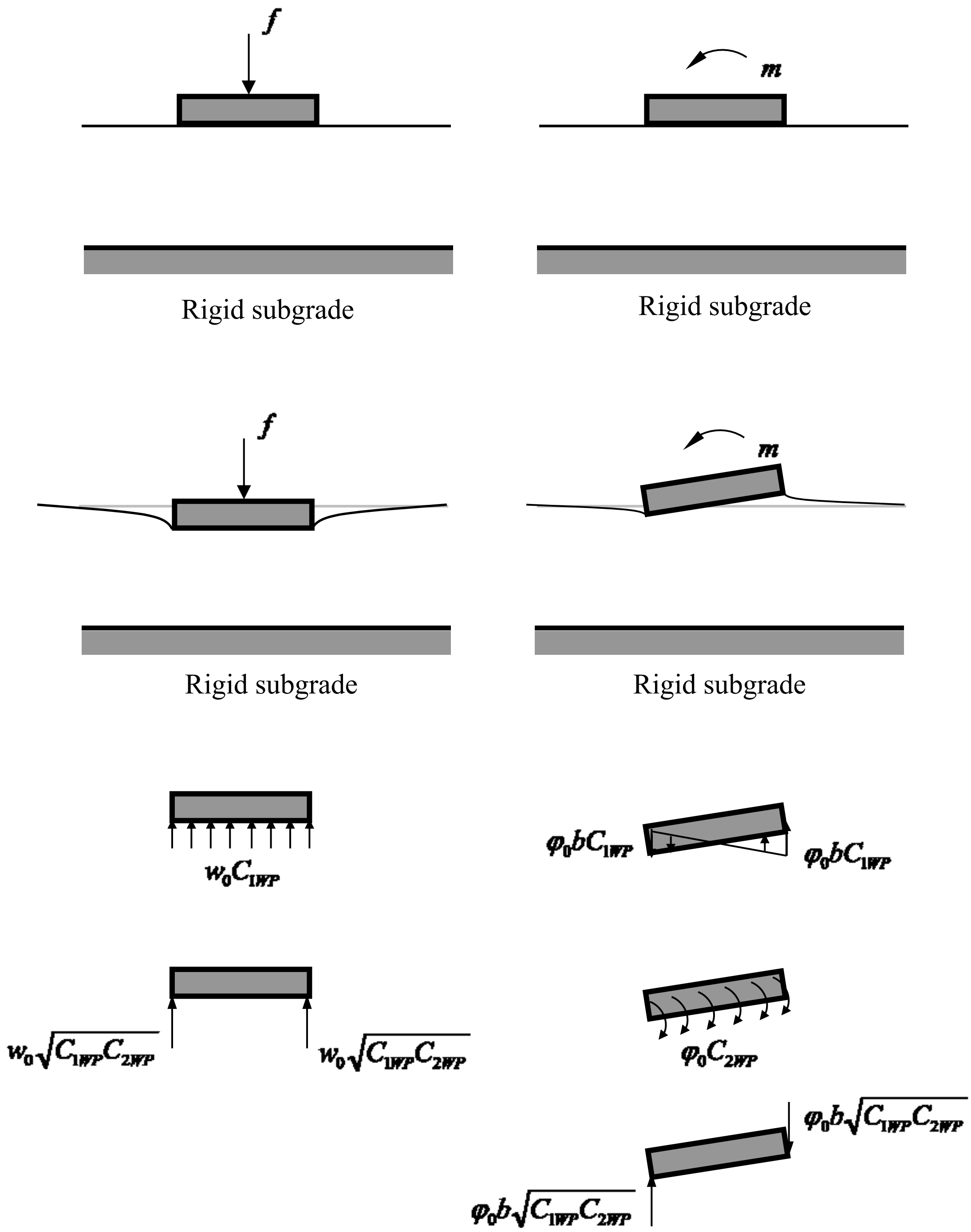

Fig. A1 Reaction of the two parametric subsoil loaded by rigid footing

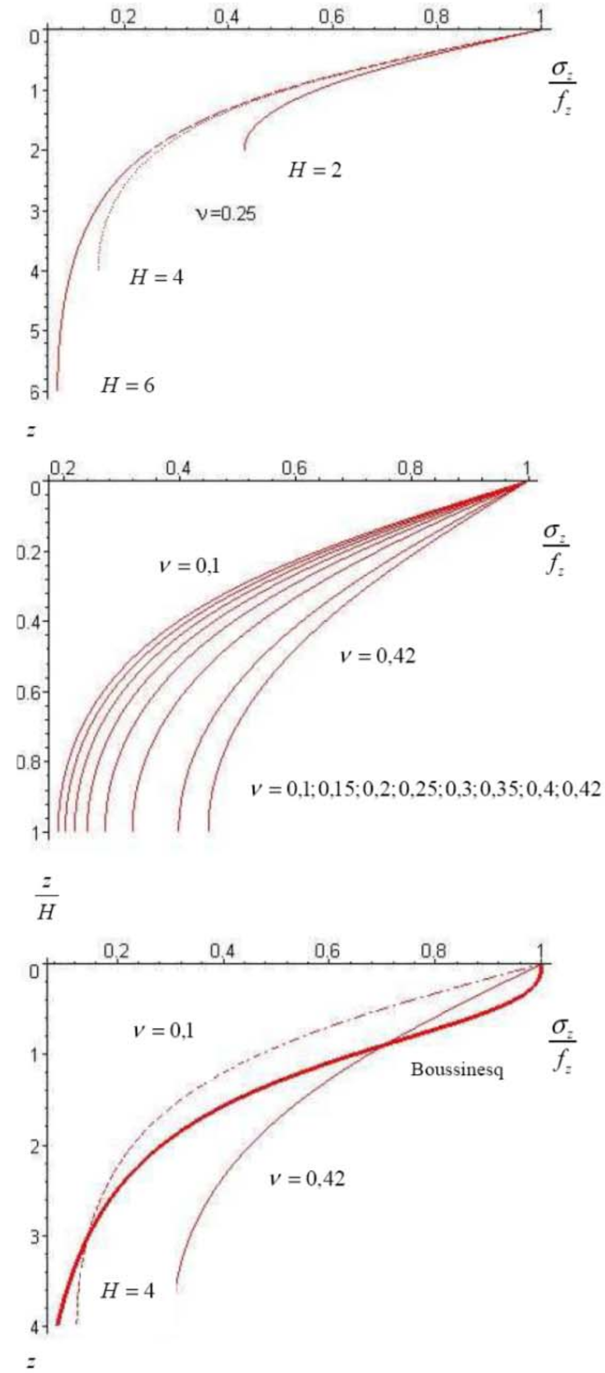

Fig. A2 Vertical stress inside the layer for different thickness and different Poisson's ratio

It can be observed, that with increasing thickness (depth) the subsoil reaction is less stiff and the solution is getting closer to half space. In case of Boussinesq's solution it is necessary to keep in mind that it was derived for domain with Poisson's ratio $\nu = 0{,}5$ and therefore the shape of the vertical stress near the top (surface) of the layer is different.

The governing ideas of influence zone (IZ) depth estimation were introduced in Chapter 5 of this thesis.

Assuming layer with thickness H placed on rigid subgrade and loaded with constant uniform load f_z (kN.m^{-2}) acting on infinite strip which width equals $2a$ (m), then the maximal vertical stress $\sigma_z(x,z)$ within interval $z \in \langle 0, H \rangle$ is reached in a point where $x = 0$:

$$\max_{x \in R} \sigma_z(x,z) = \sigma_z(0,z) = f_z - \frac{f_z}{\pi} \arctan\left(\frac{\sin(\pi z / 2H)}{\sinh \alpha a} \right) = \frac{2 f_z}{\pi} \arctan\left(\frac{\sinh \alpha a}{\sin(\pi z / 2H)} \right) ,$$

$$\alpha = \frac{\pi}{2H} \sqrt{\frac{E_{oed}}{G}} = \frac{\pi}{2H} \sqrt{\frac{2-2\nu}{1-2\nu}} . \tag{A.9}$$

The function $\sigma_z(0,z)$ is descending with increasing z and maximum of this function at the bottom of the layer yields:

$$\sigma_z(0,H) = \frac{2 f_z}{\pi} \arctan \sinh \alpha a \quad . \tag{A.10}$$

The depth of the influence zone is estimated from pre-consolidation, which is due to original geostatic stress, as:

$$\sigma_z(0,H) = \gamma h , \tag{A.11}$$

where γ is specific weight and h is the depth of foundation pit. Combining Eq. A.10 and A.11 yields:

$$\frac{\gamma h}{f_z} = \frac{2}{\pi} \arctan \sinh \alpha a \quad . \tag{A.12}$$

With help of Eq. A.9 the depth of the influence zone can be derived as

$$H = \frac{\pi a}{2}\sqrt{\frac{2-2\nu}{1-2\nu}}\,\frac{1}{\sinh^{-1}\left(\tan\dfrac{\pi\gamma h}{2 f_z}\right)} = \frac{\pi(2a)}{4}\sqrt{\frac{2-2\nu}{1-2\nu}}\,\frac{1}{\sinh^{-1}\left(\tan\dfrac{\pi\gamma h}{2 f_z}\right)}\;. \qquad \text{(A.13)}$$

Following conclusions can be made based on above introduced equations and figures.

- First, the depth of the influence zone is directly proportional to *2a* which is the width of the strip footing.
- Second, the depth of the influence zone does not depend on elastic modulus but Poisson's ratio ν has significant influence.
- The addition loading to pre-consolidation (or excavation depth) ratio is third parameter which governs the depth of the influence zone.

These conclusions are highlighted within figures A3 – A5.

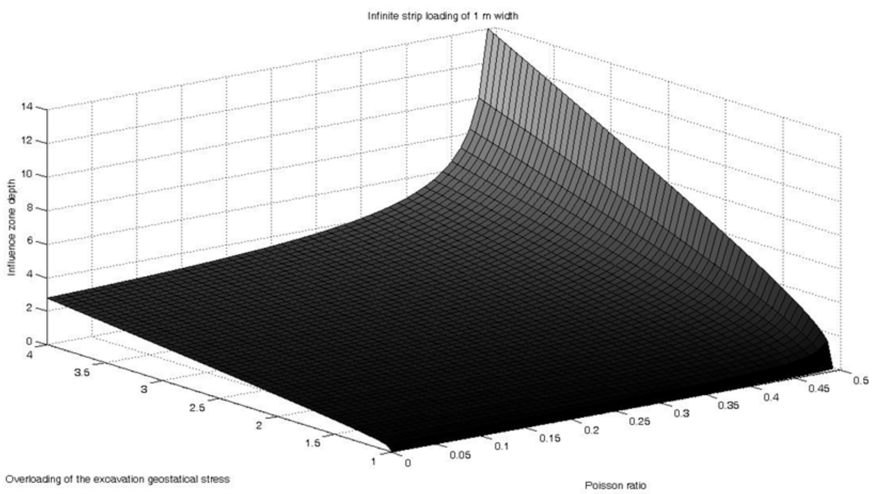

Fig. A3 Evolution of the depth of IZ for strip footing 1.0 m wide

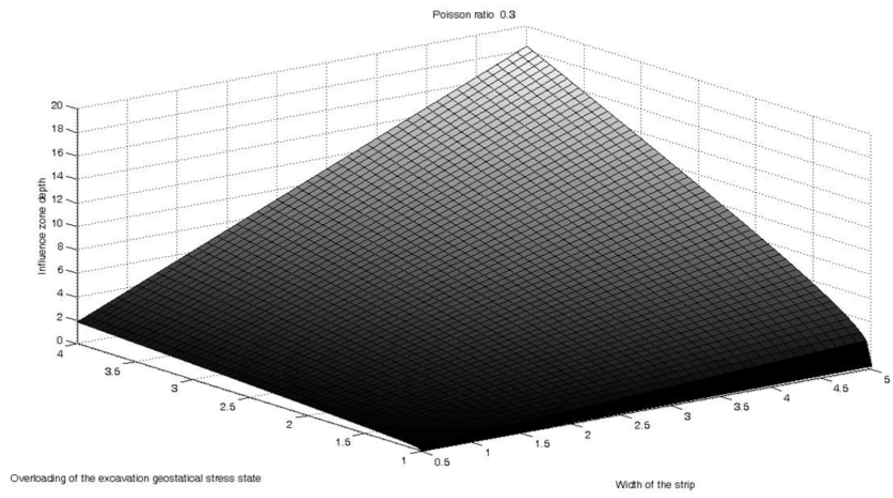
Poisson ratio 0.3
Influence zone depth
Overloading of the excavation geostatical stress state
Width of the strip

a)

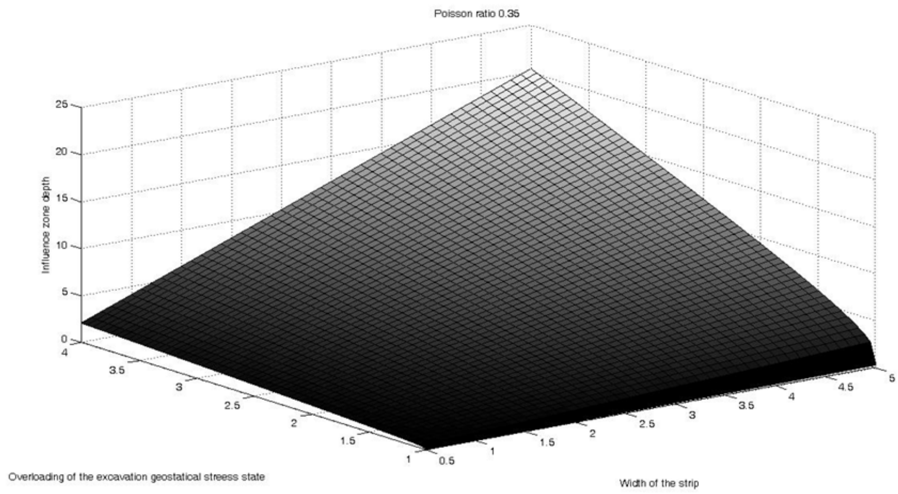
Poisson ratio 0.35
Influence zone depth
Overloading of the excavation geostatical stress state
Width of the strip

b)

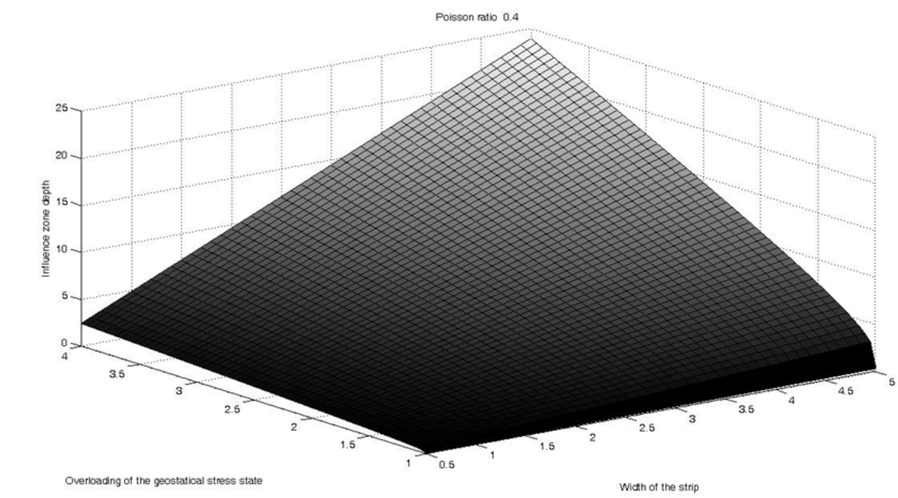
Poisson ratio 0.4
Influence zone depth
Overloading of the geostatical stress state
Width of the strip

c)

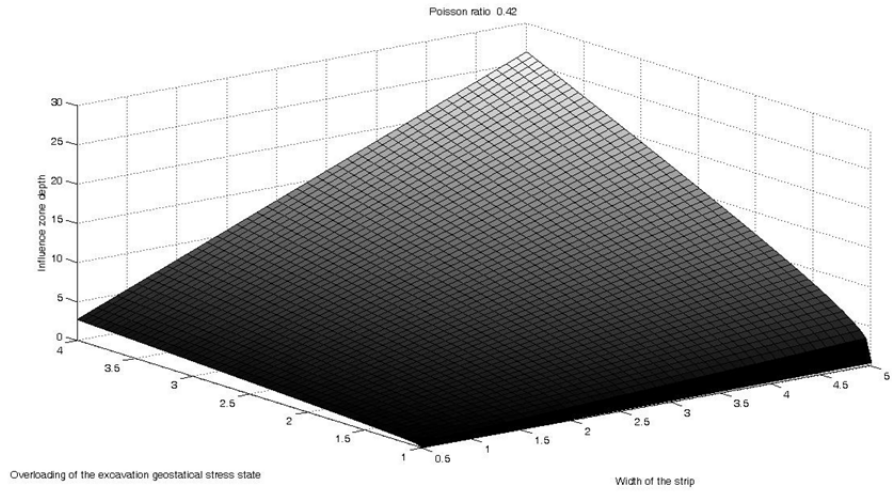

d)

Fig. A4 Poisson's ratio influence a) $\nu = .30$ b) $\nu = .35$ c) $\nu = .40$ d) $\nu = .42$

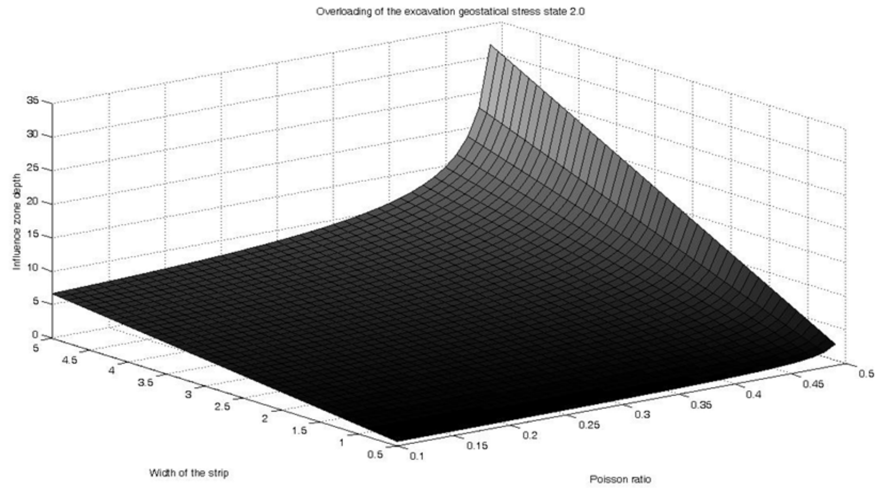

a)

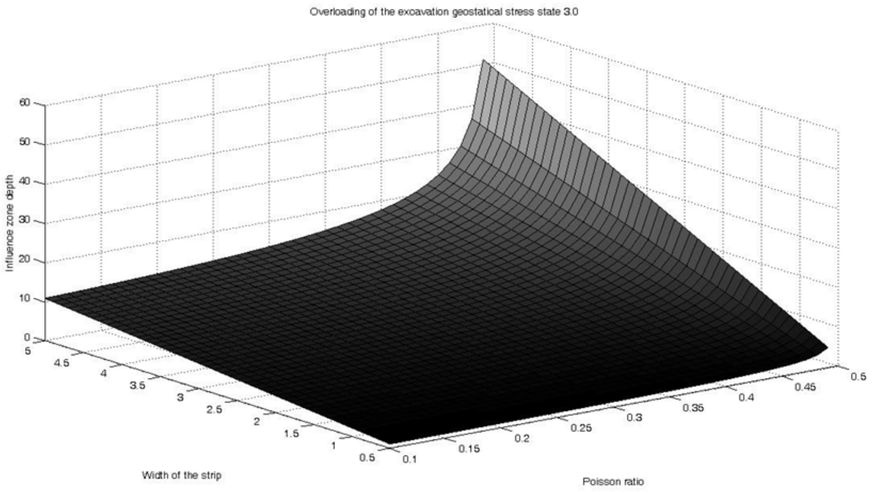

b)

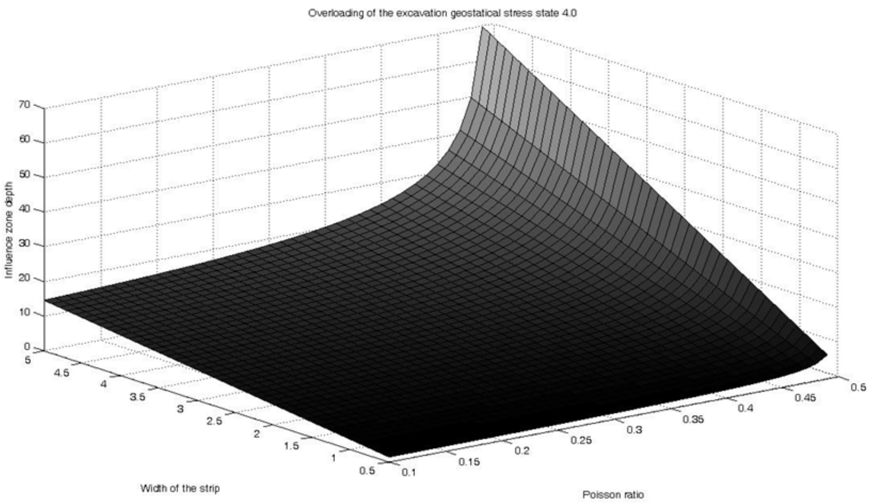

c)

Fig. A5 Influence of the depth of excavation: a) $f_z / \gamma h = 2$ b) $f_z / \gamma h = 3$ c) $f_z / \gamma h = 4$

Vertical stress in the depth H below the centre of rectangular footing can be limited accordingly to Eq. A.10. Following equation describes the idea

$$\sigma_z(0,0,H) = f_z F(\beta) = \gamma h \ . \qquad \text{(A.14)}$$

From the known value of pre-consolidation γh and surcharge f_z the value of β can be calucated with the help of function *F(β)* by inverse analysis. The algorithm of the approach described earlier is clear from following equation. earlier

$$\frac{\gamma h}{f_z} = F\left(\beta\right) \rightarrow \beta = \frac{a}{H}\sqrt{\frac{2-2\nu}{1-2\nu}} \rightarrow H \ . \tag{A.15}$$

The shapes of $F\left(\beta\right)$ function for selected width (2a) to length (2b) of the rectangular footing ratio are clear from Fig. A6 – right part. Left part presents the shape of $F_r\left(\beta\right)$ function which is used similarly for plate footings. Analogical approach should be undertaken when calculating the depth of IZ, i.e. from known value of $F_r(\beta)$ estimate value of β and finish the inverse analysis by calculating H from Eq. A.16.

$$\frac{\gamma h}{f_z} = F_r\left(\beta\right) \rightarrow \beta = \frac{r}{H}\sqrt{\frac{2-2\nu}{1-2\nu}} \rightarrow H \ . \tag{A.16}$$

Where r is the radius of the plate and H is the depth of IZ.

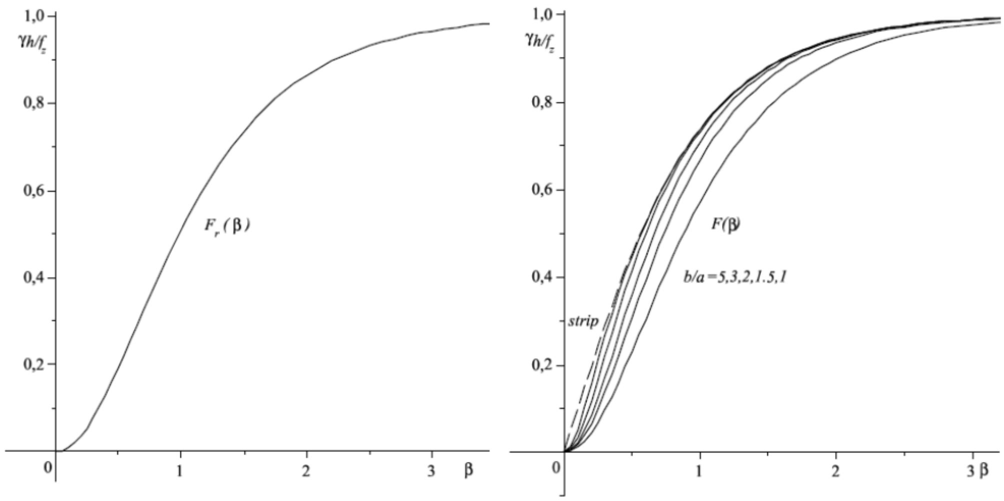

Fig. A.6 $F_r(\beta)$ and $F(\beta)$ function

For interpolating purposes following table presents values of *F(β)* function for different basic shapes of footing.

Values of $F(\beta)$ function for plate, rectangular and strip footing

β	Fr(β)	F1(β)	F1.5(β)	F2(β)	F3(β)	F5(β)	$F_{strip}(\beta)$
0.05	0.002285	0.002908	0.004354	0.005792	0.008631	0.01409	0.049949
0.10	0.009086	0.011538	0.017193	0.022715	0.033221	0.051417	0.099591
0.15	0.020241	0.025619	0.037873	0.049509	0.070437	0.101878	0.148631
0.20	0.03549	0.044725	0.065424	0.084371	0.116178	0.157082	0.196789
0.25	0.054495	0.068307	0.098662	0.125268	0.166667	0.212304	0.243812
0.30	0.076851	0.095733	0.136315	0.170219	0.218986	0.265425	0.289476
0.35	0.102112	0.126328	0.177133	0.217469	0.271126	0.315674	0.333594
0.40	0.12981	0.159414	0.219962	0.265575	0.321812	0.362878	0.376014
0.45	0.159473	0.194334	0.263795	0.313421	0.370297	0.407103	0.41662
0.50	0.190643	0.230478	0.307787	0.360185	0.416184	0.448498	0.455332
0.55	0.222884	0.267299	0.351262	0.405289	0.459300	0.487229	0.492103
0.60	0.255799	0.304319	0.393695	0.448353	0.499611	0.523456	0.526913
0.65	0.289029	0.341129	0.434698	0.489147	0.537167	0.557327	0.559768
0.70	0.322258	0.377394	0.473997	0.527554	0.572068	0.588979	0.590695
0.75	0.355216	0.412841	0.511409	0.563538	0.604445	0.618537	0.61974
0.80	0.387674	0.447257	0.546829	0.59712	0.634439	0.646118	0.646959
0.85	0.419446	0.480483	0.580210	0.628365	0.662200	0.671834	0.672420
0.90	0.450380	0.512402	0.611548	0.657363	0.687877	0.695792	0.696200
0.95	0.480359	0.542937	0.640875	0.684221	0.711613	0.718094	0.718378
1,00	0.509296	0.572042	0.668246	0.709058	0.733549	0.73884	0.739036
1.05	0.537128	0.599696	0.693733	0.731997	0.753815	0.758123	0.758259
1.10	0.563813	0.625901	0.717421	0.753160	0.772536	0.776036	0.776130
1.15	0.589330	0.650671	0.739401	0.772669	0.789828	0.792666	0.792731
1.20	0.613669	0.674039	0.759767	0.790643	0.805800	0.808097	0.808142
1.25	0.636837	0.696042	0.778616	0.807194	0.820552	0.822409	0.822439
1.30	0.658847	0.716727	0.796044	0.822430	0.834178	0.835676	0.835697
1.35	0.679723	0.736146	0.812144	0.836450	0.846764	0.847971	0.847985
1.40	0.699493	0.754353	0.827005	0.849351	0.858389	0.859361	0.859371
1.45	0.718190	0.771405	0.840716	0.861220	0.869128	0.869910	0.869916
1.50	0.735852	0.787359	0.853357	0.872140	0.879049	0.879677	0.879681
1.55	0.752518	0.802272	0.865009	0.882185	0.888215	0.888718	0.888722
1.60	0.768228	0.816202	0.875743	0.891428	0.896683	0.897087	0.897089
1.65	0.783025	0.829204	0.885629	0.899933	0.904507	0.904831	0.904832
1.70	0.796950	0.841332	0.894731	0.907759	0.911737	0.911996	0.911997
1.75	0.810045	0.852638	0.903111	0.914961	0.918417	0.918625	0.918625
1.80	0.822352	0.863172	0.910823	0.921590	0.924591	0.924757	0.924757
1.85	0.833910	0.872982	0.91792	0.927694	0.930296	0.930428	0.930429
1.90	0.844759	0.882114	0.924451	0.933313	0.935568	0.935674	0.935675
1.95	0.854938	0.890611	0.930459	0.938488	0.940441	0.940526	0.940526
2.00	0.864483	0.898514	0.935987	0.943254	0.944945	0.945012	0.945013
2.10	0.881811	0.912694	0.945751	0.951691	0.952955	0.952998	0.952998
2.20	0.897011	0.924938	0.954014	0.958855	0.959798	0.959825	0.959825
2.30	0.910326	0.935500	0.961008	0.964943	0.965645	0.965662	0.965662
2.40	0.921974	0.944602	0.966928	0.970119	0.970641	0.970652	0.970652
2.50	0.932153	0.952441	0.971941	0.974522	0.974910	0.974917	0.974917
2.60	0.941039	0.959186	0.976186	0.978271	0.978558	0.978562	0.978562
2.70	0.94879	0.964987	0.979782	0.981463	0.981675	0.981678	0.981678
2.80	0.955545	0.969972	0.982829	0.984182	0.984339	0.984341	0.984341
2.90	0.961427	0.974255	0.985412	0.986500	0.986616	0.986617	0.986617
3.00	0.966546	0.977933	0.987603	0.988476	0.988562	0.988562	0.988562
3.10	0.970999	0.981090	0.989461	0.990161	0.990225	0.990225	0.990225
3.20	0.974868	0.983799	0.991038	0.991599	0.991646	0.991646	0.991646
3.30	0.978230	0.986122	0.992377	0.992826	0.992860	0.992860	0.992860
3.40	0.981149	0.988114	0.993514	0.993873	0.993898	0.993898	0.993898
3.50	0.983681	0.989822	0.994480	0.994766	0.994785	0.994785	0.994785
3.60	0.985879	0.991286	0.995301	0.995529	0.995543	0.995543	0.995543
3.70	0.987784	0.992541	0.995999	0.996181	0.996191	0.996191	0.996191
3.80	0.989435	0.993615	0.996592	0.996737	0.996745	0.996745	0.996745
3.90	0.990865	0.994536	0.997097	0.997212	0.997218	0.997218	0.997218
4.00	0.992104	0.995324	0.997526	0.997618	0.997622	0.997622	0.997622

Appendix B

PLATE LOAD TESTS ON POORLY GRADED GRAVEL

The following pages contain processed data from full scale experiments on soil specimen made of poorly graded gravel. The data are presented in the same order in which the experiments were carried out. More detailed description of the soil sample or the placement of the soil into the stand can be found in relevant part of chapter 4.

Symbols used further in the tables and charts have following meaning. Data labelled as SM 1 or SM 2 (settlement measuring point 1 and 2) contain measured results from dial gauges located symmetrically on the top of the plate. SZ 50 and SZ 100 are measured settlements of the shear zone from dial gauges located 50 mm from the edge of the plate in case of SZ 50 and 100 mm from the edge of the plate in case of SZ 100. Column labelled as WS contains position of groundwater table inside the soil with respect to the top of the specimen. Due to the influence of the preferential paths created around the intake to the piezometer during compaction process and due to leakage from the stand, measured positions of groundwater table must be interpreted carefully and with respect to these facts. T stands for time and Avg. S. represents average settlement.

Experiment No.	1
Date	2.4.2009
Type	dry – natural moisture
Notes	----

Load (kPa)	SM1 (mm)	SM2 (mm)	Avg. S. (mm)	T (hours)
7.6	0	0	0.000	0:00
100.0	0.418	0.314	0.366	0:05
121.0	0.462	0.35	0.406	0:08
192.7	0.638	0.504	0.571	0:12
126.1	0.638	0.504	0.571	0:15
56.6	0.59	0.461	0.526	0:18
10.0	0.5	0.395	0.448	0:22

11.2	0.5	0.395	0.448	0:26
56.2	0.549	0.419	0.484	0:28
120.4	0.609	0.465	0.537	0:32
189.5	0.669	0.52	0.595	0:38
259.8	0.779	0.628	0.704	0:42
344.8	0.929	0.768	0.849	0:48
420.7	1.05	0.884	0.967	0:56
286.0	1.027	0.862	0.945	1:03
286.6	1.027	0.862	0.945	1:04
118.3	0.956	0.793	0.875	1:10
62.7	0.908	0.748	0.828	1:15
11.9	0.786	0.648	0.717	1:22
58.6	0.837	0.679	0.758	1:28
78.9	0.864	0.701	0.783	1:53
186.0	0.936	0.767	0.852	1:57
267.3	0.984	0.816	0.900	2:04
349.1	1.034	0.868	0.951	2:11
438.0	1.105	0.94	1.023	2:17
514.2	1.198	1.035	1.117	2:29
560.6	1.268	1.106	1.187	2:44
607.2	1.32	1.154	1.237	2:58
362.8	1.288	1.118	1.203	3:01
219.0	1.237	1.071	1.154	3:10
110.4	1.161	0.997	1.079	3:15
13.7	0.975	0.826	0.901	3:24
Load (kPa)	SM1 (mm)	SM2 (mm)	Avg. S. (mm)	T (hours)

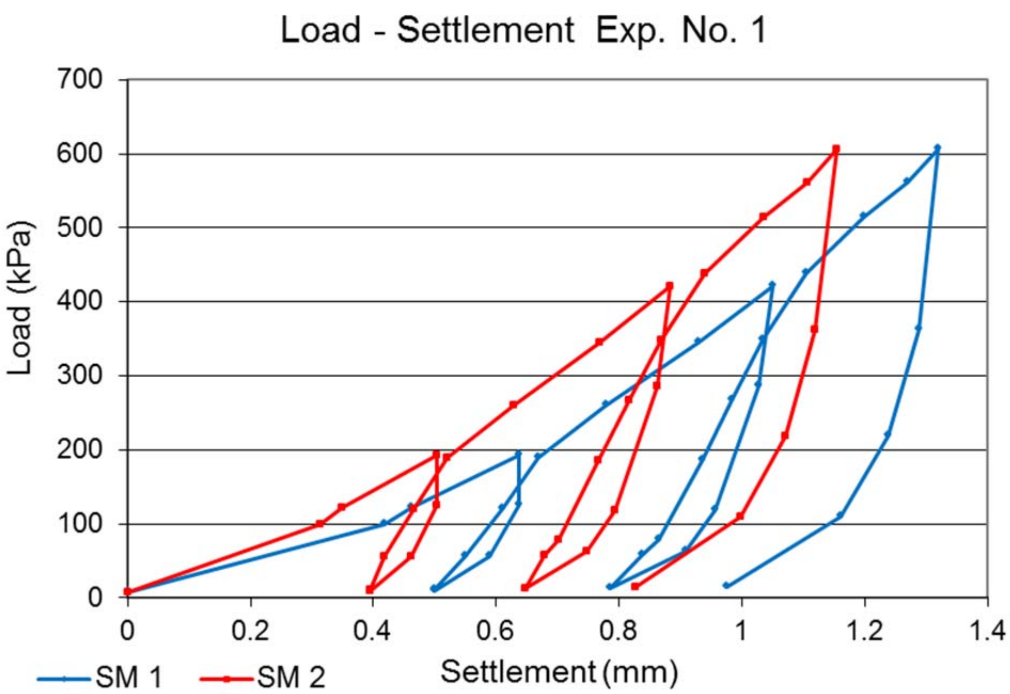

Experiment No.	2
Date	10.4.2009
Type	dry – natural moisture
Notes	creep behaviour tested for load approximately 1010 kPa

Load (kPa)	SM1 (mm)	SM2 (mm)	Avg. S. (mm)	T (hours)
8.8	0.000	0.000	0.000	0:00
68.2	0.196	0.198	0.197	0:03
140.7	0.337	0.348	0.343	0:07
204.9	0.429	0.437	0.433	0:13
261.8	0.498	0.505	0.502	0:19
76.4	0.417	0.440	0.429	0:24
9.2	0.248	0.315	0.282	0:28
11.4	0.248	0.316	0.282	0:41
62.1	0.359	0.392	0.376	0:46
144.8	0.442	0.456	0.449	0:51
205.9	0.483	0.492	0.488	0:56
267.1	0.527	0.531	0.529	1:00
340.9	0.588	0.590	0.589	1:06
410.2	0.657	0.647	0.652	1:11
471.5	0.698	0.691	0.695	1:17
552.4	0.757	0.744	0.751	1:24
340.3	0.723	0.711	0.717	1:30
207.5	0.677	0.670	0.674	1:35
89.7	0.587	0.601	0.594	1:43
40.7	0.517	0.550	0.534	1:48
9.6	0.377	0.444	0.411	1:50
64.6	0.504	0.536	0.520	1:55
135.8	0.577	0.588	0.583	2:01
199.1	0.618	0.624	0.621	2:05
262.7	0.655	0.654	0.655	2:10
346.9	0.693	0.689	0.691	2:17
413.5	0.720	0.716	0.718	2:21
483.6	0.749	0.744	0.747	2:28
558.2	0.788	0.776	0.782	2:33
607.0	0.826	0.798	0.812	2:40
410.6	0.802	0.776	0.789	2:45
204.1	0.727	0.716	0.722	2:50
41.7	0.577	0.603	0.590	2:58
56.6	0.604	0.619	0.612	7:05
8.0	0.497	0.551	0.524	7:15
10.0	0.497	0.551	0.524	7:25
61.9	0.545	0.562	0.554	7:27

202.5	0.658	0.654	0.656	7:33
301.7	0.707	0.694	0.701	7:42
409.2	0.756	0.739	0.748	7:49
505.8	0.797	0.774	0.786	7:55
610.1	0.855	0.832	0.844	8:03
714.8	0.938	0.912	0.925	8:13
809.2	1.040	0.979	1.010	8:22
911.2	1.146	1.067	1.107	8:34
1016.9	1.209	1.124	1.167	8:36
1017.9	1.264	1.174	1.219	8:52
1018.9	1.269	1.182	1.226	9:02
1016.2	1.279	1.191	1.235	9:18
1013.6	1.288	1.194	1.241	9:32
1017.9	1.289	1.201	1.245	9:43
654.0	1.247	1.153	1.200	9:49
254.0	1.098	1.017	1.058	9:51
9.8	0.779	0.761	0.770	9:57
0.0	0.688	0.686	0.687	9:58
Load (kPa)	SM1 (mm)	SM2 (mm)	Avg. S. (mm)	T (hours)

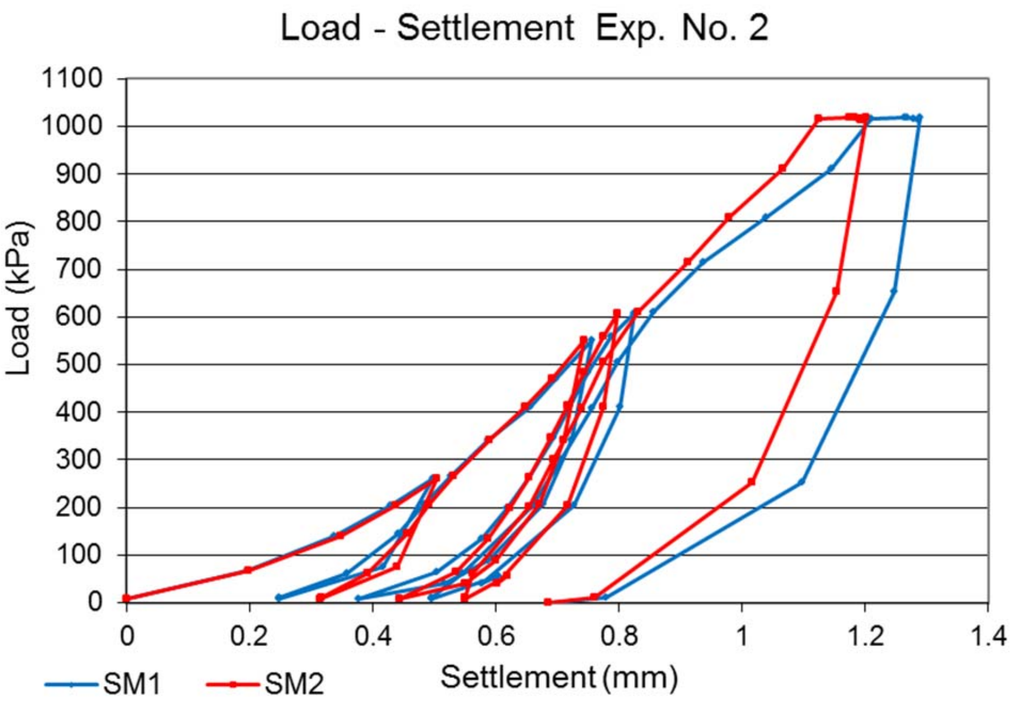

Experiment No.	3
Date	23.4.2009
Type	wetting at 1010 kPa
Notes	creep behaviour measured before wetting for load approximately 1010 kPa

Load (kPa)	SM1 (mm)	SM2 (mm)	Avg. S. (mm)	T (hours)	WS (cm)
17.0	0.000	0.000	0.000	0:00	---
68.7	0.150	0.119	0.135	0:05	---
149.1	0.289	0.264	0.277	0:13	---
207.7	0.362	0.338	0.350	0:19	---
112.8	0.347	0.313	0.330	0:23	---
12.3	0.191	0.149	0.170	0:28	---
13.3	0.187	0.148	0.168	0:42	---
117.1	0.319	0.281	0.300	0:53	---
207.9	0.391	0.361	0.376	0:59	---
302.3	0.480	0.460	0.470	1:12	---
404.3	0.574	0.568	0.571	1:20	---
510.6	0.656	0.667	0.662	1:28	---
605.4	0.735	0.757	0.746	1:35	---
708.5	0.815	0.841	0.828	1:42	---
806.6	0.898	0.930	0.914	1:52	---
914.6	0.975	1.009	0.992	1:59	---
1013.0	1.072	1.109	1.091	2:10	---
1014.6	1.083	1.119	1.101	2:21	---
1012.2	1.093	1.129	1.111	2:41	---
1012.6	1.094	1.134	1.114	2:49	---
1012.0	1.098	1.138	1.118	2:54	70.9
1012.8	1.103	1.140	1.122	2:57	60.3
1011.6	1.108	1.146	1.127	2:59	55.8
1011.8	1.122	1.157	1.140	3:04	48.3
1011.8	1.134	1.168	1.151	3:10	45.6
1014.2	1.151	1.182	1.167	3:16	44.4
1011.6	1.162	1.193	1.178	3:20	43.3
1020.1	1.178	1.207	1.193	3:25	42.5
1017.1	1.193	1.219	1.206	3:30	41.8
1015.2	1.203	1.228	1.216	3:35	41.1
1013.0	1.214	1.238	1.226	3:40	41.0
1010.6	1.232	1.256	1.244	3:47	41.2
1012.0	1.241	1.259	1.250	3:52	41.6
1011.6	1.247	1.268	1.258	3:58	41.2
1013.0	1.254	1.277	1.266	4:06	41.4
1013.6	1.264	1.281	1.273	4:14	42.2

1012.4	1.273	1.289	1.281	4:25	43.2
1016.9	1.282	1.297	1.290	4:33	43.1
1014.6	1.288	1.305	1.297	4:45	43.5
1013.4	1.292	1.308	1.300	4:53	44.3
1012.4	1.294	1.310	1.302	5:01	44.7
1012.0	1.297	1.311	1.304	5:06	44.5
1013.6	1.299	1.316	1.308	5:11	44.6
1013.2	1.302	1.318	1.310	5:17	47.7
1012.6	1.303	1.319	1.311	5:22	50.3
1011.4	1.303	1.319	1.311	5:29	53.5
1011.2	1.304	1.323	1.314	5:34	59.7
1012.8	1.304	1.324	1.314	5:38	63.5
1012.2	1.305	1.326	1.316	5:42	65.0
1012.0	1.308	1.327	1.318	5:45	66.7
1011.4	1.309	1.328	1.319	5:52	---
1011.2	1.311	1.328	1.320	6:02	---
547.2	1.210	1.217	1.214	6:09	---
400.6	1.163	1.157	1.160	6:16	---
220.6	1.043	1.016	1.030	6:22	---
9.2	0.677	0.643	0.660	6:29	---
0.0	0.587	0.569	0.578	6:34	---
Load (kPa)	SM1 (mm)	SM2 (mm)	Avg. S. (mm)	T (hours)	WS (cm)

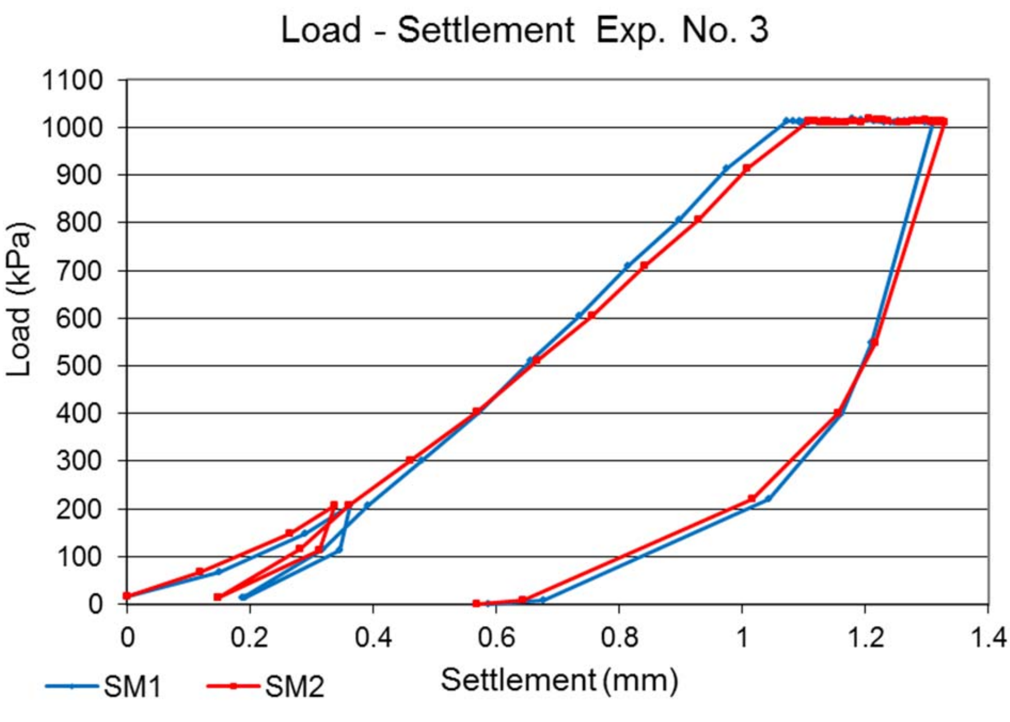

Experiment No.	4
Date	7.5.2009
Type	dry – flooded 14 days ago
Notes	creep behaviour tested for load approximately 710 kPa

Load (kPa)	SM1 (mm)	SM2 (mm)	Avg. S. (mm)	T (hours)
13.7	0	0	0.000	0:00
98.7	0.207	0.194	0.201	0:13
198.0	0.358	0.347	0.353	0:25
105.1	0.336	0.321	0.329	0:34
7.1	0.164	0.161	0.163	0:41
98.3	0.285	0.279	0.282	0:53
199.9	0.368	0.353	0.361	0:59
290.2	0.475	0.456	0.466	1:13
403.2	0.57	0.544	0.557	1:21
505.6	0.657	0.629	0.643	1:31
392.0	0.656	0.624	0.640	1:36
243.5	0.6	0.572	0.586	1:42
118.5	0.521	0.494	0.508	1:47
9.0	0.284	0.275	0.280	1:53
125.0	0.455	0.437	0.446	1:58
297.7	0.58	0.554	0.567	2:03
452.0	0.657	0.634	0.646	2:11
605.4	0.748	0.723	0.736	2:17
708.5	0.808	0.782	0.795	2:26
711.2	0.813	0.787	0.800	2:38
708.7	0.814	0.788	0.801	2:49
708.7	0.816	0.792	0.804	3:01
709.0	0.817	0.792	0.805	3:09
709.2	0.817	0.793	0.805	3:15
709.0	0.821	0.794	0.808	3:27
525.2	0.807	0.774	0.791	3:33
198.6	0.676	0.639	0.658	3:38
6.9	0.351	0.348	0.350	3:43
0.0	0.313	0.315	0.314	3:46
Load (kPa)	SM1 (mm)	SM2 (mm)	Avg. S. (mm)	T (hours)

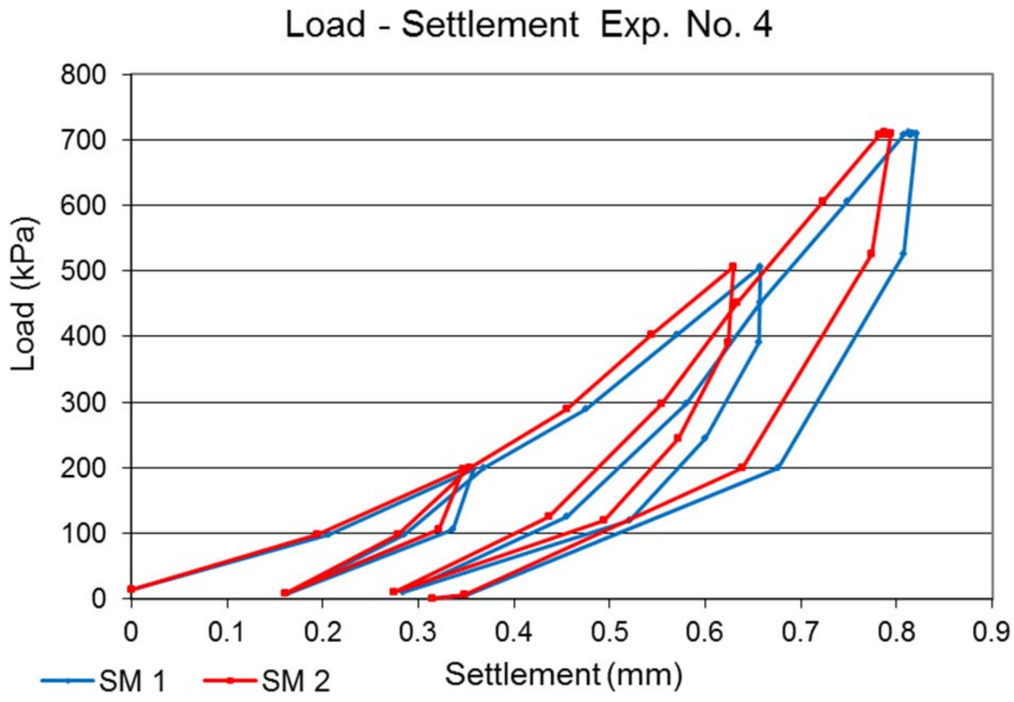

Experiment No.	5
Date	11.5.2009
Type	wetting at 710 kPa
Notes	creep behaviour measured before wetting for load approximately 710 kPa

Load (kPa)	SM1 (mm)	SM2 (mm)	Avg. S. (mm)	T (hours)	WS (cm)
6.9	0	0	0.000	0:00	---
97.7	0.182	0.155	0.169	0:05	---
198.0	0.265	0.242	0.254	0:16	---
299.1	0.33	0.31	0.320	0:29	---
192.1	0.33	0.289	0.310	0:35	---
96.0	0.26	0.232	0.246	0:43	---
7.1	0.081	0.073	0.077	0:55	---
151.3	0.25	0.232	0.241	1:01	---
299.3	0.334	0.318	0.326	1:08	---
455.3	0.42	0.405	0.413	1:17	---
605.4	0.504	0.492	0.498	1:27	---
709.8	0.559	0.546	0.553	1:33	---
709.0	0.561	0.553	0.557	1:46	---
707.9	0.568	0.554	0.561	1:52	---
708.7	0.568	0.554	0.561	1:57	---
708.5	0.569	0.555	0.562	2:01	70.5

709.0	0.571	0.559	0.565	2:17	53.0
709.4	0.571	0.561	0.566	2:25	51.3
708.3	0.576	0.563	0.570	2:33	50.1
709.2	0.576	0.564	0.570	2:43	45.0
708.3	0.576	0.565	0.571	2:53	43.7
708.3	0.581	0.566	0.574	3:04	42.6
709.2	0.581	0.569	0.575	3:20	40.2
708.7	0.583	0.569	0.576	3:31	39.0
708.1	0.583	0.571	0.577	3:41	38.0
709.8	0.585	0.573	0.579	3:47	36.3
709.0	0.591	0.576	0.584	4:19	35.0
707.1	0.592	0.582	0.587	5:30	35.6
706.9	0.601	0.587	0.594	7:37	38.6
708.1	0.601	0.589	0.595	8:07	35.0
706.3	0.601	0.592	0.597	8:45	35.3
706.7	0.601	0.593	0.597	9:26	36.1
706.7	0.601	0.594	0.598	9:56	36.5
689.8	0.612	0.606	0.609	23:37	49.6
724.7	0.647	0.627	0.637	27:22	49.0
727.8	0.652	0.635	0.644	29:52	58.5
416.6	0.595	0.576	0.586	30:10	58.5
219.4	0.519	0.492	0.506	30:21	58.5
6.9	0.18	0.189	0.185	30:35	58.5
0.0	0.114	0.129	0.122	30:37	58.5
Load (kPa)	SM1 (mm)	SM2 (mm)	Avg. S. (mm)	T (hours)	WS (cm)

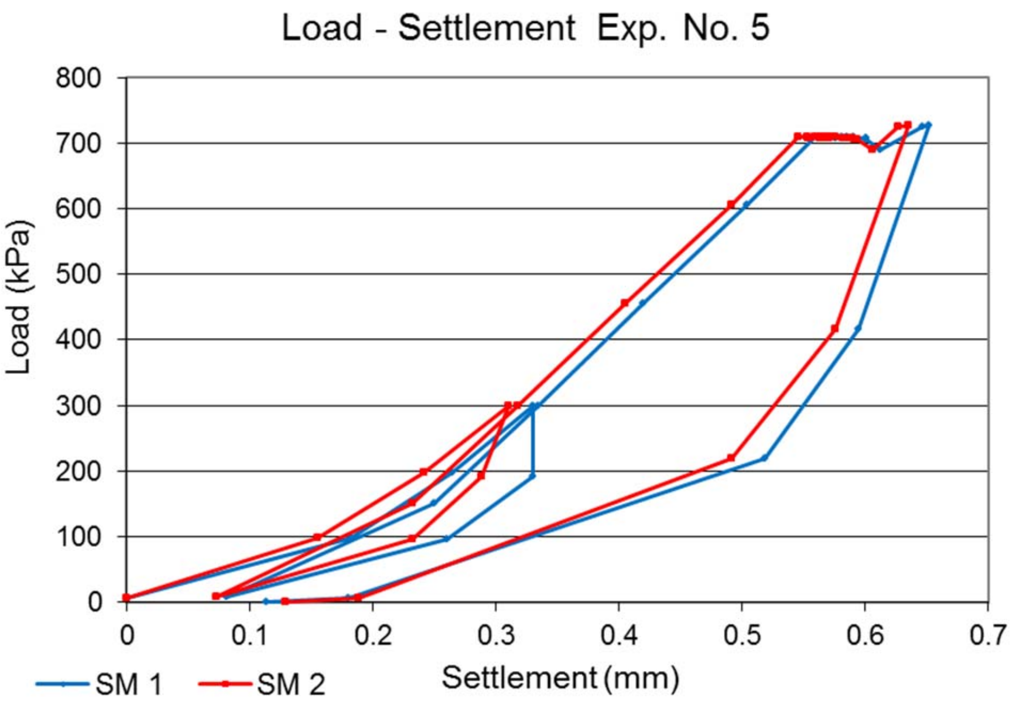

Experiment No.	6
Date	14.5.2009
Type	wetting at 1010 kPa
Notes	creep behaviour in second load cycle for load approximately 1010 kPa

Load (kPa)	SM1 (mm)	SM2 (mm)	Avg. S. (mm)	T (hours)	WS (cm)
5.3	0	0	0	0:00	---
97.5	0.179	0.157	0.168	0:09	---
199.7	0.27	0.247	0.2585	0:18	---
299.7	0.343	0.316	0.3295	0:29	---
162.4	0.309	0.272	0.2905	0:35	---
5.5	0.041	0.012	0.0265	0:42	---
152.8	0.257	0.222	0.2395	0:56	---
302.3	0.348	0.322	0.335	1:08	---
452.0	0.432	0.403	0.4175	1:22	---
606.6	0.509	0.481	0.495	1:37	---
755.0	0.588	0.555	0.5715	2:08	---
908.2	0.683	0.655	0.669	2:28	---
1012.0	0.762	0.744	0.753	2:45	---
1009.4	0.773	0.758	0.7655	3:11	---
1011.6	0.778	0.763	0.7705	3:28	---
1010.6	0.779	0.768	0.7735	3:43	---
776.1	0.763	0.742	0.7525	3:53	---
358.7	0.65	0.616	0.633	4:02	---
8.4	0.173	0.153	0.163	4:15	---
13.3	0.175	0.153	0.164	5:05	---
206.3	0.448	0.422	0.435	5:19	---
406.7	0.564	0.541	0.5525	5:37	---
605.2	0.659	0.633	0.646	5:51	---
807.4	0.743	0.724	0.7335	6:06	---
1013.2	0.848	0.839	0.8435	6:18	---
1012.6	0.849	0.844	0.8465	6:31	54.0
1014.2	0.856	0.852	0.854	6:45	49.8
1009.4	0.859	0.853	0.856	7:07	45.7
1010.8	0.859	0.857	0.858	7:23	45.0
971.9	0.876	0.876	0.876	22:22	58.5
975.5	0.882	0.883	0.8825	28:19	---
511.4	0.81	0.791	0.8005	28:28	---
235.9	0.681	0.652	0.6665	28:38	---
6.1	0.278	0.278	0.278	28:46	---
0.0	0.242	0.243	0.2425	28:50	---
Load (kPa)	SM1 (mm)	SM2 (mm)	Avg. S. (mm)	T (hours)	WS (cm)

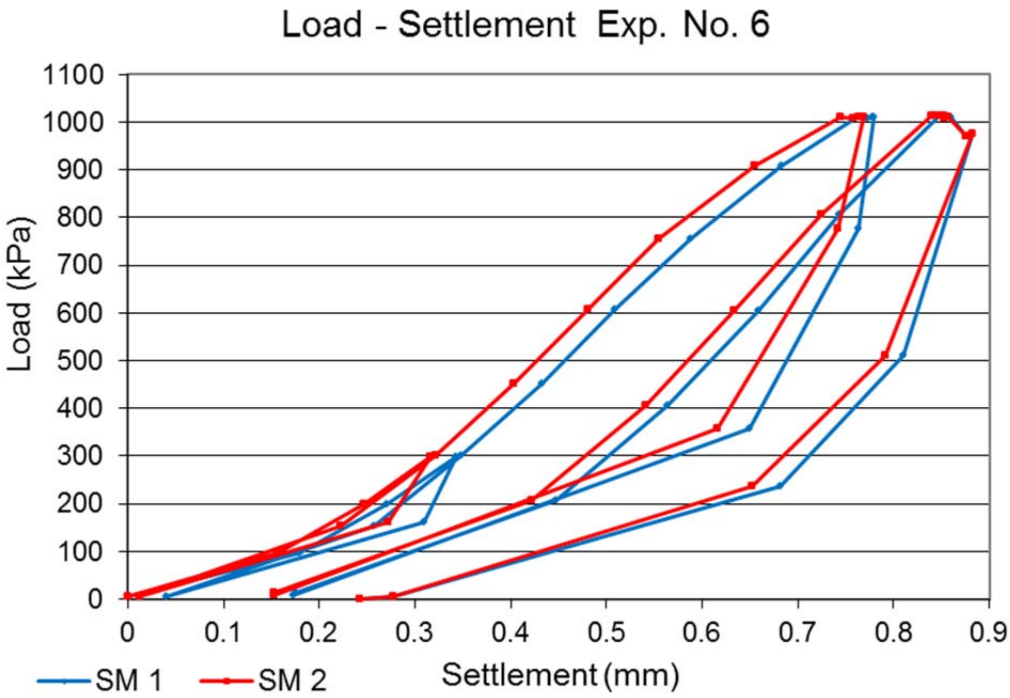

Experiment No.	7
Date	5.8.2009
Type	dry – flooded 83 days ago
Notes	creep behaviour tested for load approximately 1010 kPa

Load (kPa)	SM1 (mm)	SM2 (mm)	Avg. S. (mm)	T (hours)
7.4	0	0	0.000	0:00
98.1	0.408	0.362	0.385	0:10
202.3	0.603	0.541	0.572	0:20
299.7	0.747	0.675	0.711	0:30
403.7	0.87	0.788	0.829	0:41
501.7	0.977	0.885	0.931	0:53
606.2	1.077	0.98	1.029	1:03
412.5	1.051	0.952	1.002	1:13
224.6	0.972	0.862	0.917	1:23
113.0	0.865	0.737	0.801	1:33
7.4	0.713	0.567	0.640	1:45
104.5	0.839	0.707	0.773	1:53
209.5	0.918	0.795	0.857	2:03
299.7	0.971	0.856	0.914	2:17
405.5	1.022	0.91	0.966	2:29
505.4	1.077	0.959	1.018	2:40
607.2	1.135	1.02	1.078	2:51

Load (kPa)	SM1 (mm)	SM2 (mm)	Avg. S. (mm)	T (hours)
399.2	1.111	0.999	1.055	3:01
213.4	1.031	0.908	0.970	3:13
80.9	0.924	0.794	0.859	3:15
8.0	0.77	0.623	0.697	3:32
100.8	0.892	0.756	0.824	3:45
210.3	0.973	0.846	0.910	3:55
309.7	1.031	0.907	0.969	4:05
406.3	1.076	0.954	1.015	4:13
511.0	1.123	1.002	1.063	4:24
616.1	1.18	1.055	1.118	4:32
711.6	1.238	1.117	1.178	4:42
825.9	1.316	1.205	1.261	4:52
909.8	1.384	1.281	1.333	5:03
1012.8	1.464	1.358	1.411	5:15
1013.8	1.473	1.367	1.420	5:26
1014.4	1.48	1.37	1.425	5:33
1012.4	1.482	1.37	1.426	5:45
1011.8	1.483	1.37	1.427	5:54
641.0	1.432	1.327	1.380	6:03
408.2	1.361	1.25	1.306	6:15
211.5	1.253	1.13	1.192	6:23
80.3	1.119	0.979	1.049	6:53
7.4	0.911	0.757	0.834	7:38

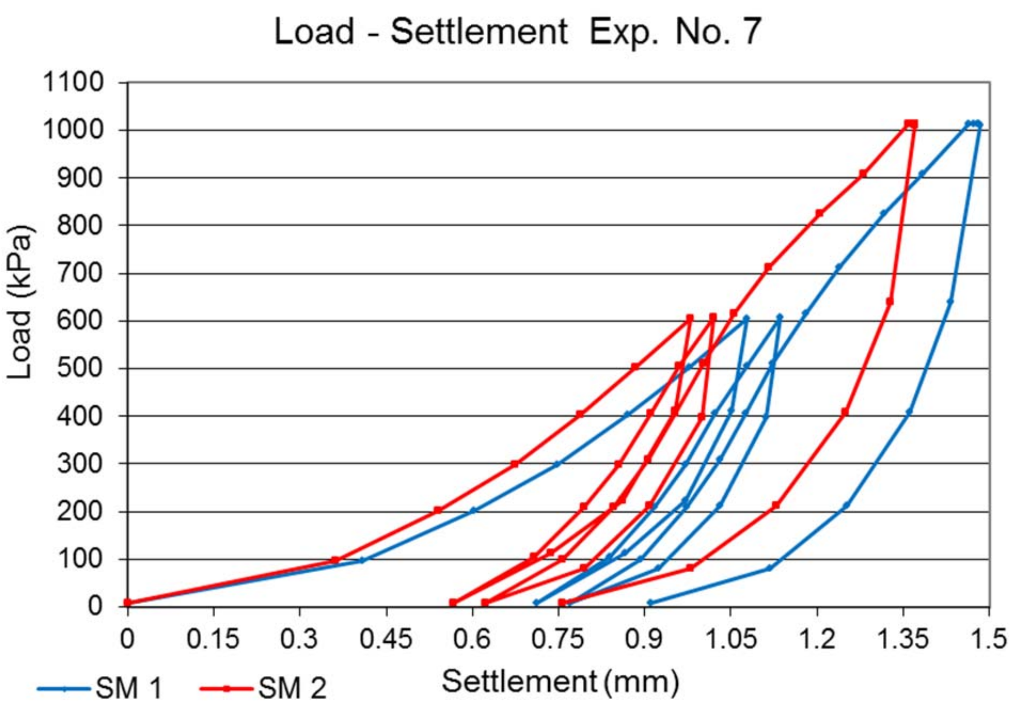

Experiment No.	8
Date	10.8.2009
Type	dry – flooded 88 days ago
Notes	-----

Load (kPa)	SM1 (mm)	SM2 (mm)	Avg. S. (mm)	T (hours)
7.6	0	0	0.000	0:00
98.1	0.256	0.283	0.270	0:14
191.9	0.385	0.41	0.398	0:24
297.9	0.482	0.502	0.492	0:35
132.6	0.423	0.44	0.432	0:49
35.4	0.312	0.33	0.321	1:00
101.2	0.364	0.378	0.371	1:08
44.3	0.327	0.344	0.336	1:22
7.2	0.173	0.214	0.194	1:31
100.0	0.37	0.378	0.374	1:40
194.0	0.441	0.448	0.445	2:01
297.5	0.502	0.515	0.509	2:13
178.7	0.474	0.484	0.479	2:23
59.1	0.379	0.394	0.387	2:31
7.4	0.223	0.227	0.225	2:41
193.5	0.46	0.466	0.463	2:53
299.1	0.521	0.531	0.526	3:06
451.4	0.618	0.634	0.626	3:14
605.6	0.721	0.737	0.729	3:25
747.0	0.814	0.832	0.823	3:40
907.3	0.905	0.921	0.913	3:54
1009.2	0.955	0.97	0.963	4:04
674.6	0.903	0.917	0.910	4:14
328.1	0.792	0.797	0.795	4:30
184.2	0.72	0.722	0.721	4:40
89.7	0.631	0.631	0.631	4:53
7.1	0.401	0.392	0.397	5:06
0.0	0.338	0.312	0.325	5:08
7.6	0	0	0.000	0:00
Load (kPa)	SM1 (mm)	SM2 (mm)	Avg. S. (mm)	T (hours)

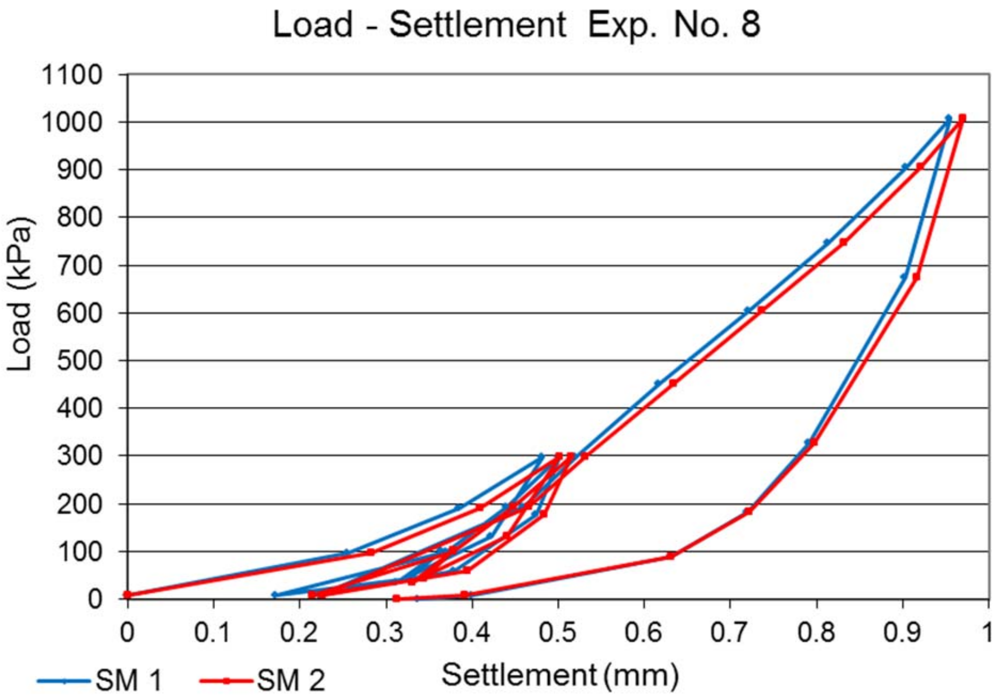

Experiment No.	9
Date	11.8.2009
Type	dry – flooded 89 days ago
Notes	originally designed to confirm the negligibility of reaction frame relaxation

Load (kPa)	SM1 (mm)	SM2 (mm)	Avg. S. (mm)	T (hours)
7.8	0	0	0	0:00
119.9	0.152	0.207	0.1795	0:11
221.0	0.234	0.299	0.2665	0:23
304.6	0.284	0.356	0.32	0:32
383.6	0.329	0.403	0.366	0:43
519.6	0.399	0.475	0.437	0:53
603.2	0.443	0.523	0.483	1:12
719.1	0.496	0.566	0.531	1:25
420.9	0.451	0.526	0.4885	1:35
247.8	0.389	0.466	0.4275	1:45
79.9	0.277	0.364	0.3205	1:55
6.7	0.129	0.226	0.1775	2:03
7.1	0.126	0.225	0.1755	2:09
0.0	0.092	0.191	0.1415	2:11

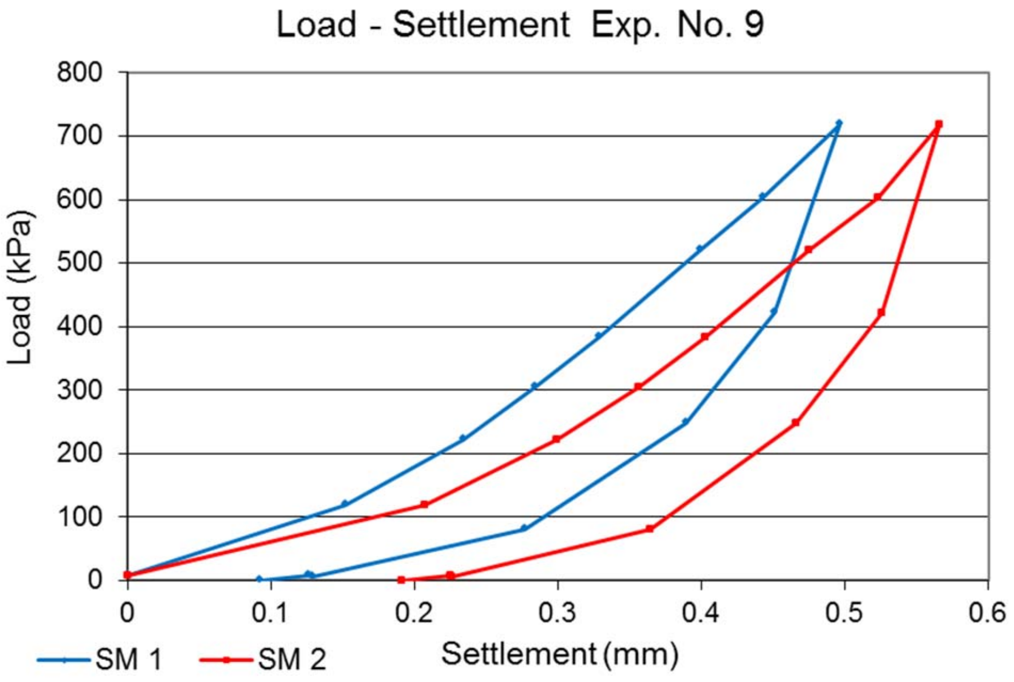

Experiment No.	10
Date	19.7.2010
Type	wetting at 910 kPa
Notes	shear zone measurement added

Load (kPa)	SM1 (mm)	SM2 (mm)	Avg. S. (mm)	SZ 50 (mm)	SZ 100 (mm)	T (hours)	WS (cm)
9.2	0	0	0.000	0.000	0.000	0:00	---
49.7	0.186	0.181	0.184	0.006	0.000	0:10	---
104.7	0.314	0.318	0.316	0.012	0.000	0:23	---
159.1	0.405	0.412	0.409	0.020	0.000	0:30	---
239.5	0.519	0.534	0.527	0.031	0.007	0:42	---
302.5	0.575	0.591	0.583	0.040	0.007	0:50	---
404.5	0.669	0.69	0.680	0.052	0.011	1:00	---
494.1	0.742	0.762	0.752	0.063	0.016	1:12	---
606.4	0.809	0.838	0.824	0.077	0.019	1:20	---
702.6	0.87	0.9	0.885	0.087	0.022	1:31	---
808.4	0.933	0.969	0.951	0.099	0.027	1:43	---
912.4	0.994	1.034	1.014	0.109	0.029	1:54	---
783.3	0.992	1.03	1.011	0.110	0.030	2:03	---
675.2	0.974	1.016	0.995	0.109	0.029	2:13	---
556.2	0.952	0.991	0.972	0.102	0.028	2:24	---
398.9	0.913	0.948	0.931	0.091	0.023	2:33	---
299.7	0.881	0.911	0.896	0.085	0.019	2:40	---

197.0	0.835	0.859	0.847	0.075	0.016	2:50	---
94.4	0.758	0.773	0.766	0.060	0.009	2:57	---
8.8	0.589	0.592	0.591	0.036	0.000	3:05	---
10.8	0.579	0.585	0.582	0.035	0.000	3:57	---
50.7	0.639	0.641	0.640	0.040	0.001	4:07	---
96.6	0.686	0.697	0.692	0.049	0.001	4:20	---
147.3	0.727	0.739	0.733	0.054	0.003	4:38	---
201.7	0.764	0.772	0.768	0.061	0.006	4:54	---
302.9	0.814	0.831	0.823	0.071	0.010	5:15	---
472.7	0.877	0.902	0.890	0.083	0.018	5:30	---
515.2	0.895	0.922	0.909	0.089	0.019	5:40	---
613.8	0.929	0.96	0.945	0.095	0.021	5:50	---
708.7	0.96	0.991	0.976	0.100	0.027	5:58	---
816.2	0.995	1.032	1.014	0.110	0.030	6:09	---
914.2	1.035	1.07	1.053	0.120	0.038	6:23	---
913.4	1.035	1.071	1.053	0.120	0.038	6:25	valve opened
913.4	1.042	1.076	1.059	0.121	0.039	6:29	> 80
913.4	1.045	1.081	1.063	0.126	0.041	6:34	> 80
913.4	1.052	1.088	1.070	0.129	0.043	6:42	> 80
913.4	1.056	1.092	1.074	0.131	0.047	6:55	> 80
913.4	1.059	1.095	1.077	0.131	0.048	6:59	> 80
913.4	1.062	1.099	1.081	0.132	0.049	7:04	> 80
913.4	1.063	1.1	1.082	0.133	0.049	7:11	> 80
913.4	1.065	1.103	1.084	0.139	0.050	7:34	> 80
913.4	1.071	1.11	1.091	0.140	0.057	7:43	> 80
914.2	1.072	1.111	1.092	0.140	0.057	8:10	valve closed
913.4	1.074	1.112	1.093	0.141	0.057	8:15	---
744.1	1.064	1.101	1.083	0.141	0.057	8:20	---
580.6	1.035	1.076	1.056	0.131	0.051	8:25	---
412.9	0.989	1.027	1.008	0.120	0.043	8:30	---
216.8	0.905	0.932	0.919	0.099	0.030	8:35	---
104.2	0.832	0.848	0.840	0.080	0.020	8:40	---
9.2	0.645	0.65	0.648	0.050	0.010	8:45	---
0.0	0.6	0.601	0.601	0.049	0.009	8:48	---
Load (kPa)	SM1 (mm)	SM2 (mm)	Avg. S. (mm)	SZ 50 (mm)	SZ 100 (mm)	T (hours)	WS (cm)

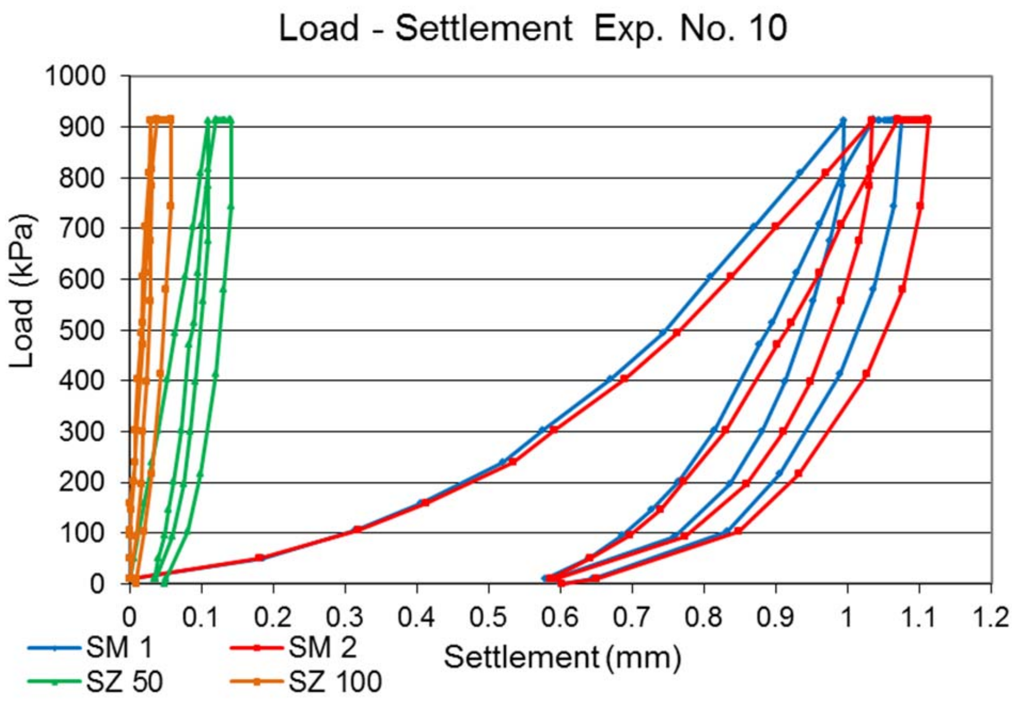

Experiment No.	11
Date	20.7.2010
Type	dry – wetted 1 day ago
Notes	shear zone measurement added

Load (kPa)	SM1 (mm)	SM2 (mm)	Avg. S. (mm)	SZ 50 (mm)	SZ 100 (mm)	T (hours)
5.7	0	0	0.000	0.000	0.000	0:00
49.4	0.106	0.114	0.110	0.009	0.003	0:08
98.3	0.166	0.178	0.172	0.016	0.004	0:15
200.5	0.245	0.264	0.255	0.030	0.012	0:23
299.7	0.302	0.326	0.314	0.044	0.017	0:31
406.7	0.35	0.383	0.367	0.056	0.025	0:40
282.8	0.335	0.363	0.349	0.054	0.024	0:45
199.3	0.306	0.33	0.318	0.045	0.023	0:51
94.0	0.245	0.263	0.254	0.033	0.016	0:55
6.3	0.067	0.072	0.070	0.009	0.009	1:00
0.0	0.026	0.023	0.025	0.016	0.006	1:04

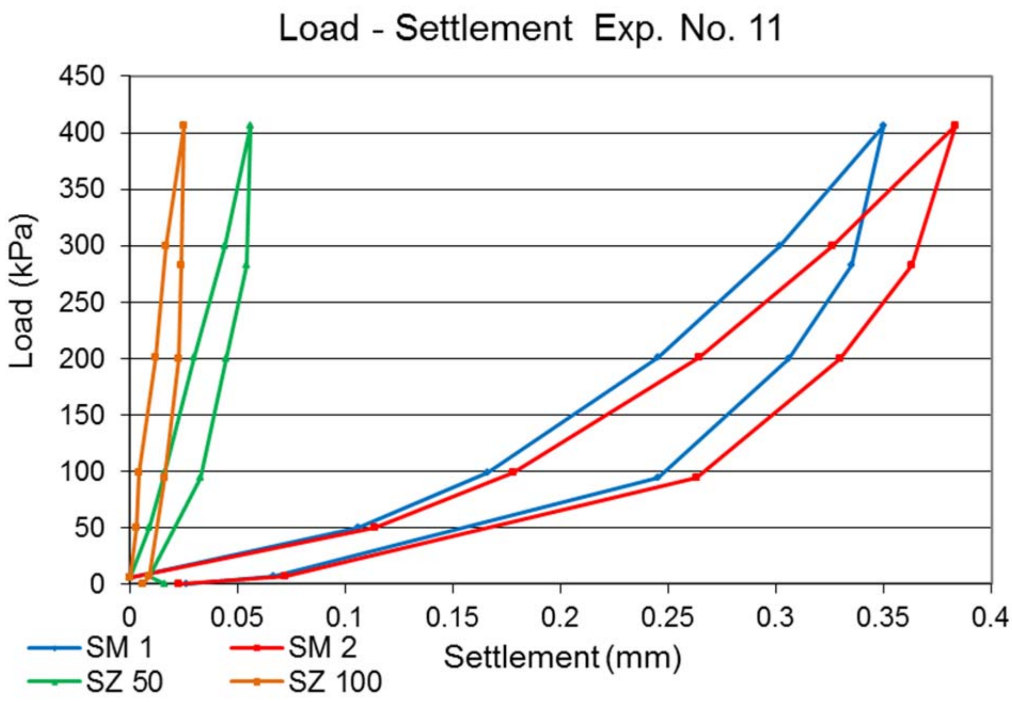

Experiment No.	12
Date	20.7.2010
Type	dry – wetted 1 day ago
Notes	11 cm excavated and plate positioned into the pit; shear zone measured but all values were zeros

Load (kPa)	SM1 (mm)	SM2 (mm)	Avg. S. (mm)	T (hours)
4.9	0	0	0.000	0:00
48.8	0.098	0.069	0.083	0:07
97.5	0.189	0.132	0.161	0:13
201.1	0.31	0.224	0.267	0:19
301.9	0.416	0.32	0.368	0:24
393.6	0.484	0.409	0.446	0:29
299.3	0.481	0.409	0.445	0:34
195.8	0.451	0.382	0.417	0:39
85.6	0.392	0.332	0.362	0:44
6.7	0.283	0.246	0.265	0:49
98.1	0.363	0.31	0.337	0:54
200.7	0.415	0.357	0.386	0:59
88.3	0.384	0.323	0.354	1:04
4.5	0.28	0.243	0.262	1:09
0.0	0.259	0.219	0.239	1:12

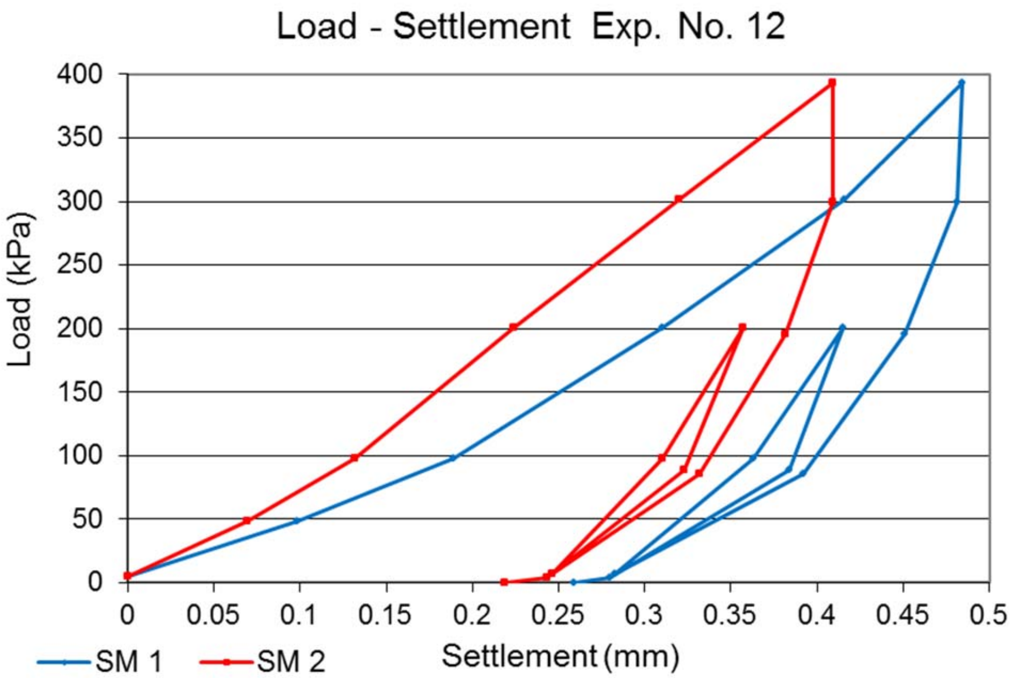
Load - Settlement Exp. No. 12
Load (kPa)
400
350
300
250
200
150
100
50
0
0
0.05
0.1
0.15
0.2
0.25
0.3
0.35
0.4
0.45
0.5
Settlement (mm)
SM 1
SM 2

Appendix C

PLATE LOAD TESTS ON SILT LOAM

The following pages contain processed data from full scale experiments on soil specimen made of silt loam. The data are presented in the same order in which the experiments were carried out. More detailed description of the soil sample or the placement of the soil into the stand can be found in relevant part of chapter 4.

Symbols used further in the tables and charts have following meaning. Data labelled as SM 1 or SM 2 (settlement measuring point 1 and 2) contain measured results from dial gauges located symmetrically on the top of the plate. SZ 50 and SZ 100 are measured settlements of the shear zone from dial gauges located 50 mm from the edge of the plate in case of SZ 50 and 100 mm from the edge of the plate in case of SZ 100. Column labelled as WS contains position of groundwater table inside the soil with respect to the top of the specimen. Due to the influence of the preferential paths created around the intake to the piezometer during compaction process and due to leakage from the stand, measured positions of groundwater table must be interpreted carefully and with respect to these facts. T stands for time and Avg. S. represents average settlement. LP contains measured lateral pressures.

Experiment No.	1
Date	6.5.2011
Type	dry – natural moisture
Notes	shear zone and lateral pressure measurement added

Load (kPa)	SM1 (mm)	SM2 (mm)	Avg. S. (mm)	SZ 50 (mm)	SZ 100 (mm)	T (hours)	LP (kPa)
4.1	0	0	0.000	0.000	0.000	0:00	0.00
49.0	0.554	0.525	0.540	0.075	0.047	0:07	2.12
97.9	1.17	1.1	1.135	0.207	0.105	0:20	5.41

199.9	2.046	1.963	2.005	0.511	0.228	0:33	12.37
300.5	3.02	2.91	2.965	0.849	0.368	0:49	18.90
195.0	2.912	2.809	2.861	0.800	0.324	1:00	15.46
95.6	2.682	2.6	2.641	0.686	0.177	1:12	11.05
3.9	1.948	1.92	1.934	0.432	0.137	1:26	3.70
7.1	1.924	1.898	1.911	0.427	0.136	1:44	3.58
97.7	2.319	2.258	2.289	0.541	0.216	1:58	7.75
199.9	2.719	2.63	2.675	0.712	0.296	2:12	13.29
299.7	3.209	3.089	3.149	0.915	0.390	2:30	18.50
397.9	4.811	4.827	4.819	1.260	0.526	2:49	23.67
498.0	9.722	9.568	9.645	1.540	0.670	3:09	26.61
503.0	10.121	9.956	10.039	1.567	0.686	3:25	26.63
291.6	9.856	9.69	9.773	1.525	0.586	3:35	20.95
197.4	9.596	9.435	9.516	1.330	0.516	3:47	17.12
97.3	9.18	9.009	9.095	1.188	0.426	3:57	11.89
4.3	8.29	8.128	8.209	0.927	0.282	4:10	4.56
0.0	8.205	8.057	8.131	0.907	0.271	4:14	0.00
Load (kPa)	SM1 (mm)	SM2 (mm)	Avg. S. (mm)	SZ 50 (mm)	SZ 100 (mm)	T (hours)	LP (kPa)

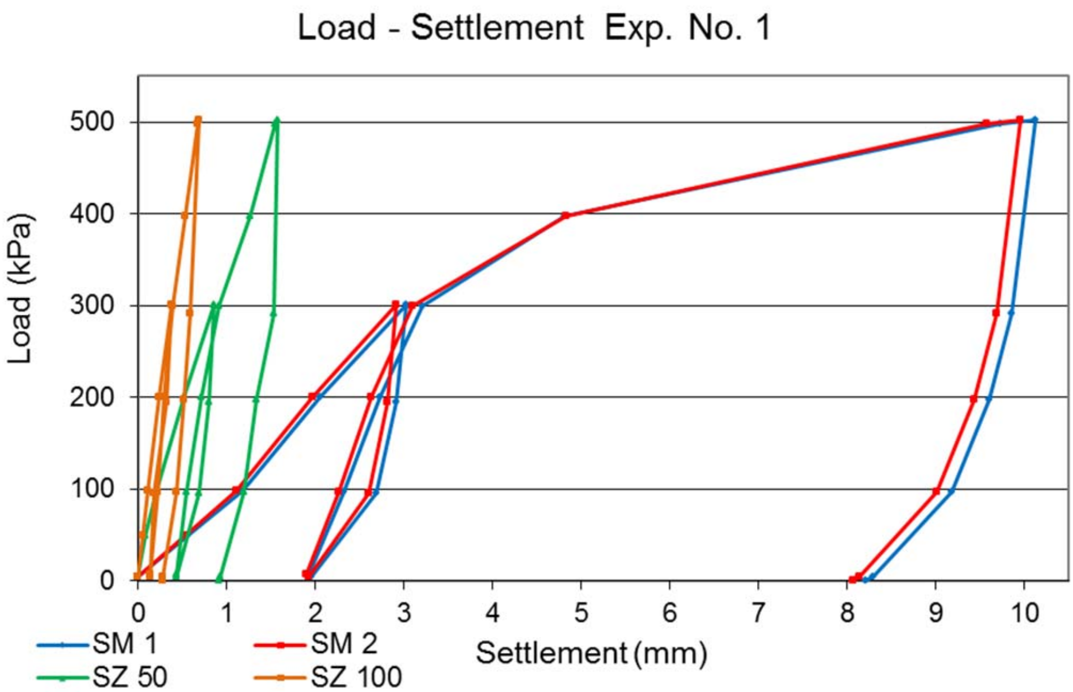

Experiment No. 2

Date	7.7.2011
Type	dry
Notes	shear zone measurement added

Load (kPa)	SM1 (mm)	SM2 (mm)	Avg. S. (mm)	SZ 50 (mm)	SZ 100 (mm)	T (hours)
5.3	0	0	0.000	0.000	0.000	0:00
30.6	0.131	0.12	0.126	0.018	0.020	0:06
50.1	0.229	0.217	0.223	0.040	0.038	0:14
67.8	0.318	0.312	0.315	0.085	0.059	0:20
96.0	0.481	0.475	0.478	0.122	0.100	0:27
148.5	0.762	0.746	0.754	0.226	0.179	0:33
201.1	1.06	1.033	1.047	0.350	0.278	0:43
251.4	1.35	1.315	1.333	0.476	0.378	0:54
300.1	1.63	1.593	1.612	0.592	0.480	1:04
351.4	1.952	1.906	1.929	0.712	0.600	1:14
402.2	2.252	2.205	2.229	0.819	0.701	1:25
401.8	2.311	2.263	2.287	0.841	0.720	1:38
402.0	2.352	2.304	2.328	0.860	0.737	1:49
402.4	2.388	2.336	2.362	0.872	0.748	2:04
398.5	2.422	2.375	2.399	0.884	0.762	2:35
221.6	2.228	2.198	2.213	0.787	0.676	2:51
107.7	1.955	1.955	1.955	0.649	0.564	3:04
6.1	1.403	1.423	1.413	0.404	0.387	3:11
6.5	1.379	1.4	1.390	0.393	0.377	3:15
0.0	1.331	1.347	1.339	0.380	0.369	3:17

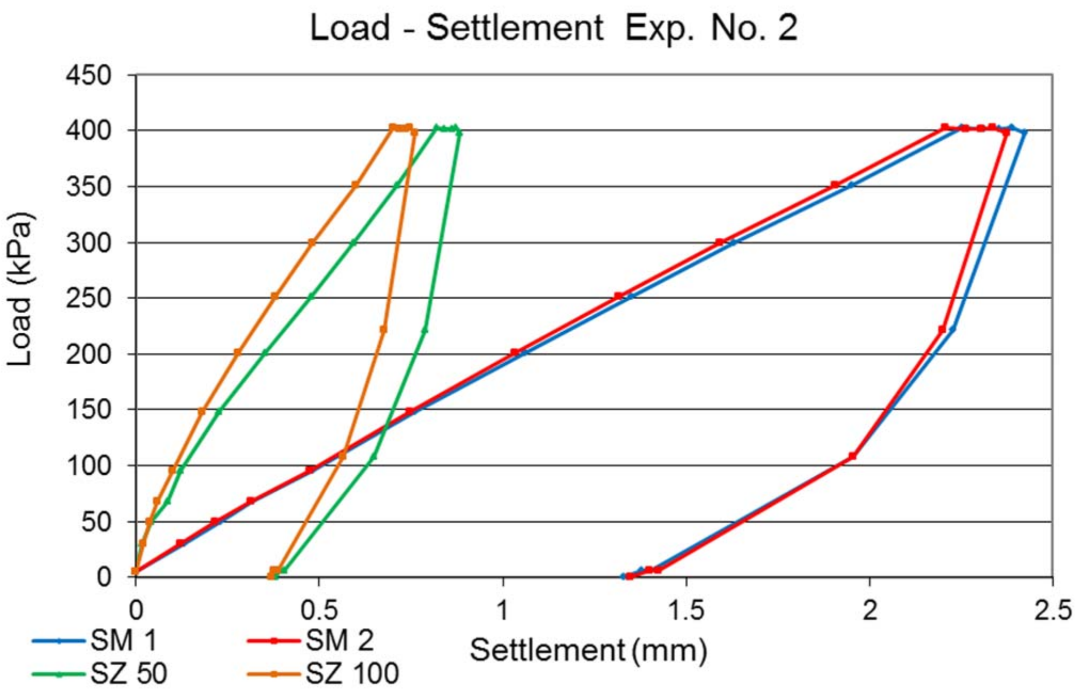

Experiment No.	3
Date	8.7.2011
Type	wetting at 400 kPa
Notes	shear zone measurement added

Load (kPa)	SM1 (mm)	SM2 (mm)	Avg. S. (mm)	SZ 50 (mm)	SZ 100 (mm)	T (hours)	WS (cm)
6.3	0	0	0.000	0.000	0.000	0:00	---
50.1	0.145	0.152	0.149	0.033	0.026	0:06	---
97.3	0.297	0.301	0.299	0.087	0.066	0:14	---
148.9	0.474	0.458	0.466	0.162	0.126	0:31	---
199.9	0.634	0.603	0.619	0.240	0.188	0:42	---
250.4	0.795	0.759	0.777	0.327	0.263	0:58	---
300.3	0.948	0.904	0.926	0.414	0.334	1:14	---
351.8	1.102	1.049	1.076	0.495	0.404	1:29	---
402.2	1.281	1.221	1.251	0.583	0.475	1:45	---
402.6	1.305	1.25	1.278	0.595	0.485	1:56	valve open
392.4	2.435	2.431	2.433	1.795	1.635	2:04	NM*
389.3	2.985	3.001	2.993	2.285	2.115	2:08	NM
400.4	3.245	3.251	3.248	2.450	2.285	2:13	NM
400.0	3.413	3.421	3.417	2.574	2.393	2:18	NM
404.5	3.493	3.511	3.502	2.630	2.445	2:23	NM
399.8	3.55	3.561	3.556	2.660	2.480	2:28	NM
402.2	3.63	3.641	3.636	2.725	2.534	2:33	NM
398.7	3.75	3.761	3.756	2.812	2.615	2:39	NM
400.2	3.87	3.871	3.871	2.880	2.690	2:47	NM
403.4	3.947	3.946	3.947	2.925	2.735	2:54	NM
402.2	4.02	4.021	4.021	2.977	2.785	3:00	NM
403.4	4.12	4.119	4.120	3.032	2.840	3:08	NM
398.7	4.234	4.24	4.237	3.115	2.913	3:21	NM
374.4	4.564	4.576	4.570	3.326	3.106	3:56	NM
401.6	4.79	4.809	4.800	3.419	3.192	4:03	NM
402.2	5.04	5.044	5.042	3.495	3.265	4:13	NM
397.7	5.545	5.56	5.553	3.635	3.404	4:35	NM
391.8	6.255	6.241	6.248	3.725	3.493	4:53	NM
235.7	6.083	6.061	6.072	3.608	3.394	5:01	NM
144.2	5.777	5.772	5.775	3.493	3.286	5:14	NM
6.1	4.637	4.681	4.659	3.170	3.003	5:24	NM
0.0	3.526	4.569	4.048	3.135	2.971	5:29	valve close
0.0				3.114	2.950	23:39	---

*NM…not measured due to clogging of the open piezometer

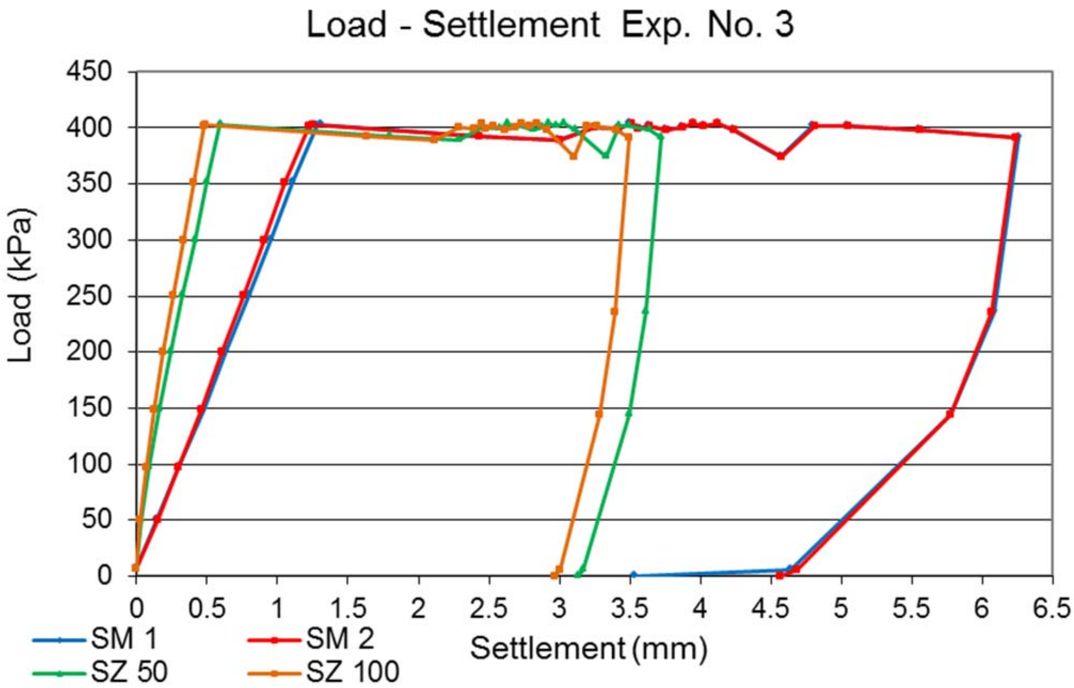

Experiment No.	4
Date	5.10.2011
Type	dry – flooded 89 days ago
Notes	shear zone and lateral pressure measurement added; still saturated from previous experiment

Load (kPa)	SM1 (mm)	SM2 (mm)	Avg. S. (mm)	SZ 50 (mm)	SZ 100 (mm)	T (hours)	LP (kPa)
3.9	0	0	0.000	0.000	0.000	0:00	0.00
49.0	4.416	4.931	4.674	0.936	0.588	1:14	2.77
49.0	4.798	5.331	5.065	1.067	0.701	1:35	2.86
49.0	5.068	5.597	5.333	1.160	0.773	1:47	2.94
49.0	5.204	5.739	5.472	1.211	0.816	2:00	2.85
65.6	7.968	8.599	8.284	1.434	0.995	2:07	4.22
68.0	9.598	10.189	9.894	1.518	1.093	2:17	4.35
69.5	10.283	10.889	10.586	1.561	1.144	2:27	4.33
71.9	10.788	11.389	11.089	1.614	1.209	2:42	4.27
71.9	11.313	11.909	11.611	1.656	1.263	2:54	4.30
80.7	14.918	15.549	15.234	1.746	1.343	2:57	5.50
71.5	15.118	16.739	15.929	1.746	1.350	3:07	4.63
68.2	15.143	16.779	15.961	1.756	1.365	3:20	4.25
46.4	15.034	16.693	15.864	1.724	1.345	3:32	3.62
18.4	14.503	15.139	14.821	1.631	1.281	3:50	2.13
4.1	14.018	14.659	14.339	1.582	1.243	3:57	1.28
0.0	13.791	14.438	14.115	1.564	1.233	4:08	1.09

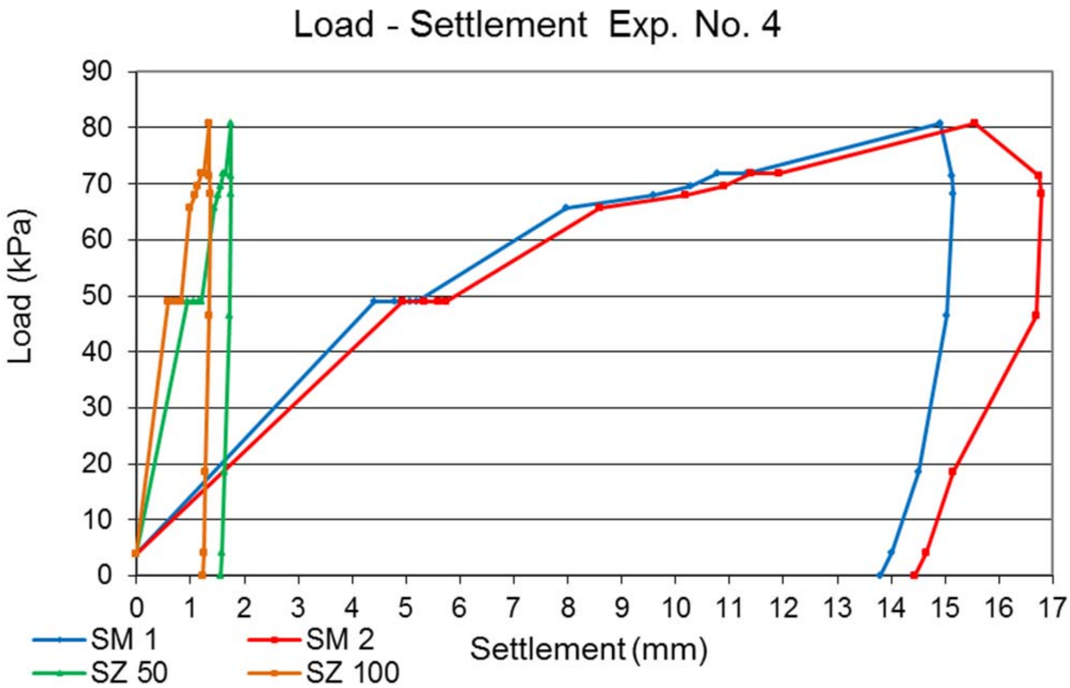
Load - Settlement Exp. No. 4
Load (kPa)
90
80
70
60
50
40
30
20
10
0
0 1 2 3 4 5 6 7 8 9 10 11 12 13 14 15 16 17
Settlement (mm)
SM 1
SM 2
SZ 50
SZ 100

Appendix D

SMALL SCALE EXPERIMENTS

Small scale experiments were proposed only to confirm the similarity of phenomenon of soil cancellation for undisturbed soil samples. That means to exclude the possibility that due to the loss of soil structure and compaction process which took place during the large specimen preparations we have crated conditions which are irrelevant for soils in a natural state.

As for their limited impact and expected results only small number of data was measured however nearly all small specimens went through the wetting procedure before they were subjected to high hydraulic gradients.

Experiment No.	1
Date	25.9.2006
Soil class	S-F
Load (kPa)	6.4

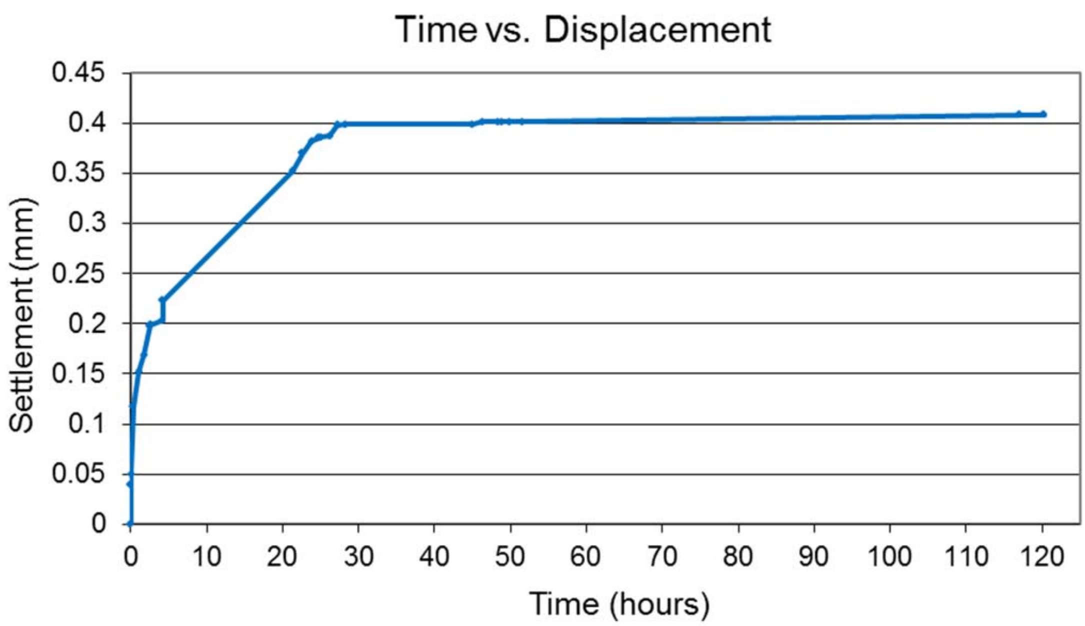

Experiment No.	2
Date	5.8.2006
Soil class	S-F
Load (kPa)	26.9

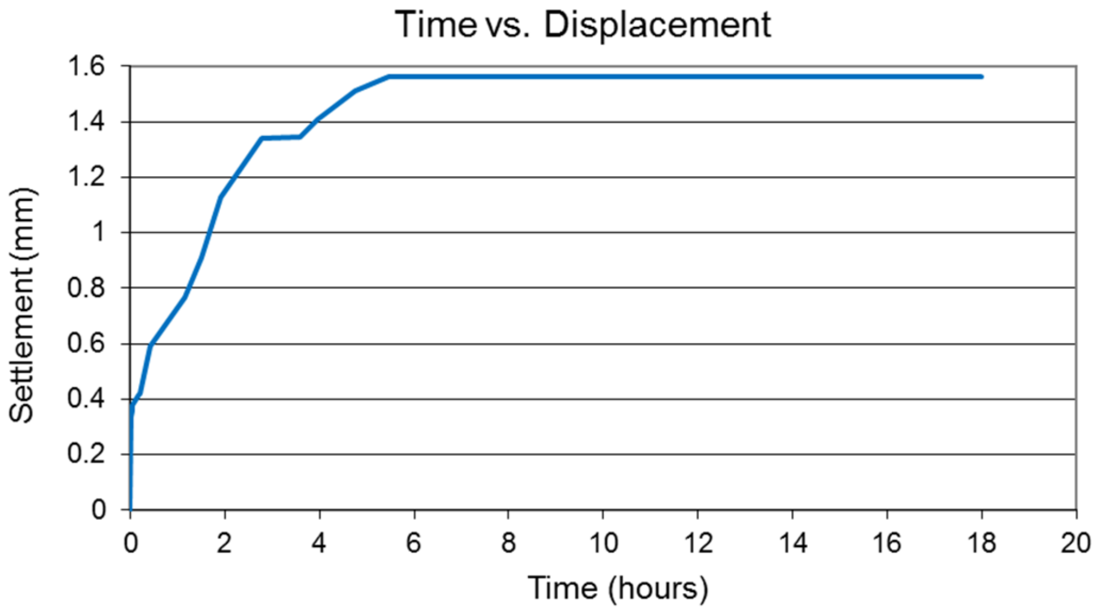

Experiment No.	3
Date	25.8.2006
Soil class	S-F
Load (kPa)	26.9

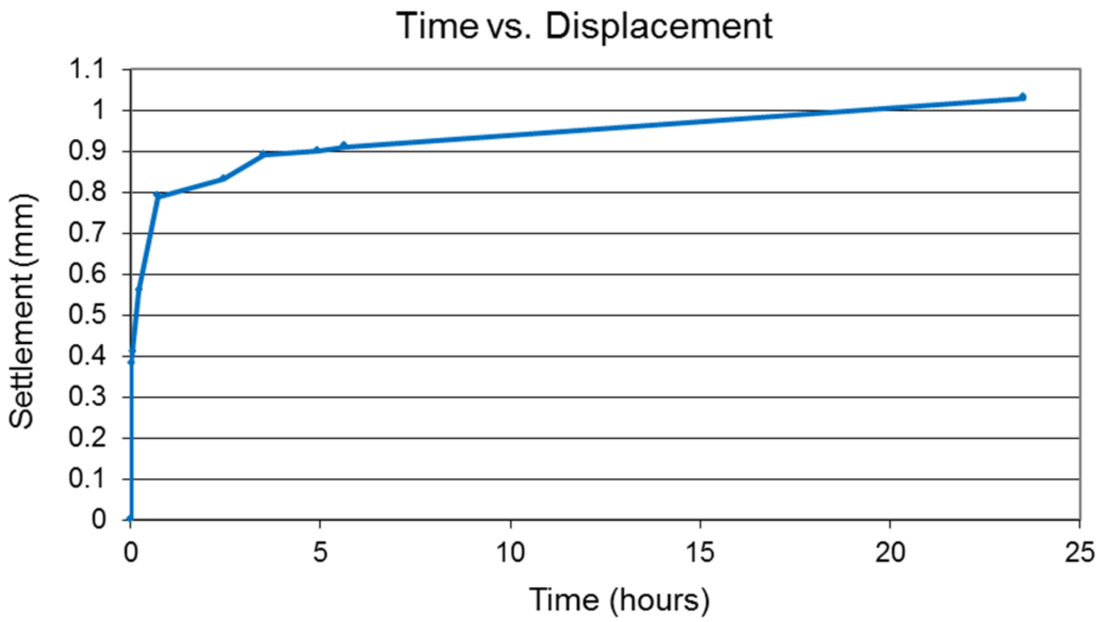

Appendix E

EROSION UNDER EXTREMELY HIGH GRADIENTS

The following pages contain processed data from experiments on small undisturbed soil specimen made of sands. More detailed description of the soil samples can be found in relevant parts of chapter 4. Flow and settlement charts are presented with basic data about the soil sample. If the specimen should collapse, the grain distribution of the erode particles and original specimen is presented.

Due to the fact, that except sand class samples, all the specimens sustained even phase III. of the experiment, i.e. hydraulic gradient over 14, for sufficiently long time, only result from sand samples are introduced followed brief photo documentation.

Experiment No.	1
Date	13.6.2007
Soil class	SP
Collapse	no; but particles were eroded

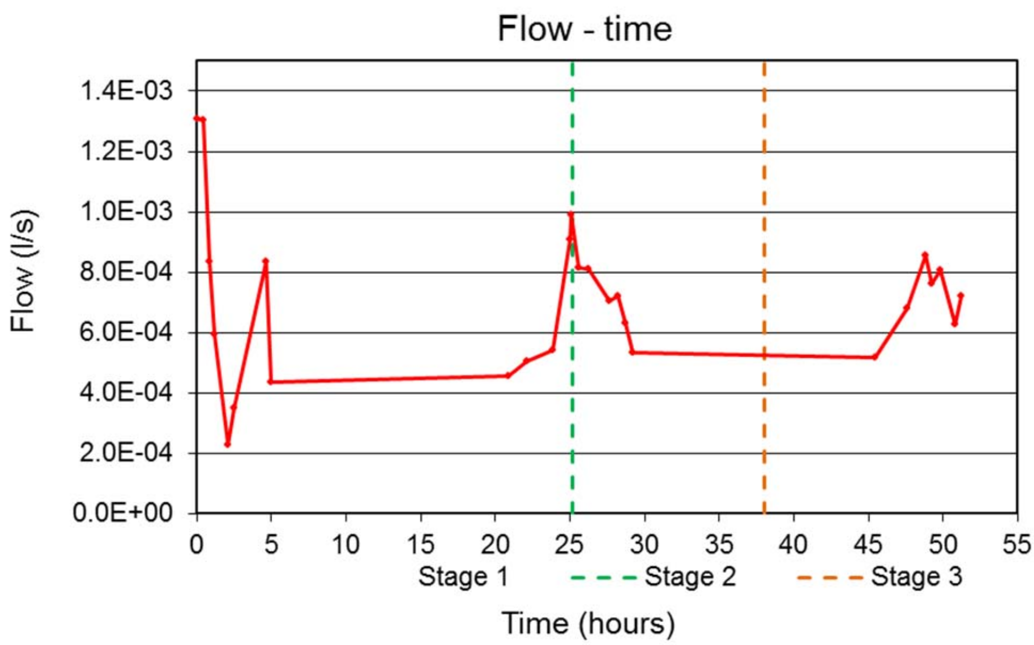

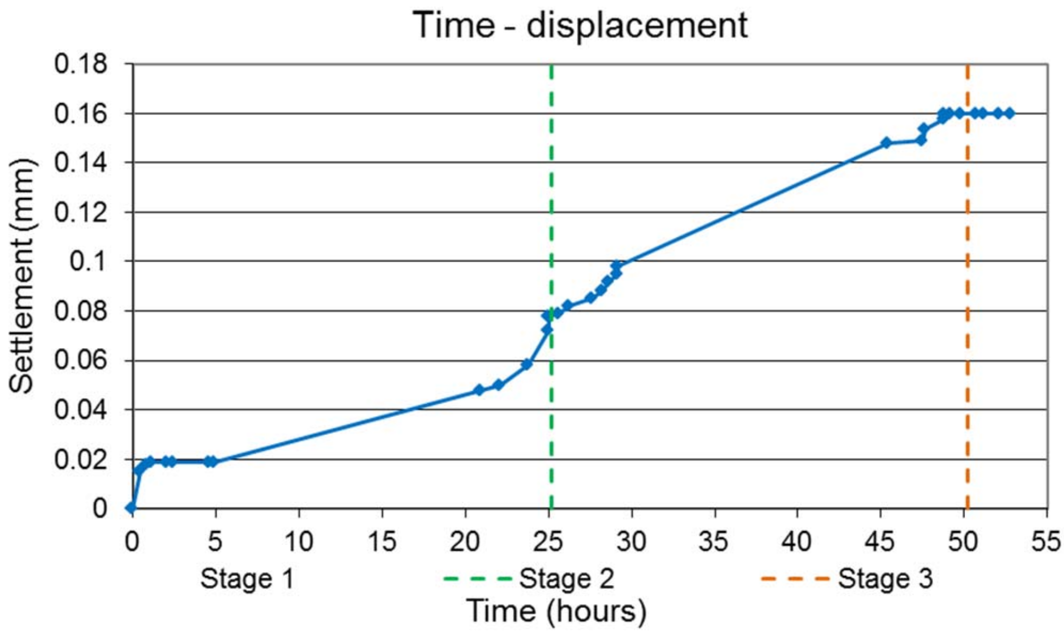

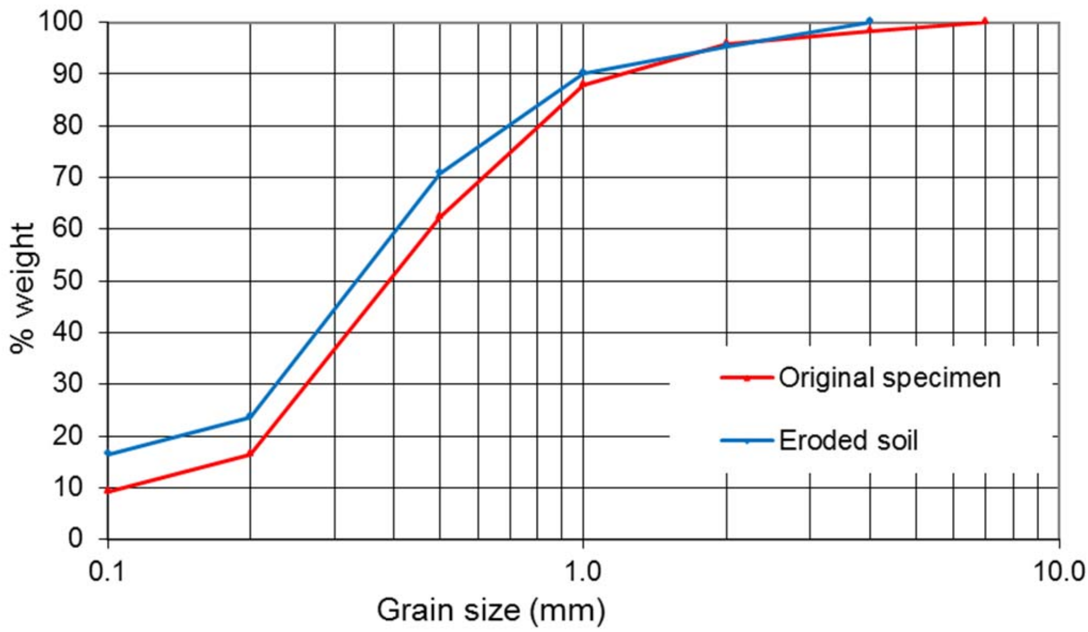

Experiment No.	2
Date	15.6.2007
Soil class	SP
Collapse	yes; III. phase

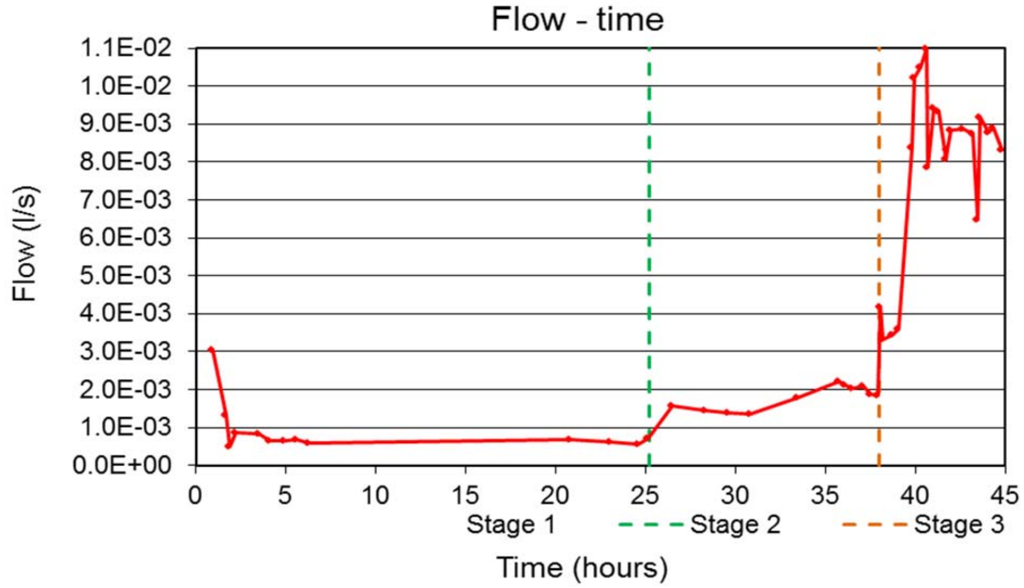
Flow - time
Flow (l/s)
1.1E-02
1.0E-02
9.0E-03
8.0E-03
7.0E-03
6.0E-03
5.0E-03
4.0E-03
3.0E-03
2.0E-03
1.0E-03
0.0E+00
0
5
10
15
20
25
30
35
40
45
Stage 1
Stage 2
Stage 3
Time (hours)

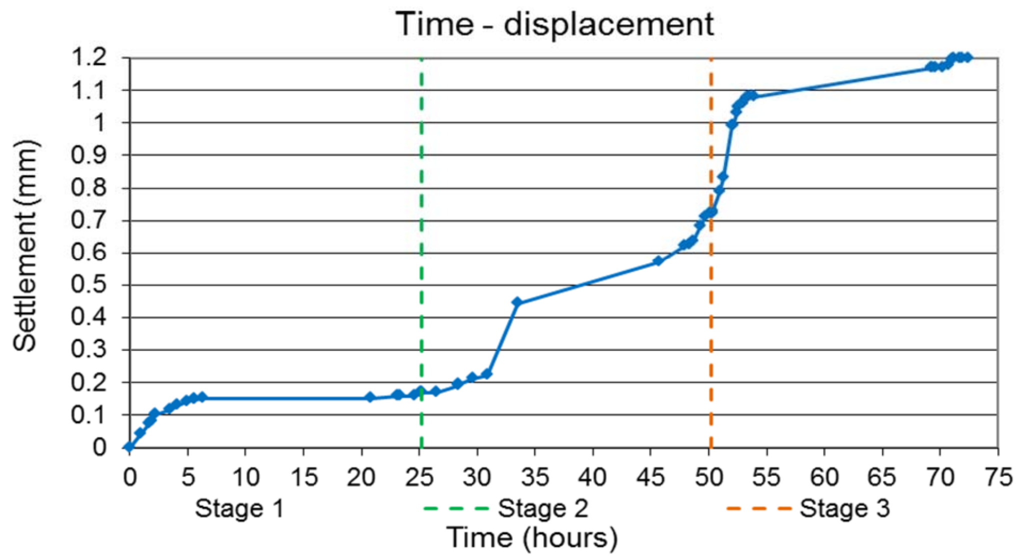
Time - displacement
Settlement (mm)
1.2
1.1
1
0.9
0.8
0.7
0.6
0.5
0.4
0.3
0.2
0.1
0
0
5
10
15
20
25
30
35
40
45
50
55
60
65
70
75
Stage 1
Stage 2
Stage 3
Time (hours)

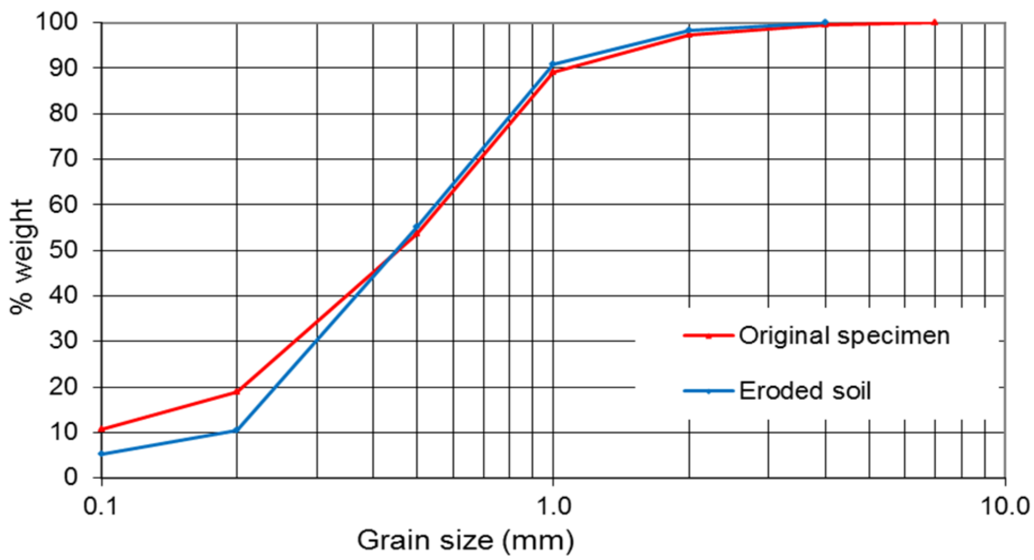
% weight
100
90
80
70
60
50
40
30
20
10
0
0.1
1.0
10.0
Grain size (mm)
Original specimen
Eroded soil

Experiment No.	3
Date	22.6.2007
Soil class	SP
Collapse	no

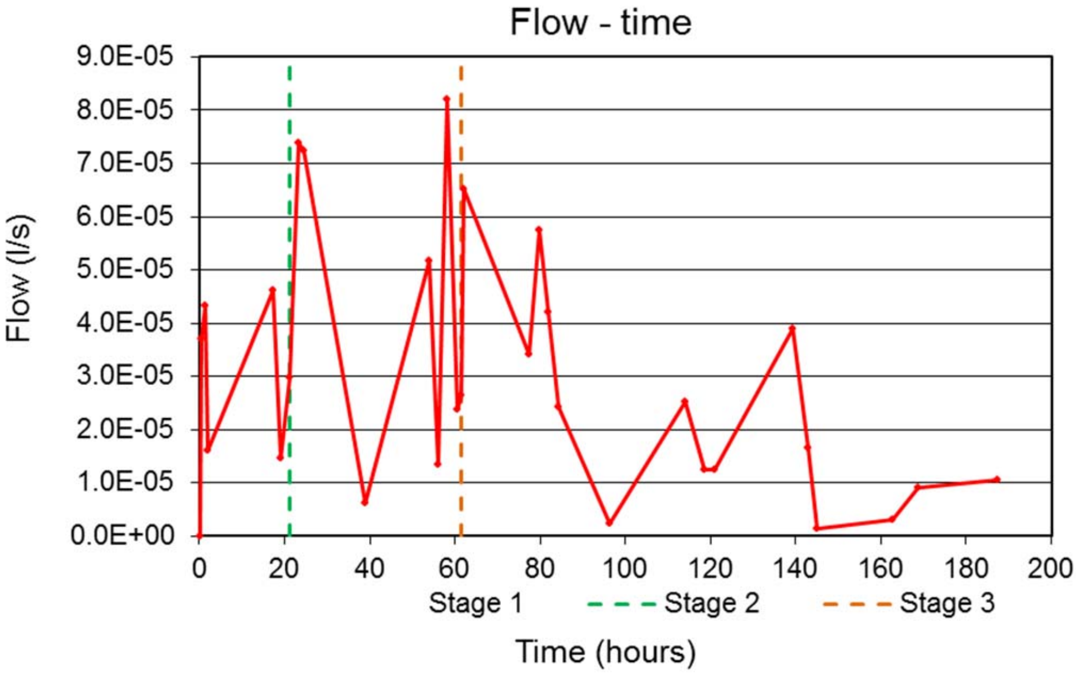

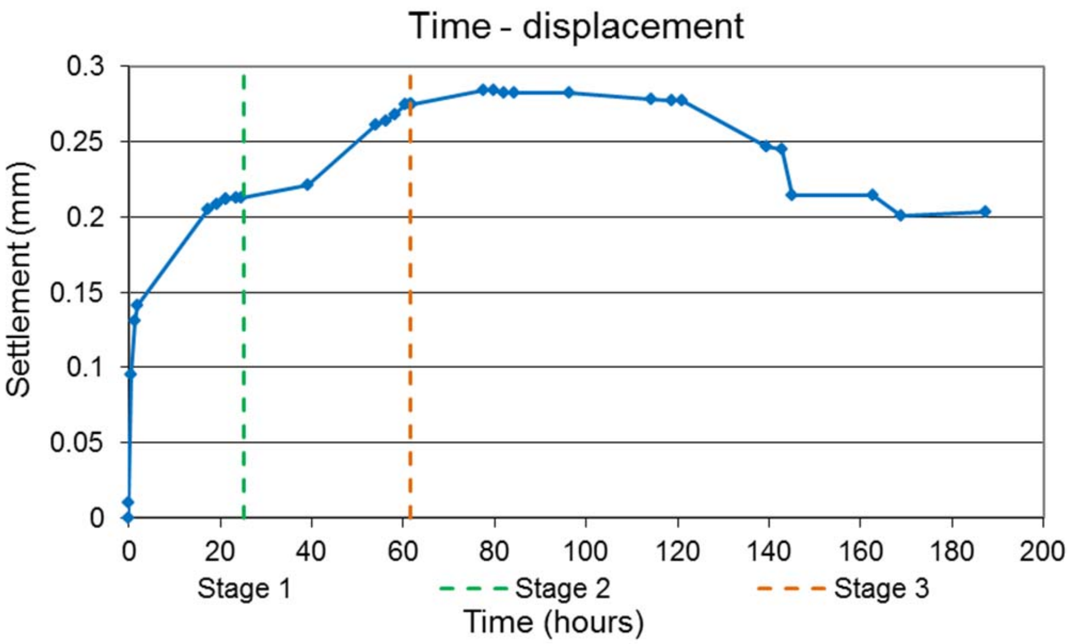

Experiment No.	4
Date	4.7.2007
Soil class	SP
Collapse	yes; II. phase

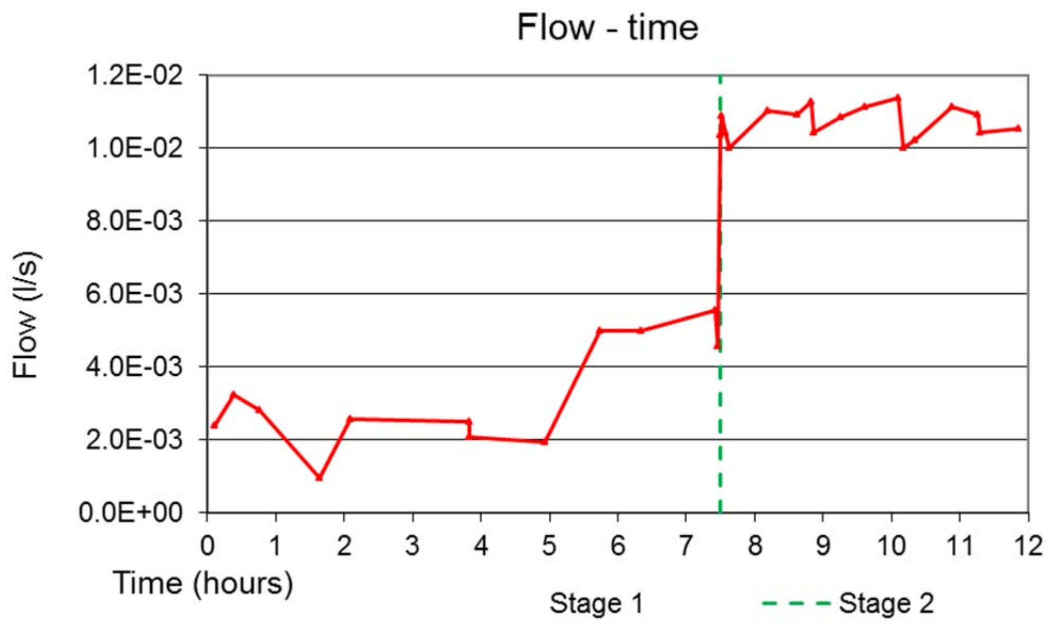

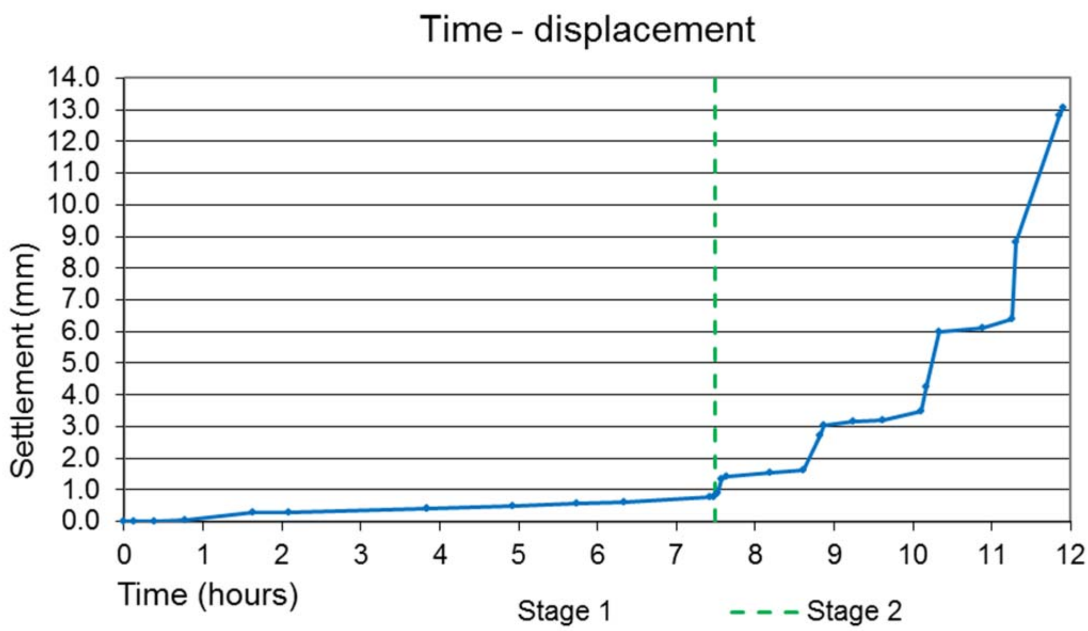

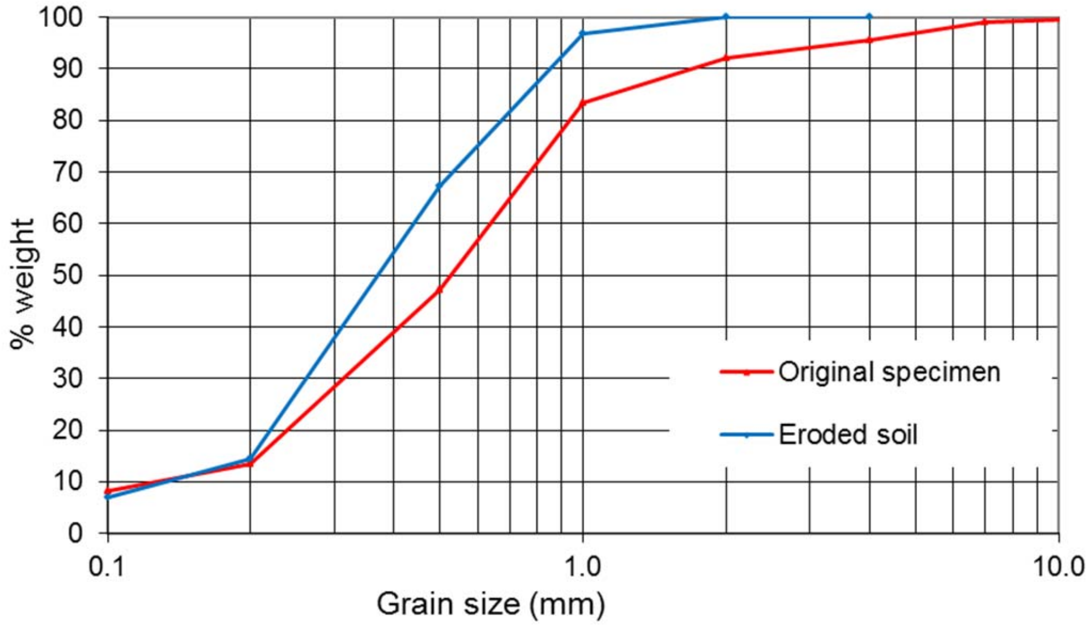

Experiment No.	4
Date	13.7.2007
Soil class	SP
Collapse	yes; III. phase

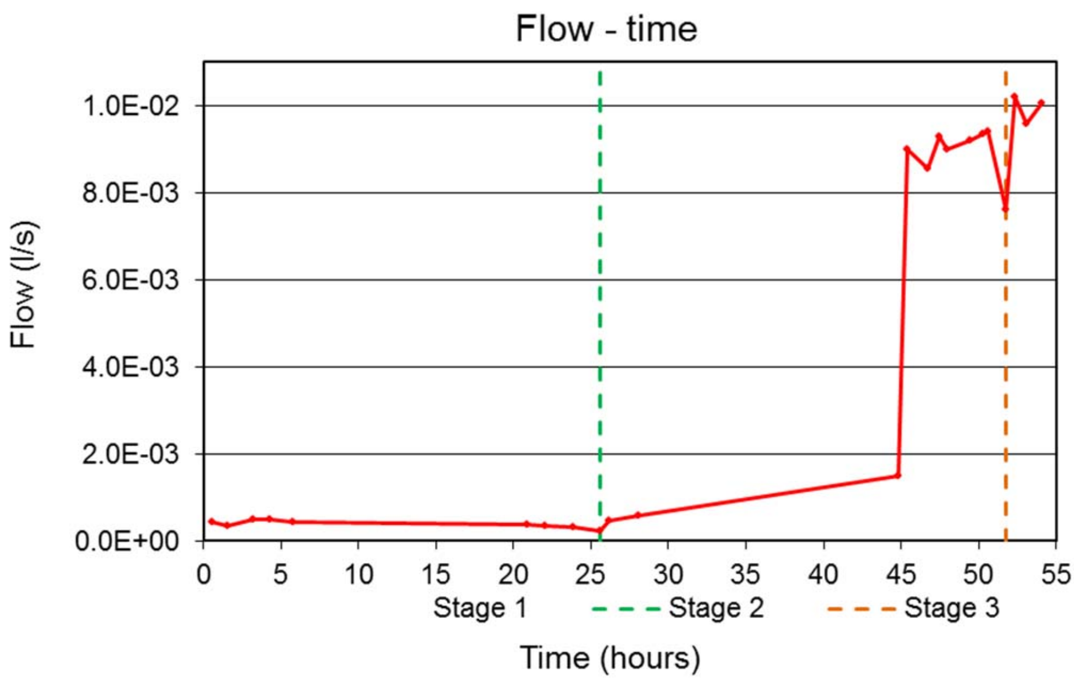

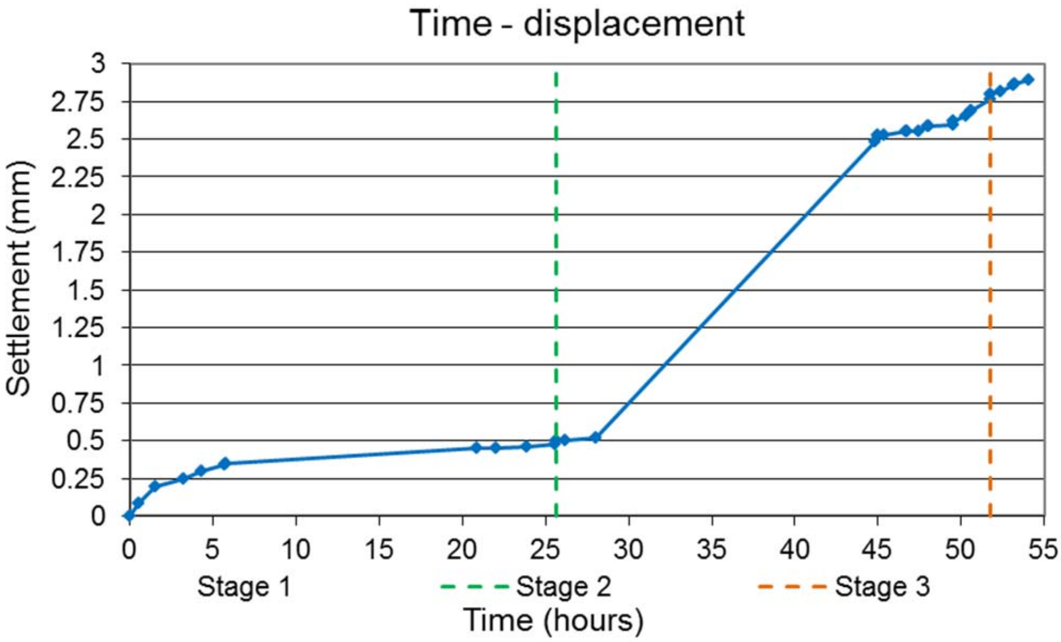
Time - displacement
Settlement (mm)
3
2.75
2.5
2.25
2
1.75
1.5
1.25
1
0.75
0.5
0.25
0
0 5 10 15 20 25 30 35 40 45 50 55
Stage 1
Stage 2
Stage 3
Time (hours)

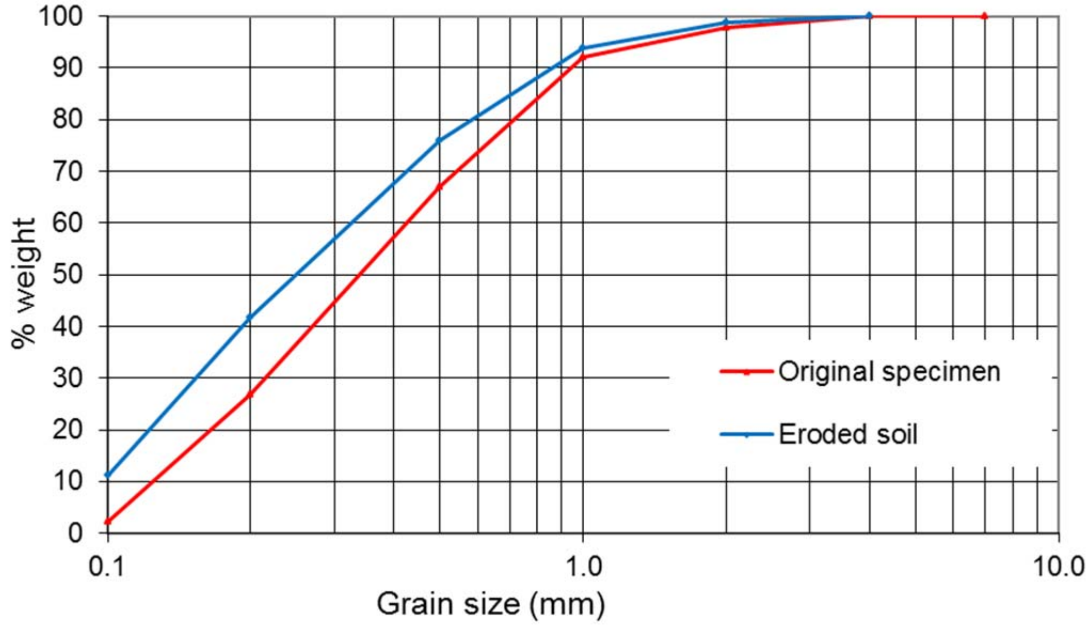
% weight
100
90
80
70
60
50
40
30
20
10
0
0.1
1.0
10.0
Grain size (mm)
Original specimen
Eroded soil